

Design and Implementation of a Humanoid Climbing Robot

A DISSERTATION SUBMITTED TO THE
GRADUATE SCHOOL OF ENGINEERING AND SCIENCE OF
SHIBAURA INSTITUTE OF TECHNOLOGY

by

NGUYEN ANH DUNG

IN PARTIAL FULFILLMENT OF THE REQUIREMENTS
FOR THE DEGREE OF

DOCTOR OF ENGINEERING

SEPTEMBER 2015

To my parents for their inspiration and motivation to meet my
dreams.

To my wife, Vu Thanh Lan. Thanks to her love and sacrifice I can
keep my mind on my research.

To my son, Nguyen Anh Khoa.

Acknowledgments

First of all, I would like to express my sincere thanks to my supervisor, Professor Akira SHIMADA, for his inexhaustible wisdom. He has given me the guidance to be a better researcher, thinker, speaker, writer, and teacher, and for this I offer my sincerest appreciation. This dissertation could not have been possible without his instructive comments at every stage of the dissertation process.

Next, I would like to thank all my committee members, Prof. Yutaka UCHIMURA, Prof. Yoshinobu ANDO, Prof. Takeshi SASAKI, and Prof. Toshiaki TSUJI for participating in my defense and their valuable comments. Their suggestions and discussions during my presentations help me to significantly improve my results.

I would also like to extend my gratitude to the faculty and staff members of Shibaura Institute of Technology for their support. Thanks to all the Motion Control Laboratory (MCL) members who are very kind to me, I strongly appreciate their helps for my life in Japan.

My deepest thanks go out to my wife, Thanh-Lan, whose emotional and physical support has given me strength and joy during the writing of this dissertation. Many thanks to my parents for their lifelong support. Special thanks to my mother, Thanh-Ha, who is a fountain of love. Thanks to younger brother Duc-Manh.

I will end with a baby-sized thank you to my one year-old son Anh-

Khoa, who will hopefully be able to understand this thesis someday.

Tokyo, Jun 28, 2015

Nguyen Anh Dung

Abstract

This dissertation describes a research with respect to humanoid free climbing robot. The design, implementation, and experimentation of humanoid climbing robot are presented. The goal of my research is develop a humanoid climbing robot, which can climb up autonomously a vertical climbing wall while using the climbing technical similar to those develop by climber. It means that humanoid climbing robot uses only his hands and feet to make contact with terrain feature to maintain static equilibrium.

In order to develop humanoid robot in a similar way, four fundamental challenges must be addressed: robot design, sensing, motion planning and motion control. Our work focuses on robot design (including sensors) and motion planning. At that point, our robot is an integrated system consisting of a sensing system and global and local planner running offline.

The presented robot can be modified to improve the inherent ability of the humanoid robot to climb complex terrain. It may also lead to better performance and make other issues easier, such as motion planning and control. Therefore, our work starts with rudimentary analysis of mechanical structure and kinematic aspects of humanoid robot. Then, the climbing robot simulation was design to optimize performance, in particular to maximize the work-space reachable by the robot hands.

In the motion control part, the method to calculate valid area to keep balance is presented considering the equilibrium condition in order to perform motion control. A four limb model is analyzed to clarify

those useful climbing technical should be apply for humanoid climbing robot.

In the motion planning part, this dissertation focuses on a path planning and local planning algorithm for humanoid robot wall climbing as the initial phase of our development. The first step is to acquire a depth map to extract accurate information about climbing holds on the vertical wall. Secondly, we propose a global planning algorithm for the humanoid robot using data from Kinect. The proposed algorithm ensures that the climbing robot finds the best route to climb up the wall. During climbing, the humanoid robot utilizes the local planning algorithm, based on quasi static equilibrium, to adjust its body posture in order to remain in equilibrium state. Finally, all algorithms are evaluated with a simple practical example for a humanoid climbing robot system, and its effectiveness is demonstrated experimentally in a real environment.

Contents

Abstract	iv
Acknowledgments	iv
List of Figures	xii
List of Tables	xiii
List of Algorithms	xiv
List of Abbreviations	xiv
1 Introduction	1
1.1 Background and Challenges	1
1.1.1 Aid Climbing Robots	2
1.1.2 Free Climbing Robots	5
1.1.3 Challenges of Humanoid Climbing Robots	7
1.2 Objectives	8
1.3 Contributions of this Dissertation	10
1.4 Structure of this Dissertation	11
2 Literature review	13
2.1 Humanoid Robot Researches	13
2.1.1 The Humanoid robot at Waseda University	14
2.1.2 Honda humanoid robots	16
2.1.3 The HRP project	18
2.1.4 Universities and Research Institutes	20

2.1.5	Companies	21
2.2	Previous Review on Humanoid Climbing Robot	22
3	Humanoid climbing Robot System Design	25
3.1	Hardware platform	25
3.1.1	KONDO KHR-3HV	25
3.1.2	Geometric dimensions	26
3.1.3	Hardware modification	26
3.1.4	Shoulder joints	27
3.1.5	Elbow joints	28
3.1.6	Actuators	29
3.2	Control System and Sensors	30
3.2.1	Microprocessor board	30
3.2.2	Gyro Sensor	31
3.3	Climbing Wall	32
4	Humanoid Climbing Robot Modeling	34
4.1	Introduction	34
4.2	Climbing Technique	35
4.2.1	Climbing Technique with The Simplest Model of Climbing	36
4.2.2	Climbing Technical for my Humanoid Climbing Robot . .	40
4.3	Humanoid Climbing Robot: Kinematics	40
4.3.1	Definition of coordinate frames	41
4.3.2	Inverse kinematics of Humanoid climbing robots	44
4.3.2.1	Inverse kinematic for the hands	44
4.3.2.2	Inverse kinematic for the legs	46
4.3.3	The stability analysis of humanoid climbing robot	48
4.4	Modeling of Humanoid Climbing Robot by Using Simmechanics .	50
4.4.1	Introduction of Simmechanics	50
4.4.2	Export CAD to Simmechanics diagram	50
4.4.3	Modeling of humanoid climbing robot	51
4.4.3.1	Moderling the bodies, legs, hands and joints for the climbing robot	51
4.4.3.2	Modeling the servomotor and actuated joint . . .	52

4.5	Simulation results	53
4.5.1	Humanoid climbing robot model in Matlab	53
4.5.2	Perform simple task of the climbing activities	53
4.6	Discussion	55
5	Equilibrium Control on Four-Limbed Climbing Robot	57
5.1	Four limb model	57
5.2	Climbing Condition	60
5.2.1	Static equilibrium constrain	60
5.2.2	Equilibrium condition of movement	61
5.2.3	Relationship between Torque and Length of Limb	61
5.2.4	Examples	62
5.3	Discussion	65
5.3.1	Platform for Humanoid Robot	65
5.3.2	Proposition of Position Control	66
6	Global Path and Local Motion Planning for Humanoid Climbing Robot	68
6.1	Introduction	68
6.2	Precondition and Preliminary Work	71
6.2.1	Hardware Structure	71
6.2.2	Assumptions on the research	72
6.2.3	Climbing Wall Structure	73
6.3	Observation part	73
6.3.1	Pre-processing of Kinect Depth Data	73
6.3.2	Searching Climbing Holds Position (pixel data)	74
6.3.3	Climbing holds position (real data-mm)	76
6.4	Global Path Planning	77
6.4.1	Defining robot “reachable area”	78
6.4.2	Scanning Phase	78
6.4.2.1	Scanning Valid Right Hand Holds	78
6.4.2.2	Cost Evaluations and Building the Graph of “Right Hand Reachable Holds”	82
6.4.3	The Query Phase	84

6.5	Local Motion Planning	86
6.6	Experiment with an Example	88
6.7	Conclusion and Future work	95
6.7.1	Future work	95
7	Conclusion and Future Work	96
7.1	Conclusion	96
7.2	Future works	97
	References	109

List of Figures

1.1	Samples of climbing robots	4
1.2	Stickybot climbs at surfaces, while Spinybot climbs surfaces with tiny texture.	5
1.3	A few examples of legged robots.	6
1.4	These example of free-climbing robots	7
1.5	Climber keeps balance on the climbing wall.	9
2.1	Humanoid robots from Waseda University	14
2.2	The WABIAN and WABIAN RV humanoid robots	16
2.3	The WABIAN 2R humanoid robot [71].	17
2.4	These example of free-climbing robots	18
2.5	The WABIAN and WABIAN RV humanoid robots	19
2.6	The HRP-2, HRP-3 and HRP-4 humanoid robots.	20
2.7	Small Humanoid Robots	22
2.8	These example of humanoid ladder climbing robots	23
3.1	Kondo robot and an application of the robot.	26
3.2	Dimension of Kondo KHR-3HV robot	27
3.3	The original and modified hand	28
3.4	KRS-2552HV ICS servo motor red version	29
3.5	RCB-4HV robot controllers	31
3.6	KRG-4 gyro sensor	32
3.7	Humanoid climbing robot on the wall: the first type of hold is a small ring (left), and the second type is a climbing hold(right) . .	32
4.1	Climbing motion at a natural wall	36

4.2	Simplest Humanoid Climbing Robot	37
4.3	Equilibrium forces between climber and wall	38
4.4	Typical holds for climbing	39
4.5	Appropriate force with the different shape of holds	39
4.6	Base coordinate frame "O"	42
4.7	Link coordinate frames of the Left Hand/Leg	43
4.8	Left hand is initial position	45
4.9	Left leg is initial position	46
4.10	The three components of the force applied to each hold are recorded with respect to the reference system (LF, i, j, k)	48
4.11	Mass properties from Solidwork.	51
4.12	Mechanical model of HCR in Simmechanics	52
4.13	Modeling a Servo motor system	53
4.14	3D model of HCRobot in Matlab	54
4.15	Snapshot of stop motion and COG's position	55
4.16	Snapshot of dynamic motion	56
5.1	Humanoid Climbing Robot	58
5.2	The center model keep balance by using 4 limbs. The others main- tain equilibrium by just 3 limbs, one free limb is used to reach a new hold.	58
5.3	Basic structure and real climbing example	59
5.4	Reachable Area and Equilibrium Line Segment	62
5.5	Jount angles and Torques at equilibrium points	63
5.6	Equilibrium line segment position changing	64
5.7	Humanoid robots platform	66
5.8	Position control diagram	67
6.1	General Overview	69
6.2	Climbing Wall and System Location	70
6.3	Climbing holds	73
6.4	Overview proposed Systems	74
6.5	Pixel Data	75
6.6	Convert and Label Climbing Holds	76

6.7	Definition of “reachable area” and “reference point for scan”-S . . .	77
6.8	Scan example using “Right hand reachable holds”	79
6.9	The updating information of RHRHs when point S at(910,290) . . .	80
6.10	Adjacent hold V1 and V2 as an example	83
6.11	The new graph RHRHs	86
6.12	Detail local motion planning	87
6.13	Joint trajectories example	88
6.14	Robot start to climb at V1	89
6.15	Sequence of family hold group from V[2] to V[7]	90
6.16	Sequence of family hold group from V[7] to V[16]	91
6.17	Sequence of family hold group from V[16] to V[19]	92
6.18	Sequence of family hold group from V[19] to V[22]	93
6.19	Snapshots of humanoid climbing robot along the best route. . . .	94

List of Tables

3.1	Kondo KHR-3HV robot-Body measures	28
3.2	Physical parameters of the KRS-2552HV ICS Servo robot	29
4.1	Deegree of freedom of a Kondo KHR-3V robot	41
6.1	The storing rule of Kinect depth values	75
6.2	3 First right hand reachable holds for S (910,270-mm)	81

List of Algorithms

1	Scanning “Right Hand Reachable Hold”	81
2	Cost Evaluations and Building the Graph of “RHRHs”	84
3	Apply Dijkstra Algorithm	85

Chapter 1

Introduction

This chapter starts out by describing the humanoid climbing robot problem. Then, the specific challenges are discussed and why current researches are not up to meeting these challenges, which will later be used to motivate my proposal. The end of this chapter presents the main contributions of this dissertation and an outline of its organization.

1.1 Background and Challenges

Suppose it is possible that a humanoid robot could independently free-climb vertical rock, much the same as the human climber. A humanoid climbing robot has to figure out where he is going to put his foot and where he is going to try to grab onto next holds. The robot can be fall down, swing against rock hard, twist an ankle, and lose precious time at any misstep. Therefore, the robot must examine the cliff above he to choose a sequence of hand and footholds. He always look forward to plan the best route, and then climbs step by step with tremendous care. We believe that humanoid climbing robot will be applied in the following scenario: climbing over the already-rugged terrain to support rescue teams, searching trapped climbers on the mountain, or even exploring rock faces on the solar system. It is definitely a challenge and sort of a puzzle. Humanoid climbing robot not only must decide how to adjust its posture to reach the next hold

without falling, but also it must plan an entire sequence of steps. These activities present a new level of challenges for robotics.

Motivated by the challenges mentioned above, the main objectives of my research is develop a humanoid robot equipped with appropriate sensing, planning, and control and control capabilities to “free-climb” vertical and irregular terrain to reach goal locations.

1.1.1 Aid Climbing Robots

Nowadays robotics is one of the most dynamic fields in scientific researches. During the last decades, interest in studying climbing robots has been increased. This increasing interest has been appeared in many areas: mechanics, electronics, medical engineering, cybernetics, controls, and computers. It seems that climbing robots are useful devices that can be adopted in a variety of applications like maintenance, building, inspection and safety in the process and construction industries. These systems are mainly used in places where direct access by a human operator[84].

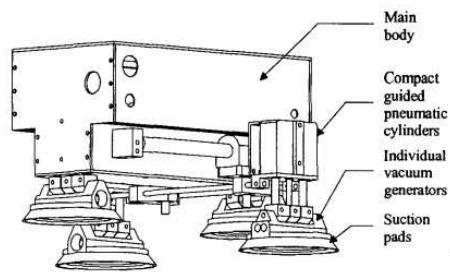
Up to now a lot of research has been devoted to wall climbing robots and various types of experimental models have been already proposed. The major two issues in design of the wall climbing robots are their locomotion and adhesion methods. According to the adhesion method, these robots are generally classified into four groups: magnetic, vacuum or suction cups, gripping to the surface and propulsion type. Recently, new methods for assuring adhesion, based in biological findings, have been proposed. The magnetic type principle implies heavy actuators and is used only for ferromagnetic surfaces[83]. The vacuum type principle is light and easy to control though it presents the problem of supplying compressed air. With respect to the locomotion type, three types are often considered: the crawler type, the wheeled type and the legged type. Although the crawler type is able to move relatively faster, it is not adequate to be applied in rough environments. On the other hand, the legged type easily copes with obstacles found in the environment, whereas generally its speed is lower and requires complex control systems[66].

In the last decades, different applications have been envisioned for these robots, mainly in the technical inspection, maintenance and failure or break-down diagnosis in dangerous environments. These tasks are necessary in bridges [13, 75], nuclear power plants [80], or pipelines [77], for scanning the external surfaces of gas or oil tanks [56, 77], and offshore platforms [13], for performing non-destructive tests in industrial structures [30, 48], and also in planes [29, 74, 75], and ships [59, 75]. Furthermore, they have been applied in civil construction repair and maintenance [13], in anti-terrorist actions [91], in cleaning operations in sky-scrapers [27, 31, 42, 67], for cleaning the walls and ceilings of restaurants, community kitchens and food preparation industrial environments [26], in the transport of loads inside buildings [60] and for recon-naissance in urban environments [78]. Their applications were also proposed in the human care [13] and education [43] areas.

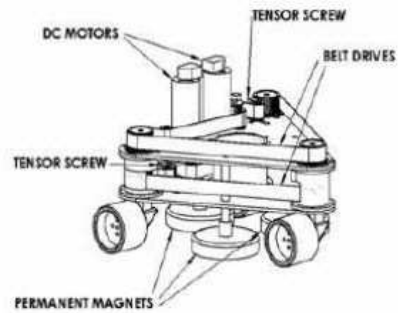
With respect to the locomotion type, the simpler alternatives usually make use of sliding segments, with suction cups or magnets that grab to surfaces, in order to move [26, 30, 31, 42, 67, 74, 80] (Figure 1.1(a)). Although the crawler type is able to move relatively faster, it is not adequate to be applied in rough environments, being its main disadvantage the difficulty in crossing cracks and obstacles.

Another possibility of locomotion is to use wheels [27, 56, 77] (Fig. 1.1(b)) being these robots able to achieve high velocities. The main drawback of some wheeled robots using the suction force for adhesion to the surface is that they need to maintain air gaps between the surface where they move over and the robot base. A final alternative for implementing the locomotion is adoption of legs. Presently there are many biped robots (Figure 1.1(c)) with the ability to climb in surfaces with different slopes [19, 39, 40, 41, 50, 59, 62, 75, 78, 82] or quadrupeds [48, 59] (Fig. 1.1(d)) and robots with larger number of legs [59, 91].

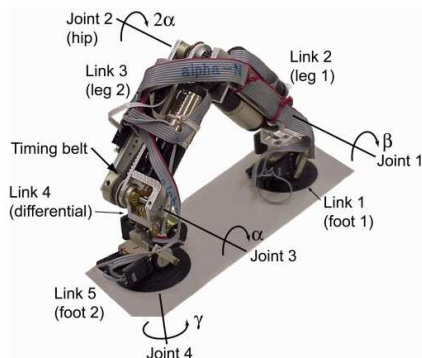
Consequently, they are limited to environments consisting of glass, metal, or other smooth surfaces. Recently, bio-inspired robot feet have been developed to create robots that can climb on building walls, tiles, and other smooth surfaces. Among them, Stickybot [49] uses a rubber-like material with tiny polymer hairs made from a micro-scale mold to mimic gecko's feet, while Spinybot [12] has



(a) ROBICEN III climbing robot. [80]



(b) Wheeled climbing robot[66]



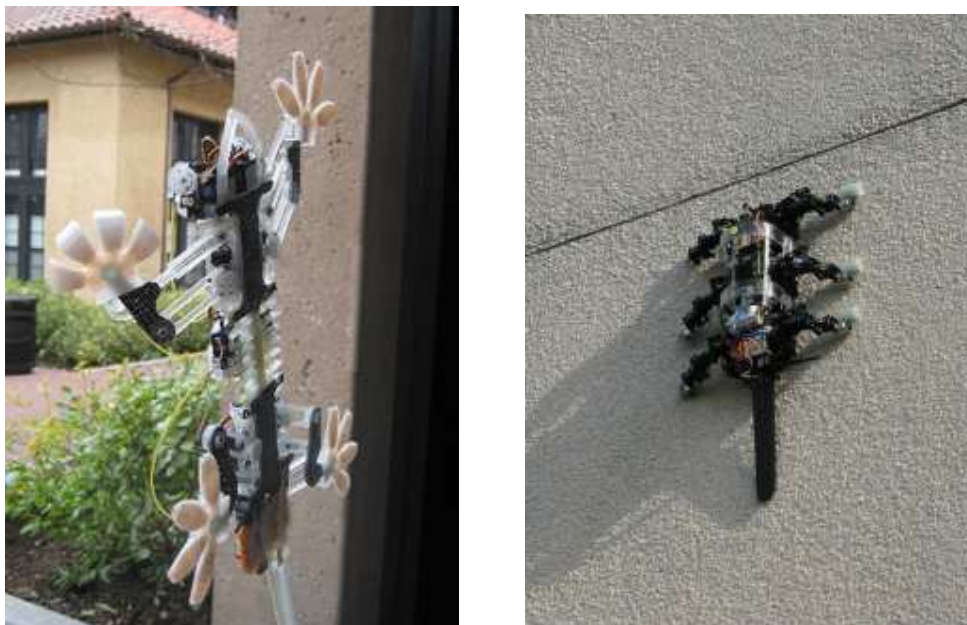
(c)(RAMR1) biped climbing robot[62]



(d) Quadruped climbing robot[48]

Figure 1.1: Samples of climbing robots

feet equipped with many tiny claws. See Figure 1.2. None of these robots could free-climb vertical terrain with both small and large irregular features.



(a) Stickybot (Stanford) [49] (b) Spinybot (Boston Dynamics) [12]

Figure 1.2: Stickybot climbs at surfaces, while Spinybot climbs surfaces with tiny texture.

1.1.2 Free Climbing Robots

Compared to aid climbing robots, legged robots are potentially more capable of traveling over challenging (e.g., steep and irregular) terrain. So, it is not surprising that much research has been carried out in recent years to design such robots, for instance humanoid robots [1], quadruped robots [61], and other multi-limbed robots [89]. Figure 1.3 shows a few of these robots.

Unlike aid climbing that takes advantage of special equipment, tools and/or engineered terrain features, free climbing robot only relies on friction at the contacts between the climber and the rigid terrain. So, a human free climber moves on a steep rock crag or an artificial climbing wall using nothing else but her body

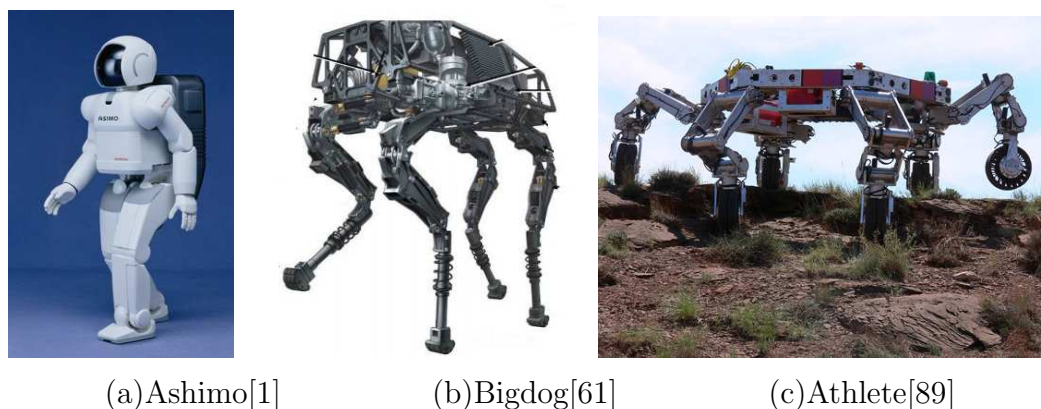


Figure 1.3: A few examples of legged robots.

(mostly her hands and feet) to make contacts with irregularly distributed terrain features, such as protrusions, holes, ledges, and cracks.

To our knowledge, there has not been any major research project aimed at developing an integrated autonomous multi-limbed robot equipped with appropriate sensing, planning, and control capabilities to “free-climbing” quasi-vertical and irregular terrain to reach user-specified goal locations. To the best of my understanding, Lemur IIb (Figure 1.4(a)) represents the first attempt to build a free-climbing robot in steep terrain found in space exploration. It is a planar fourlimbed climbing robot created by NASA’s Jet Propulsion Laboratory[22], LemurIIb robot consists of four identical limbs mounted on a circular chassis with equal spacing between them. Each limb has three revolute joints, the two first joints like a “shoulder” and “elbow” (in plane) and one out of plane degrees of freedom. At the end of each limb is a “finger”, a cylindrical peg wrapped with high-friction rubber. A planner was developed for Lemur IIb [15, 18]

A continuation of previous research done at Stanford by Tim Bretl [15, 16, 17, 18], Kris Hauser [32, 33, 34] and Teresa Miller [64, 65] Capuchin robot was designed and developed by Ruixian Zhang [94, 95, 96]. Capuchin robot (Figure 1.4(c)) is a four-limbed free climbing robot. It does not take advantage of special tools, only relies on friction at the contacts between the its limbs and the rigid terrain in order to remain its body in equilibrium. While moving, Capuchin adjusts its body posture (hence, the position of its centre of mass) and exerts

appropriate forces at the contacts in order to keep balance.

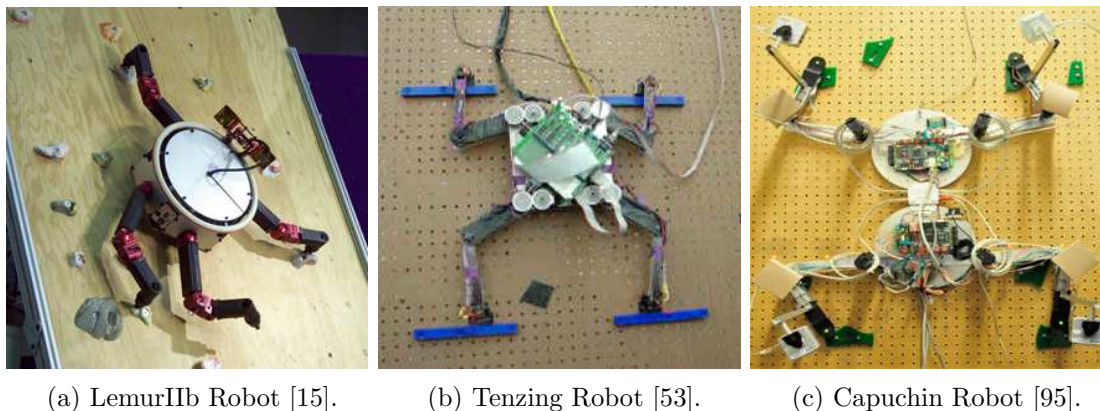


Figure 1.4: These example of free-climbing robots

Tenzing (Figure 1.4(b)), another free-climbing robot, was built at Dartmouth College [53]. Like Lemur, it is a four-limb planar robot with two revolute joints in each limb. A hobbyist servo motor is used on each elbow and shoulder joint. Tenzing is designed to climb a planar wall with artificial terrain features. A force sensor is mounted on each limb endpoint to control the magnitude of the contact force along the vertical direction. The body has a tilt sensor used to keep the body upright. A camera, not mounted on the robot and located at some distance away from the wall, is used to determine the position of the robot and locate terrain features on the wall. It is reported in [53] that the robot can climb in an interactive mode and in an automatic mode. In the interactive mode, a human user enters a sequence of holds on a graphic interface. In the automatic mode, a program automatically plans a path up the wall. The details of the control and planning algorithms are not available.

1.1.3 Challenges of Humanoid Climbing Robots

The objective of these projects mentioned above is to create a multi-limbed robot capable of climbing vertical terrain autonomously. Nevertheless, in this dissertation, I want to introduce a new approach in this field by enlarging enhancing the capabilities of humanoid robot to autonomously climb up configurable climbing

walls using techniques similar to those used by human free climbers. Humanoid climbing robot (HRC) is subject to the same constraints as a humanoid free-climber. At each configuration, some of HRC's hands must be in contact with holds, on which it can stand and balance without falling (see in Figure 1.5). To reach a goal location, HRC must move along a continuous path through such configurations, walking up the rock surface on a sequence of holds. Typically, there is no repeated pattern of limb motions (no gait), nor is there any local indication of the direction in which to climb. Therefore, multi-step planning is necessary in order to decide which hold the robot should grab next, and how it should adjust its posture in order to do so.

Creating a humanoid climbing robot is obviously a challenging project. The main objective is interesting, however to achieve this goal there are several of important technical areas of robotic should be developed. For example complex planning, multi-contact control, equilibrium maintenance, and delicate use of sensor feedback, not to mention the larger number of degree of freedom of a humanoid robot.

1.2 Objectives

Motivated by the challenges mentioned above, the main objectives of the dissertation was to enable a humanoid robot to climb an indoor, artificial rock surface. This surface is near-vertical, planar, and is covered with the same small features of irregular shape that are used in indoor "climbing gyms" for human climbers such as the climbing wall in Figure 1.5. The features are easily attached or removed from the surface, so many different environments can be constructed. Human climbers typically refer to each environment as a route or problem to be "solved." HRC are intended method to give humanoid robots the capability to autonomously climb without equipped tools, such as drills or, section cups in a real environment in order to accomplish search and rescue tasks on mountain faces or broken urban terrains.



Figure 1.5: Climber keeps balance on the climbing wall.

As we have already mentioned, a humanoid climbing robot is challenging because it only relies on friction at the contacts between the robot and selected holds. For a robot to free climb, four fundamental objectives must be considered: System design, sensing, planning and control. These main objectives of the dissertation are as follows:

- **System design and modeling robot.** Design and construction of a humanoid climbing robot system should be presented. Moreover, rock climbing technique should be master to apply for humanoid robots. A humanoid climbing robot modeling should be created in Matlab-Simmechanics.
- **Sensing.** Using vision (Kinect Microsoft) to observe the entire climbing wall, and detect the holds 's position.
- **Motion Planning.** Global motion planning is developed to identify the best route, and robot can follow this route to climb up the wall with the

current climbing wall configuration. In addition, a local planner should be developed to support humanoid robot during climbing process.

- **Motion Control.** An four limb climbing robot is analyzed to explore how this model can maintain robot's body in equilibrium. How this model make contact with holds to make sure that reaction forces keep the robot in static equilibrium.

1.3 Contributions of this Dissertation

The overall objective of the schemes proposed in this dissertation is to develop a humanoid robot capable of climbing vertical terrain autonomously using techniques similar to those used by human free climbers. The contributions of the dissertation are as follows:

- Firstly, in order to make robot climb walls successfully, the robot model is designed considering equilibrium of force and moment. Then, amount of useful climbing technical of climber apply for humanoid robot is present throughout this dissertation. Moreover, I study the problem of forward kinematic and inverse kinematics for the Kondo KHR-3HV and propose a complete analytical solution to both problem, including a software library implementation. In addition, humanoid climbing robot modeling in Simmechanics is finally present. Simulation results show that the modeling could keep balance on the wall and continue to free climb.
- Secondly, the method to calculate reachable area to keep balance is presented considering the equilibrium condition in order to perform motion control. In addition, I propose the theory for position control for humanoid climbing robot.
- Finally, I propose global path and local motion planning for humanoid climbing robot. The first step is to acquire a depth map to extract accurate information about climbing holds on the vertical wall. Then, we propose a global planning algorithm which ensures that that the climbing robot finds

the best route to climb up the wall. During climbing, the humanoid robot utilizes the local planning algorithm, base on quasi static equilibrium, to adjust its body posture in order to remain in equilibrium state. At last, a simple practical example is experiment, and its and its effectiveness is demonstrated experimentally in a real environment.

1.4 Structure of this Dissertation

This section discusses an overview of each chapter, which is detailed below

Chapter 2 is “Previous study”: It discusses the history and origin of a humanoid robot, and a humanoid climbing robot. Where does the word humanoid climbing robot come from? Evolution of the robot are recorded from the past to the present. It aims for fundamental stage before into the research.

Chapter 3 introduces a “Methodology”. An overview of humanoid climbing robot system is described. It discusses physical and components of the model robot are used to research climbing simulation and experiment. In this research, a Kondo robot (KHR-3HV) is used as a prototype climbing robot.

Chapter 4 starts with climbing technique analysis. After that, a rudimentary analysis of mechanical structure and kinematics of HC robot is shown. Secondly, a 3D humanoid climbing robot is built and simulated in Matlab-Simscape environment, and next, this model is used to perform statics and dynamics motions as some basic climbing motions

Chapter 5 presents in detail the equilibrium control, and a four limb model is proposed. Also, the strategy to compute valid area to keep balance is described considering the balance condition to perform movement control.

Chapter 6 focuses on a global path planning and local planning algorithm for humanoid robot wall climbing as the initial phase of our development. The first step is to acquire a depth map to extract accurate information about climbing holds on the vertical wall. Secondly, we propose a global planning algorithm for the humanoid robot using data from Kinect. The proposed algorithm ensures

that the climbing robot finds the best route to climb up the wall. Finally, all algorithms are evaluated with a simple practical example for a humanoid climbing robot system, and its effectiveness is demonstrated experimentally in a real environment.

The dissertation ends with conclusions and future works in the chapter 7.

Chapter 2

Literature review

This chapter deals with the history of some humanoid robots developed by a few groups around the world, mainly concentrated in Japan.

2.1 Humanoid Robot Researches

A humanoid robot is a robot that has a human-like shape, though normal people consider robots as humanoid robots because the robot's appearances are described like humans in many fiction books. Humanoid robots can be devised to fulfill tasks, such as working with human tools or to be used for experiments to study human behaviors, such as balancing, walking, running and so on. Overall, humanoid robots comprise all main parts of a human body including head, torso, two arms, and two legs or just a portion of body like upper and lower bodies. Sometimes, the head is equipped with eyes, nose and mouths to simulate facial features.

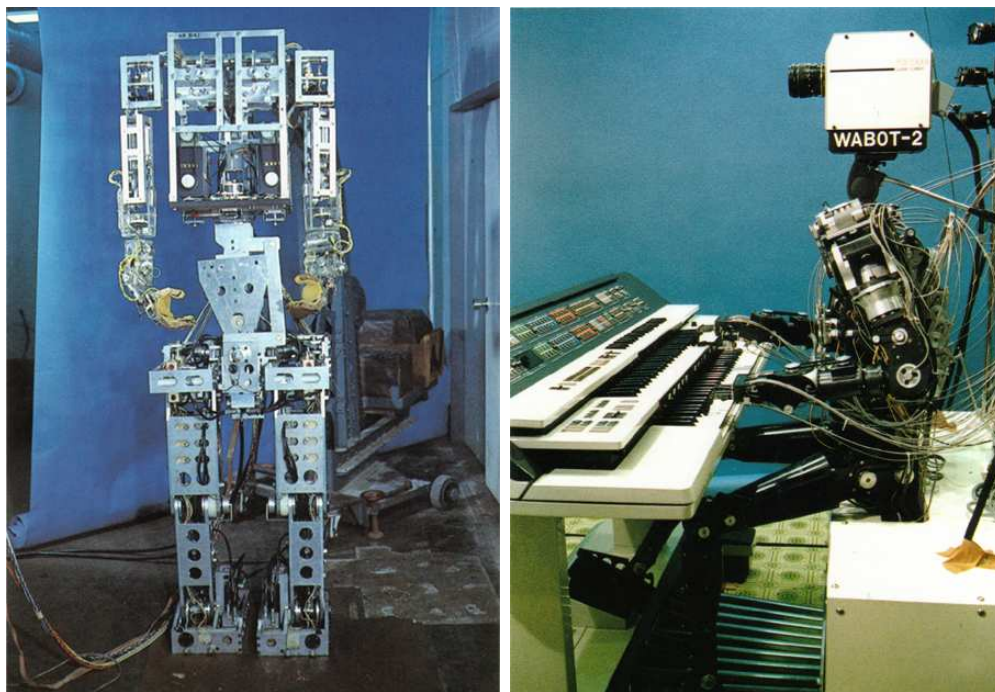
Robotics Researchers have put the humanoid in their goals/objectives from which dream up variety of applications. On the whole, researchers approach humanoid in purely intellectual or practical ways. In the first way, MIT, NASA, ERATO and the ATR groups study artificial intelligence and human manners based on computational scientific methods. On the other hand, people develop a humanoid from which invent practical applications; one of typical examples is

the Humanoid Robotics Project (HRP) of the Ministry of Economy, Trade and Industry (METI). [86]

2.1.1 The Humanoid robot at Waseda University

WABO - Waseda robot

In the dawn of humanoid robots, research groups on the world mainly located in Japan. Ichiro Kato and his colleagues started the WABOT Project in 1970 [2]. Since then, just about ten years, with the state of art technologies, they have developed a diversity of humanoid robots especially the WABOT-1 [36], (see in Figure 2.1(a)).



(a) WABOT-1(1973) [36].

(b) WABOT-2(1984) [85].

Figure 2.1: Humanoid robots from Waseda University

WABOT-1 could perform a lot of human-like behaviors, for instance, perceiving and manipulating the objects by vision and two hands, communicating with people in Japanese, and walking on two legs. The WABOT-1 approximately had

the mental ability like a one-and-half-year-old child. Ichiro Kato's group also developed WABOT-2 in 1984 [85] (see in Figure 2.1(b)). Besides communication ability, the robot musician Wabot-2 could operate more difficult behaviors such as reading and playing electronic organ. The WABOT-2 was also able to accompany a person while he listened to the person singing. WABOT-2 played a piano at Tsukuba Science Expo's85 in Japan. He was the first milestone in developing a "personal robot".

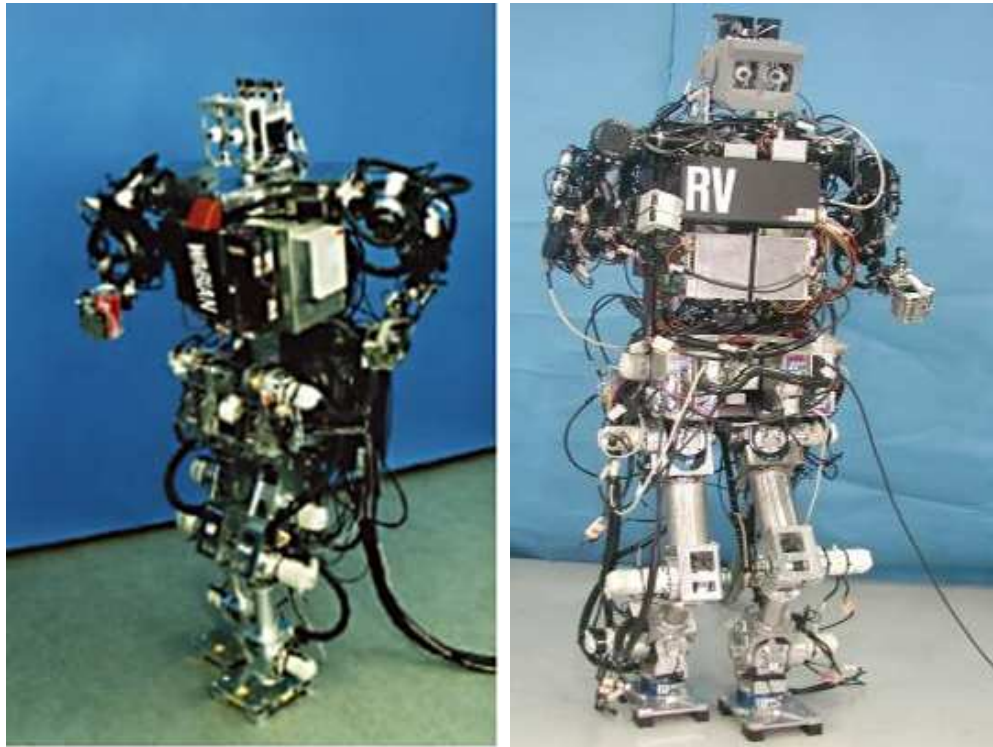
WABIAN - Waseda biped humanoid

In 1996, in purpose of cooperative dynamic walking and co-operate working with humans, a biped humanoid robot called WABIAN was developed with following designs. (1) The biped robot should have the average size of an adult Japanese woman to co-operate with humans in working. (2) The robot could walk at approximate human speed. (3) The robot should have 3 DOF trunk and 6 DOF arm. (4) The joints of the robot should use electric servomotors. (5) A control computer and motor drives except power supply should be installed. WABIAN had a total of thirty-five mechanical DOFs; twelve DOF legs, fourteen DOF arms, a two DOF neck, four DOFs in the eyes and a torso with a three DOF waist. They have carried out a variety kinds of walking such as dynamic forward and backward walking, marching in place, dancing, carrying a load, emotional walking, etc [72] (see in Figure 2.2(a)).

The next version, WABIAN-RV [20] (see in Figure 2.2(b)), WABIAN-RV has a total of forty-three mechanical DOFs and control systems. He could perform different walking motions based on the online pattern generation method boosting environmental adaptability. Moreover, thanks to combining the methods of "generating and teaching macro command by voice command" and a voice recognition system, WABIAN-RV walking motions was generated in both the on-motion-mode and the off-motion-mode.

The Wabian 2R project

The humanoid WABIAN-2R [71], as shown in Figure 2.3 developed by Waseda University, Japan could simulate the walking gait of a human due to a 2-DoF waist mechanism and a passive joint on the foot for bending toe motion, which



(a) WABIAN (1996) [2].

(b) WABIAN-RV(2003) [20].

Figure 2.2: The WABIAN and WABIAN RV humanoid robots

allows it to execute stretched knee walking with heel-contact and toe off motions,. WABIAN-2R has the height of 1.48m and weight of 67.5 kg with batteries. The mechanical framework of WABIAN-2R is mainly made of Aluminum alloy in order to achieve antithetical concepts: light weight, high stiffness and wide movable range.

2.1.2 Honda humanoid robots

In 1986, Honda started a humanoid robots project, then 10 years later they introduced a Honda humanoid robot P2 [1] (see in Figure 2.4(a)), 180 cm height and 210 kg weight, which opening the new era of humanoids. It is the first time in the world, one humanoid robot can walk on biped legs in such a stable way and carry on body a computer and batteries. After that, Honda continued to release

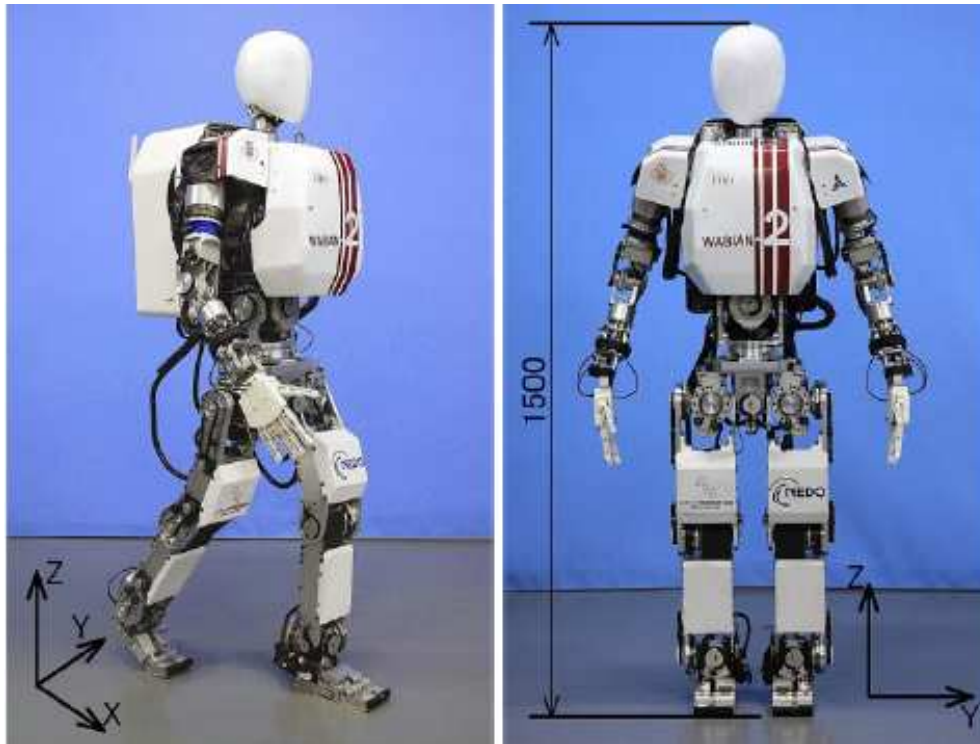
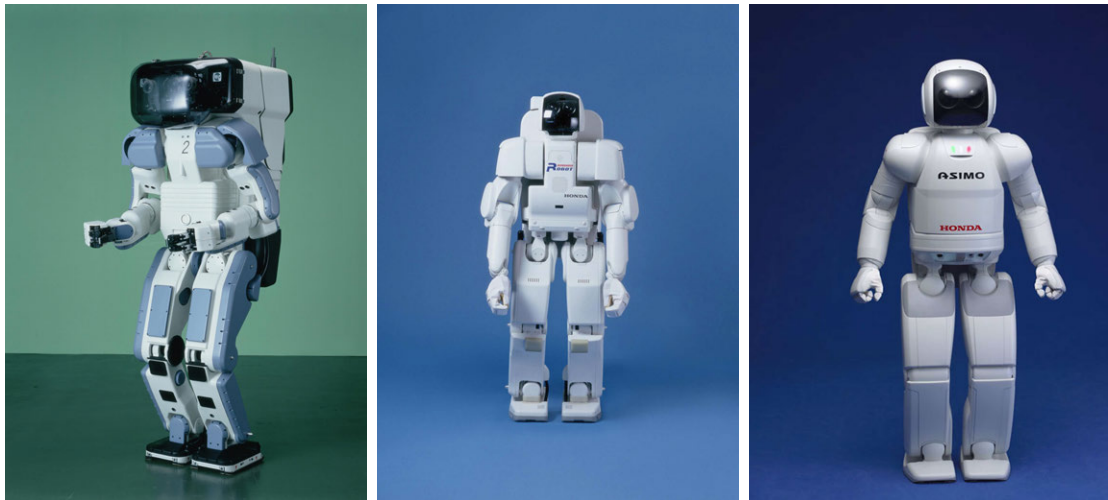


Figure 2.3: The WABIAN 2R humanoid robot [71].

P3 (Figure2.4(b)), 160 cm height and 130 kg weight, in 1997, and ASHIMO (Figure2.4(c)), 120 cm height and 43 kg weight, in 2003.

Most the old humanoid robot used heavy gears with large backlash and mechanical links made by bending or cutting that made robot's structure was not rigid enough, since those robots were mainly manufactured with limited budget mostly from graduate students and small companies. Honda humanoid robots, on other hand, used not only harmonic driver with high torque capacity and no backlash, but also cast mechanical links with high rigidity and light weight with support of most advanced mechanical CAD. Since then, the configuration of Honda humanoid robots became the standard to be compared with for most advanced humanoid robots.



(a) P2 (1996).

(b) P3 (1997).

(c) ASHIMO (2000).

Figure 2.4: These example of free-climbing robots

2.1.3 The HRP project

The Humanoid Robotics Project (HRP) is a project for development of general domestic helper robots, sponsored by Japan's Ministry of Economy , Trade and Industry (METI) and New Energy and Industrial Technology Development Organization (NEDO), spearheaded by Kawada Industries and supported by the National Institute of Advanced Industrial Science and Technology (AIST) and Kawasaki Heavy Industries, Inc. The HRP series also goes by the name Promet.

There are two essential characters of humanoid robots for HRP consisting of abilities to work in the environments for human as it is and to can use tools for human as it is. The first feature is exploited by apply humanoid robots in maintenance jobs of industrial plant such as Humanoid robot HRP-1 [37, 38](see in Figure 2.5(a)) being able to operate the tasks in a modeling industrial plant encompassing stair, ramps and pits. The second feature is utilized by fulfilling a teleoperation system for an industrial vehicle where a human operator controls a humanoid robot to drive an industrial vehicle. In Figure 2.5 (b) a backhoe is driven by humanoid robot HRP-1S [92].

HRP-2 [46] (see in Figure 2.6) is the final robotic platform for the Humanoid

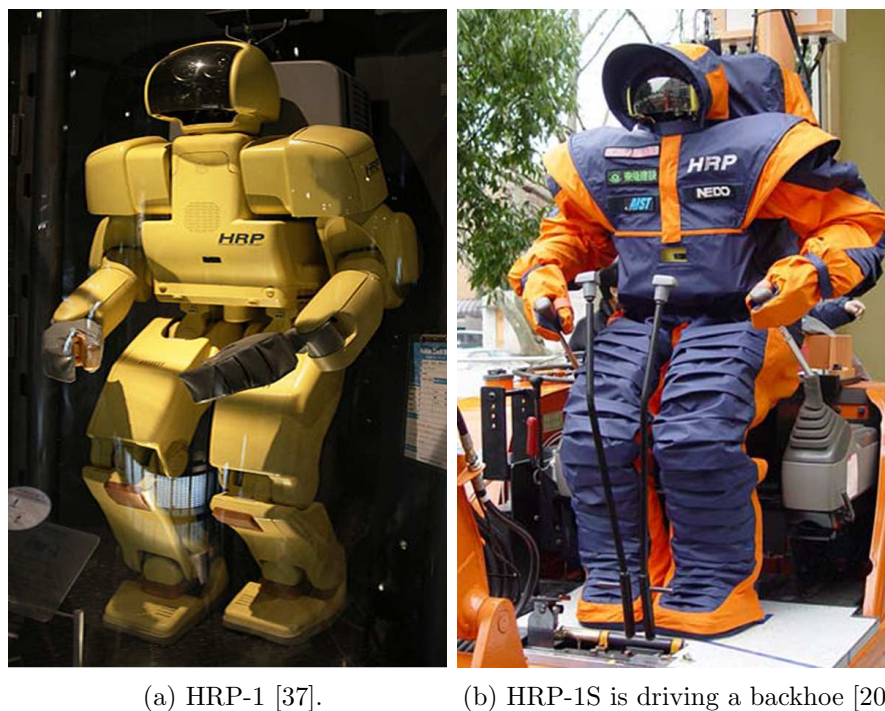


Figure 2.5: The WABIAN and WABIAN RV humanoid robots

Robotics Project headed by the Manufacturing Science and Technology Center (MSTC). Kawada Industries, Inc. together with the Humanoid Research Group of National Institute of Advanced Industrial Science and Technology (AIST) developed whole robotic system. HRP-2s, 154 cm height and 58 kg weight, has 30 degrees of freedom (DOF) including two DOF for its hip, and its highly compact electrical system packing enables it to forsake familiar "backpack" equipped for other normal robots. In addition, it can walk in a circumscribed space.

The next model of HRP-2 is Humanoid Robotics Platform 3, HRP-3 [45], whose the mechanical configuration is the almost same as that of HRP-2, while the number of driven joints is slightly increased (see in Figure 2.6). Thanks to new design of main mechanical and structural components and, HPR-3 can inhibit the penetration of dust or spray. Besides, not only new designs of wrist and hand enhance manipulation, but also the software improves performance in real environment. Two outstanding features of HRP-3 are walking on a low



Figure 2.6: The HRP-2, HRP-3 and HRP-4 humanoid robots.

friction surface like a frozen road, manhole covers with rain water and stable turning during a shower without any troubles.

Slim and lightweight HRP-4 [47] (see in Figure 2.6), 154 cm height and 58 kg weight, has 34 degrees of freedom with 7 degrees of freedom for each arm to facilitate object handling and has a slim. The HRP-4 software system used the software platform OpenRTM-aist and a Linux kernel with the RT-Preempt patch.

2.1.4 Universities and Research Institutes

Waseda University has been one of the main research destinations for humanoid robots since the late Prof. Ichiro Kato and his associates began the WABOT Project in 1970. From that point forward, pretty much ten years, they have built up an assortment of humanoid robots including WABOT-1 which is the first full-scale human-like robot made in 1973, the musical artist robot WABOT-2 in 1984,

and the biped walking robot WABIAN in 1997.

In addition, University of Tokyo presented HRP-2 in 2010 which can deal with objects of obscure weight base on online estimation of the operational force[70]. Also a biped robot with ability to balance - even after being kicked has been researching by a group which is led by professor Masayuki Inaba [87].

Obviously, humanoid robot exploration is not constrained in Japan. For example, we can see HUBO2 by Korea Advantaged Institute of Science and Technology (KAIST)[21], LOLA by Technische Universitat of Muchen (TUM) [55], CHARLI by Virginia Polytechnic Institute and State University [51], BHR-2 by Beijing Institute of Technology [90], iCub by Italian Institute of Technology (IIT), the university of Genoa [63], and TORO by the German Aerospace Center (DLR) [73].

2.1.5 Companies

There also exists many humanoid robot developed by companies. Several of prominent companies will be reviewed in this part. **Honda** Honda's been working on ASIMO robot series for the better part of two decades. The latest ASIMO comes with an amount of physical improvements, counting new legs that'll adapt to uneven landscape, walk rearward and even run at rates of about six miles an hour. At that point there are the overhauled hands, which now have 13 degrees of freedom, allowing the robot to hold and control objects without smashing or dropping them.

Toyota Toyota Motor Corporation presented a trumpet playing humanoid robot at the EXPO 2005. In addition, at the Shanghai World Expo Toyota's famed violin-playing robot excited the swarm of visitor with a performer of Chinese song. **Samsung** A South Korean company Samsung Electronics, has been also developing humanoid robots with the Korean Institute of Science and Technology (KIST). They presented the latest humanoid robot, Robaray, at IROS 2012 in Portugal. This robot can perform natural walking motion compared to the conventional knee bent walkers [52].

Boston Dynamics [3] Boston Dynamics is an engineering and robotics design company that is best known for the development of BigDog, a quadruped robot designed for the U.S. military. In 2012, they develop a humanoid robot PETMAN for testing chemical protection clothing [68]. The bipedal robot weighs about 80kg (180lb) and is nearly six feet tall (1.75m). PETMAN demonstrated a top walking speed of about 4.4mph (7.08km/h), making it the fastest bipedal robot in the world (Honda’s Asimo robot has a top walking speed of 7km/h).

There are numerous sorts of little humanoid robots for interest or examination. These humanoid robots are worked in distinctive stages grew by diverse organizations. Such as, we can choose NAO by Aldebaran Robotics [4], DARwIn-OP by ROBOTIC [5], PALRO by FujitSoft [6], or or KHTI serie by Koudo Kagaku Co. Ltd [7].

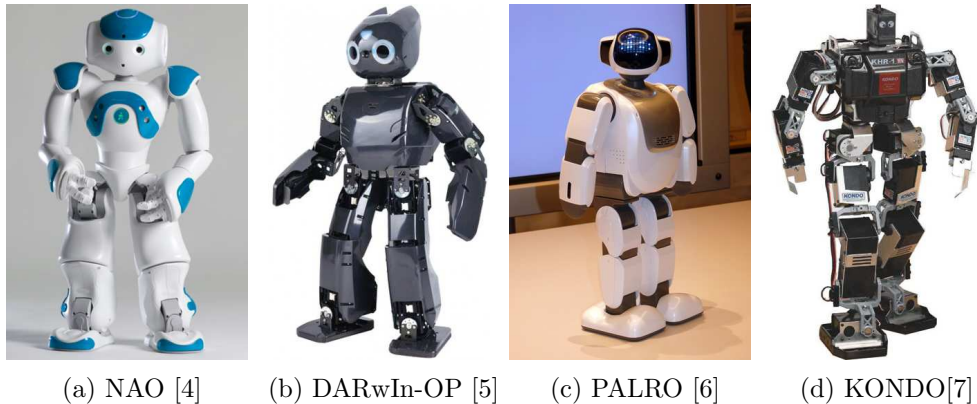
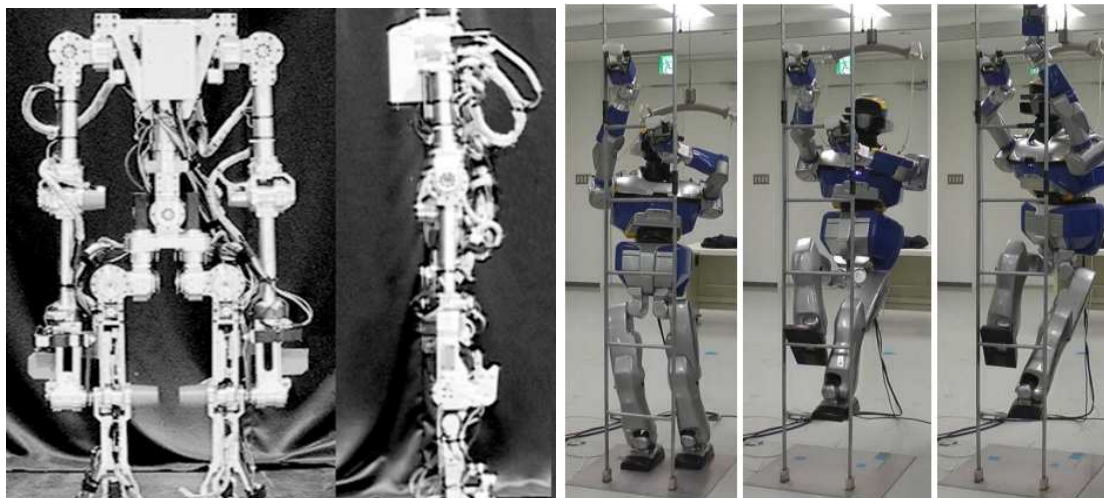


Figure 2.7: Small Humanoid Robots

2.2 Previous Review on Humanoid Climbing Robot

There are a number of humanoid robots that have been recently built throughout the world. The prototypes Gorilla III [57], HRP-2 [69, 88], SCHAFT [8], and DRC-HUBO [58] could climb general ladder and stair-like structures. In [57] Gorilla-type robot (shown in Figure 2.8(a)) was shown to climb a vertical ladder having in mind transitions toward multi-modal locomotion capabilities. They



(a) Gorilla Robot [57].

(b) HRP-2 Robot [88].



(c) Schaft Robot [8].

(d) DRC-HUBO Robot [58].

Figure 2.8: These example of humanoid ladder climbing robots

achieved three different climbing gaits: transverse, pace with constant velocity and trot with acceleration. Motivated by the DARPA Robotics Challenge (DRC) [9], the HRP-2 humanoid robot (Figure 2.8(b)) was integrated multi-contact planner and multi-objective QP control as basic components to can climb vertical industrial norm ladders. In fact, the winning SCHAFT (Figure 2.8(c)) team could

2.2 Previous Review on Humanoid Climbing Robot

climb the DRC ladder without even using its arms. The The DRC-HUBO humanoid robot (Figure 2.8(d)), based on multi-contact planning [97], could climb almost all of it [58].

Chapter 3

Humanoid climbing Robot System Design

This chapter we introduce an overview of my humanoid climbing robot system. This system include a humanoid climbing robot and a climbing wall. The system design requires making trade offs among many factors, such as functional capability and complexity, weight and strength of mechanical parts, weight and power of actuators, cost and performance of sensors, and so on. It is a complicated process that has not a single optimal solution. There is no standard method to comparatively evaluate the end result. The high-level guideline that we used throughout our work is to achieve the functions needed for free-climbing with the simplest possible design.

3.1 Hardware platform

3.1.1 KONDO KHR-3HV

We select KHR-3HV manufactured by Kondo[7] as a prototype to develop humanoid climbing robot. Then, I have implemented my motion planning and motion control on this robot. Since there is no model to be emulated, every part of this project has to be developed. The humanoid robot KHR-3HV is the third

generation of humanoid robots developed by KONDO KAGAKU Co.Ltd. This robot has 22 degrees of freedom (DOF), and two of degrees of freedom of the 22 degrees of freedom have been added in order to enable climbing in the open leg.

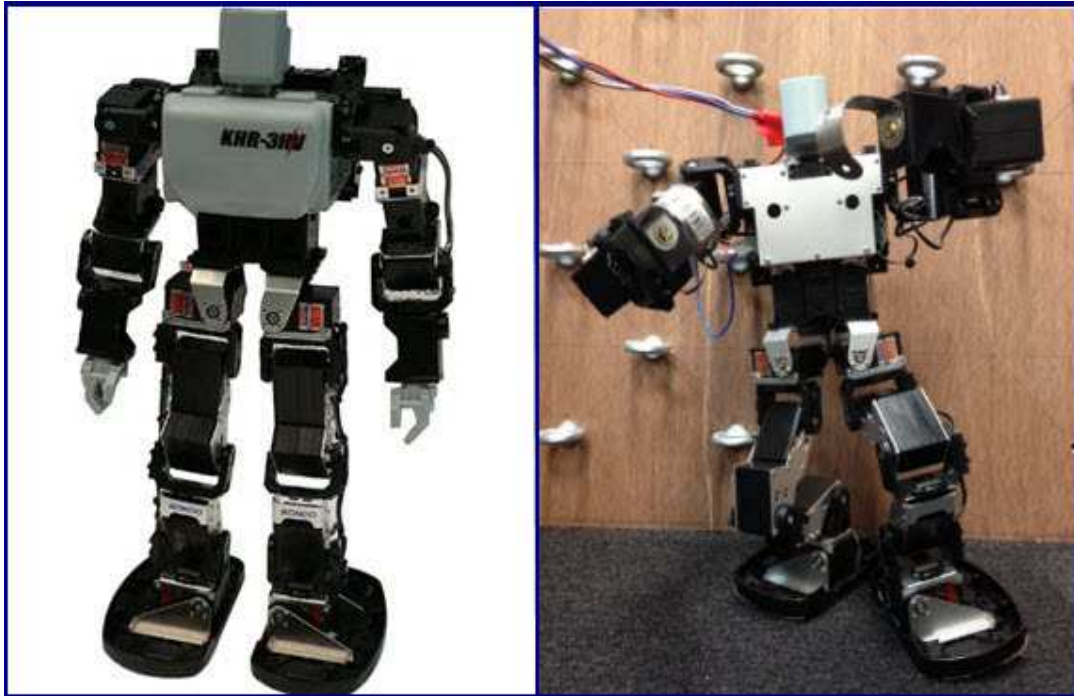


Figure 3.1: Kondo robot and an application of the robot.

3.1.2 Geometric dimensions

The humanoid robot in Figure 3.1 consists of a lot of rigid segments interconnected with joints. The humanoid robot mechanism has 22-DOF. The dimension of the Kondo KHR-3HV robot is presented in Figure 3.2 and Table 3.1

3.1.3 Hardware modification

Although human climbers sometime use their fingers to grip climbing hods, in this research I focus on the basic moves based on simple contacts. I found that at the point when numerous fingers are utilized together, the generalized force will

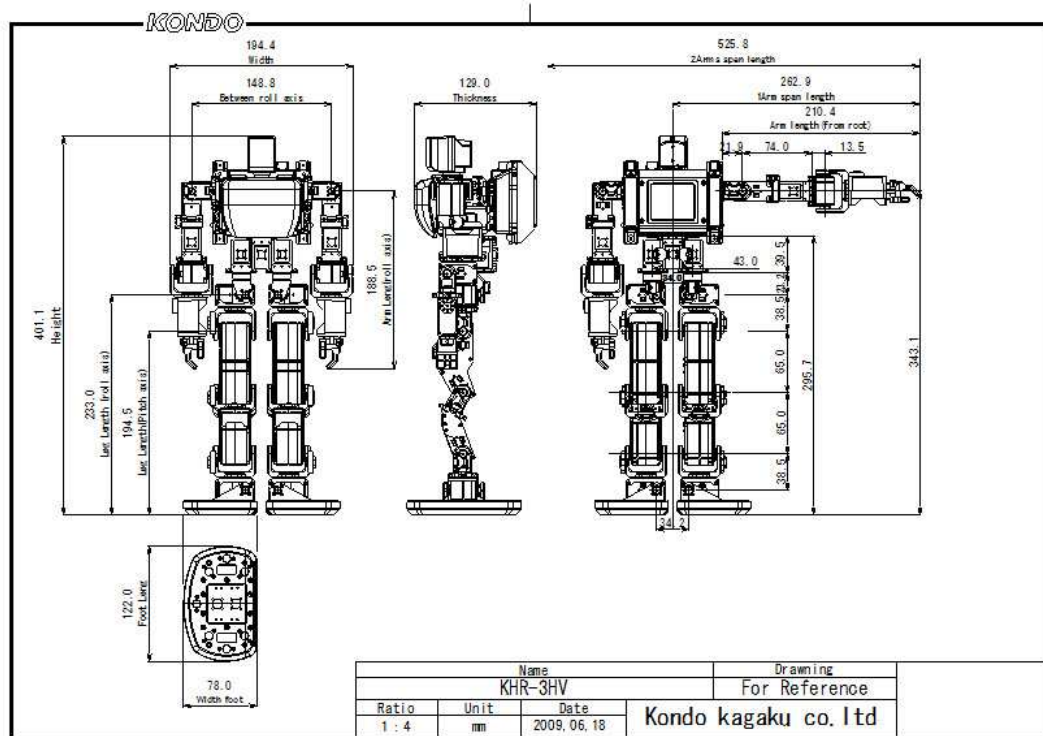


Figure 3.2: Dimension of Kondo KHR-3HV robot

be generated. This force is same with a force which is generated by open hand grip (lock like rigid angle bracket).

The humanoid robot does not have any mechanism to grasp holds, but it comes with an angles bracket as hand. Hence, the only chance to grab holds is obtained by pressing its arms together. To be able to climb, the hands of humanoid robot needs to be modified so the modified hands can hold into grips, hold their positions and pull themselves as shown in Figure 3.3.

3.1.4 Shoulder joints

Each HRC's shoulder joint has an angular range of 0 to 210 degrees.

Table 3.1: Kondo KHR-3HV robot-Body measures

Part name	Length[m]	Mass[kg]
Head	0.035	0.052
Torso	0.148	0.678
Single leg	0.233	0.264
Single arm	0.188	0.126
Whole body	0.401	0.151

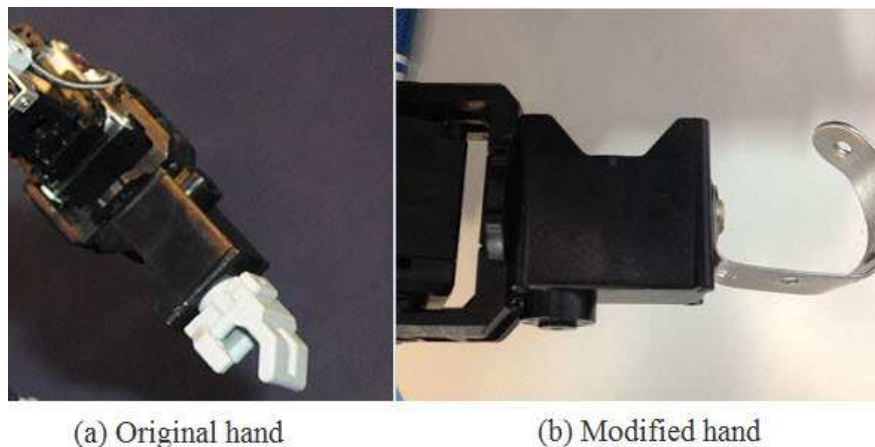


Figure 3.3: The original and modified hand

3.1.5 Elbow joints

Almost free climbing robots have elbow angle from -90 to 90 degrees. There are two limitations in this decision. To start with, the elbow of this sort of robot can't curve past 90 degrees (in any case) and as an outcome the work-space reachable by a hand is restricted to a moderately limited district. This constraint keep robots from accomplishing some essential climbing postures regularly utilized by human climbers, which require folding a climbs almost completely. Furthermore, since the joint has the capacity twist to both sides in respect to its straight design, every appendage has two reverse kinematics arrangements, making control possibly more confounded. Rather, my humanoid robot's elbow point can change between 45 to 245 degrees. This peculiarity expand the work-space area reachable by hands (Will be mentioned in detail in Chapter 5)

Table 3.2: Physical parameters of the KRS-2552HV ICS Servo robot

Physical parameters	value	unit
Maximum Operating Angle	270	°
Maximum torque	14	kg/cm
Maximum speed	0.14	S/60°
Dimension	41 X 21 X 30.5	mm
Weight	41.5	g

3.1.6 Actuators

Kondo KRS-2552HV ICS Red Version Servo Figure 3.4, Tab.3.2

The Kondo KRS-2552HV ICS Servo Motor Red Version was first introduced in KHR 3HV and is compatible with RCB-4HV as well as with the ICS USB Programmer HS (High Speed). The use of a serial protocol allows the connection of several servos in a Daisy chain. By connecting in a Daisy chain the number of cables is reduced and therefore prevents troubles regarding disconnection while improving cable routing.



Figure 3.4: KRS-2552HV ICS servo motor red version

3.2 Control System and Sensors

This section introduces the electronic components which are mounted in body of the humanoid climbing robot. They are separated to 3 parts as the processor part, the sensor part, and the actuator part. The new micro controller board RCB-4 enables the control of up to 35 serial servos. It is compatible with ICS3.0 (serial) servo protocol and a wide range of options parts. The board also includes several extension ports (10x A/D and 10x PIO) which enable use of a wide range of sensors and extension options. KHR 3HV uses KRS-2555HV servos, the first Kondo servo to use ICS 3.0. Use of a serial protocol allows connection of several servos in a Daisy chain. By connecting in a Daisy chain the number of cables are reduced and therefore it prevents troubles regarding disconnection and improves cable routing, and their specifications are written as the followings:

3.2.1 Microprocessor board

Kondo - RCB-4HV Robot Controller is shown in Figure 3.5

Features:

M16C/26A microcomputer by Renesas Technology has been adopted. It contains eight SIO ports for two systems of ICS3.0 compliant device, and it can connects up to sixtyfour ICS3.0 devices. With ten AD ports, multiple analog sensors can now be used. Further, AD input for power management is available separately. Ten PIO ports have been newly mounted. In addition, the microprocessor board also use ON/OFF switch and light up of LED. The COM ports enable a maximum speed of 1.25 Mbps. EEPROM, known for its high-speed and high capacity, has been adopted:

Specifications:

Dimensions: 45 x 35 x 13 (W x H x D) mm. Weight: 12g Interface: SIO port, COM port, AD port, PIO port Power Supply Voltage: Our specific HV power source is recommended. Minimum 6 V, Maximum 15 V. (Does not necessarily guarantee motion of device.) Internal Voltage: Set at 5 V by a regulator (for 1 A). Power Supply Terminal: Use battery or stabilized power supply corresponding to



Figure 3.5: RCB-4HV robot controllers

the above operating voltage. Com port: It is used for data communication by connecting to PC using serial USB adapter HS. Conventional serial USB adapter can also be used. (When using conventional product, communication speed may be limited.) AD port: For connecting analog device. Operating voltage is 0 to 5 V. Check maximum current for device needing power supply. PIO port: For connecting digital binary input/output device. Can be used as an output and operating voltage is 0 V (LOW), 5 V (HIGH). Resistance is connected in series, so LED can be connected directly. However, please check operating voltage for the LED. SIO port: For connecting device corresponding to ICS. Operating voltage is the same as power supply voltage. DO NOT CONNECT device corresponding to 0 to 5 V (such as analog sensors). Operation may be limited according to the corresponding version of the connected device.

3.2.2 Gyro Sensor

Kondo KRG-4 Gyro Sensor Figure 3.6 The KRG-4 gyro sensor detects angular velocity quickly and correctly, helping a stable autonomous function. It is compatible with RCB-3 (KHR-1HV, 2HV and Manoi) and is also compatible with RCB-4 (KHR-3HV). We get two of these for your robot to assist in Forward as well as Side Stabilization simultaneously.



Figure 3.6: KRG-4 gyro sensor

3.3 Climbing Wall

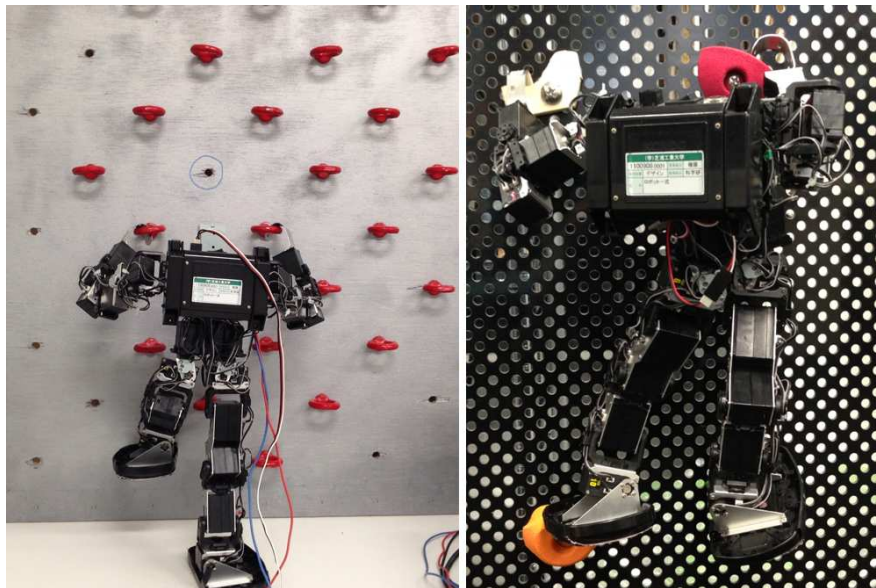


Figure 3.7: Humanoid climbing robot on the wall: the first type of hold is a small ring (left), and the second type is a climbing hold(right)

Two climbing walls used in our experiments is a vertical planar board with artificial terrain holds mounted on it (Figure 3.7). We consider two type of holds. The first type is a small ring (see in Figure 3.7(left)) and the second type is same with holds which often are used in climbing gym clubs (see in Figure3.7(right)). Each hold can easily be mounted any where on the board with any orientation. By selecting and distributing such holds differently on the climbing wall, terrains with various levels of difficulty can be created to perform climbing experiments (Chapter 5 and Chapter 6).

Chapter 4

Humanoid Climbing Robot Modeling

This research is undertaken to improve technologies that enable the design and implementation of a humanoid robot able to climb vertical natural terrain. Humanoid climbing robot (HC Robot) is designed to climb up a climbing wall totally autonomously, and it is expected to be useful to rescue in disaster area. It seems more difficult to analyze the dynamic character of humanoid climbing robot because of the complexity of mathematical description. Therefore, this chapter starts with climbing technique analysis. After that, a rudimentary analysis of mechanical structure and kinematics of HC robot is shown. Secondly, a 3D humanoid climbing robot is built and simulated in Matlab-Simscape environment, and next, this model is used to perform statics and dynamics motions as some basic climbing motions.

4.1 Introduction

Nowadays, engineers are, more and more, supported from software in the designing, manufacturing process. The benefits of using the software are to reduce time, early find errors, and decrease cost [83]. SolidWorks, Inventor, Pro/Engineer, etc., are the strong Computer Aided software in terms of designing, simulating and

preparing for manufacturing process, whereas to physically model and simulate the operation of the system, we also have many choices such as: Matlab/Simulink, MapleSim, Vizard, Robotic studio and so forth. In this study, we take advantage of the strong points of 3D modSoftware as well as physical modeling software to simulate the humanoid climbing robot.

D.Le, H.Kang and Y.Ro [24], C.Yun, C.Rong and S.Jian [93] and J.Liu, G.Chen, Y.Gong and H.Chen [54] showed two ways to establish the SimMechanics diagram: the first one is through converting the model from 3D software to XML file and the other way is by building the model directly in the Simscape environment. The first method (SimMechanics first generation) is faster, more convenient than the second one; however, the disadvantage of these models are that they were built in Simulink platform with dimensionless Simulink signals and it is difficult to pan, zoom or rotate the models during simulation. In the second method, it takes quite lot of time and labor to build the 3D model, however after that we will have physical signal model and have better performance of simulation.

The new version of Matlab R2012b supports for code generation and import of CAD models through second generation in SimMechanics. As a result, it overcomes the drawbacks of the first method and takes advantage of the second one that is mentioned above. In this paper the process of using SimMechanics second generation of Simscape platform to convert the humanoid climbing robot from 3D Solidworks environment was shown. After that simple PID controller for the system was applied to control the 3D model perform some basic climbing motions.

4.2 Climbing Technique

Free climbing and bouldering have been recognized as fascinating sports[14, 81]. Then many climbing gyms are opened. It is not only fun but tells us some important clues to understand human body nature. On the other hand, climb technique is useful to move to desired place in uneven dangerous terrain. If

practical climbing robots are developed, it seems to be very convenient and safe for us. The reason that we use type of humanoid is that the conventional climbing technique and knowledge can be made use of to robots without the change of structure.

To perform the above object, climbing technique and structure of humanoid robots should be analyzed theoretically. However, it is not easy to develop high-quality climbing robots in short period. Therefore, this paper starts the explanation of the analysis using the simplest model.

4.2.1 Climbing Technique with The Simplest Model of Climbing



(a) Face climbing.

(b) Abseil

Figure 4.1: Climbing motion at a natural wall

Climbing walls are categorized into natural walls and artificial walls, but the

principle of climbing technique is equal to each other. As shown in Figure 4.1, the climber uses his four limbs. The soles of his shoes can be watched because his toes support his body weight on tiny foot-holds. Generally, Hand-holds and foot-holds are often tiny, so climber needs to master special technique to keep his balance and to move up his body.

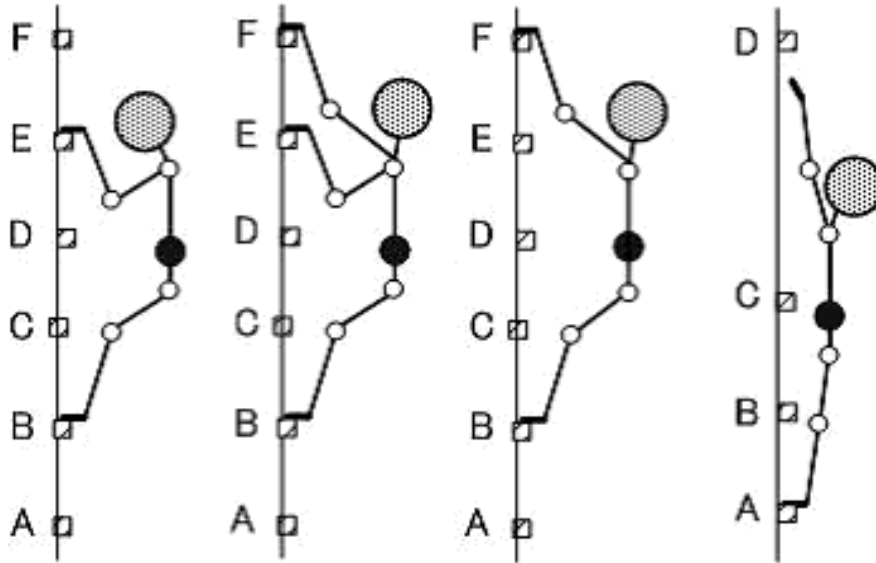


Figure 4.2: Simplest Humanoid Climbing Robot

Basic climbing motion is called ladder climbing because it is similar to real ladder climbing. Figure 4.2 illustrates the image of ladder climbing. It is natural that climber cannot move up when he cannot reach the next hold.

The first priority for climbing is to keep the body still by proper distribution of power. The principle of the distribution is given by $\Sigma \mathbf{f}_i = 0, \Sigma \mathbf{n}_i = \Sigma \mathbf{p}_i \times \mathbf{f}_i$. Where $\Sigma \mathbf{f}_i$ is a supporting force vector acting at end-effector i . And \mathbf{p}_i is a position vector denoting the position of end-effector i .

Figure 4.3 illustrates an example using the simplest model of climbing. The climber is expressed by a mass and two sticks. The upper stick simplifies the arms and the lower stick simplifies the legs in two dimensional representation space. The arrows represent forces to the climber. The corresponding forces and

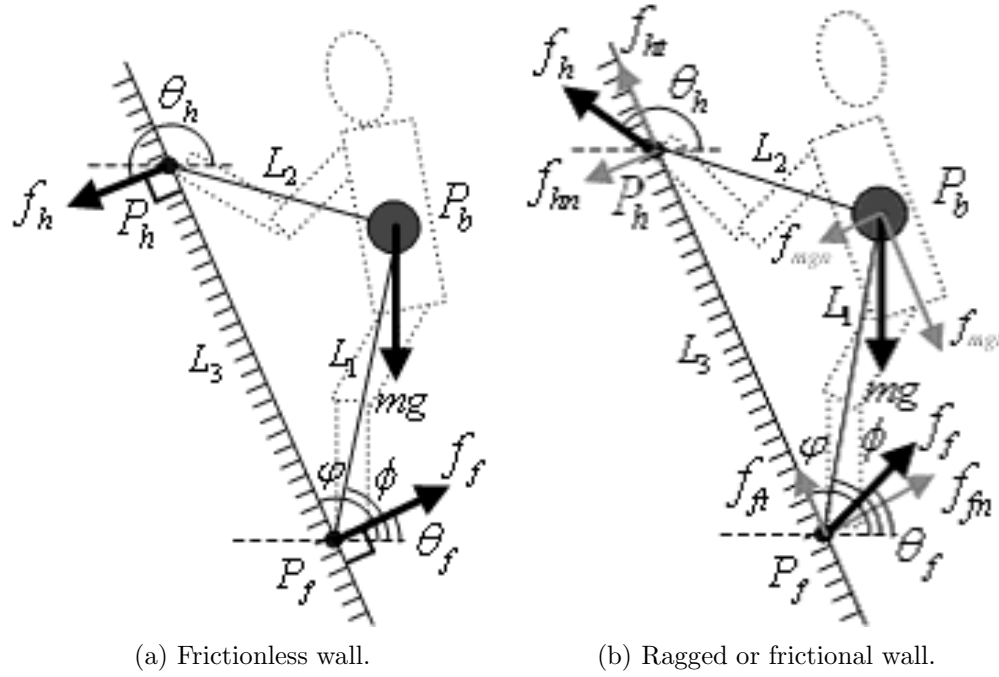


Figure 4.3: Equilibrium forces between climber and wall

moment equilibriums are expressed as

$$f_h \cos \theta_h + f_f \cos \theta_f = 0 \quad (4.1)$$

$$f_h \sin \theta_h + f_f \sin \theta_f - mg = 0 \quad (4.2)$$

$$(x_h f_h \sin \theta_h - y_h f_h \cos \theta_h) - mg L_1 \sin \phi = 0 \quad (4.3)$$

Where f_h denote the force vector to hand. f_h denotes the absolute value of the force f_h . f_f denotes the force vector to the foot. f_f denotes the absolute value of the force f_f . Furthermore, $x_h = L_3 \cos \phi$, $y_h = L_3 \sin \phi$. Such the forces are generated by climber as the reaction forces.

Figure 4.3 (a) shows a climber and pure normal forces. In this case, the shape of hand hold should be bracket shown in Figure 4.4 (b). Other types of shape shown in Figure 4.4 (a),(c),and (d) are not available. On the other hand, for the foot hold, variety of shapes shown in Figure 4.4 is available.

As the next Figure 4.3 (b), the possibility of the equilibrium should be ex-

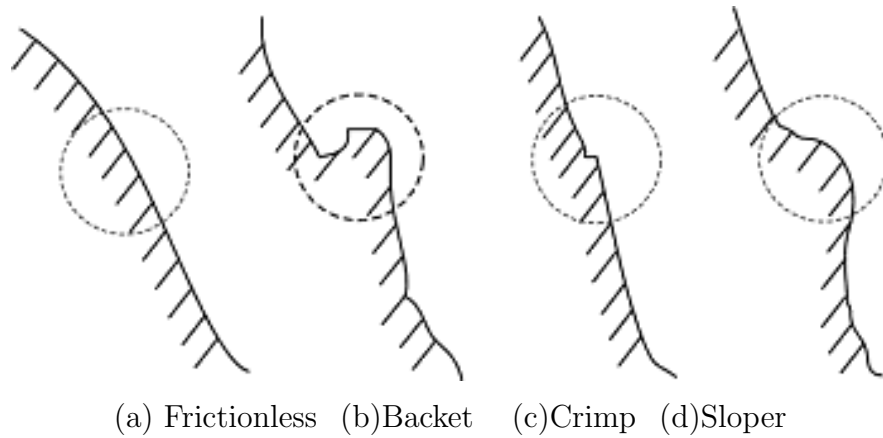


Figure 4.4: Typical holds for climbing

plored. When the direction of \mathbf{f}_h or \mathbf{f}_f is not orthogonal to the climbing wall respectively. \mathbf{f}_h and \mathbf{f}_f can be divided into normal and tangential components, \mathbf{f}_{hn} and \mathbf{f}_{ht} , \mathbf{f}_{fn} and \mathbf{f}_{ft} respectively. In this case, the possibility of keeping the

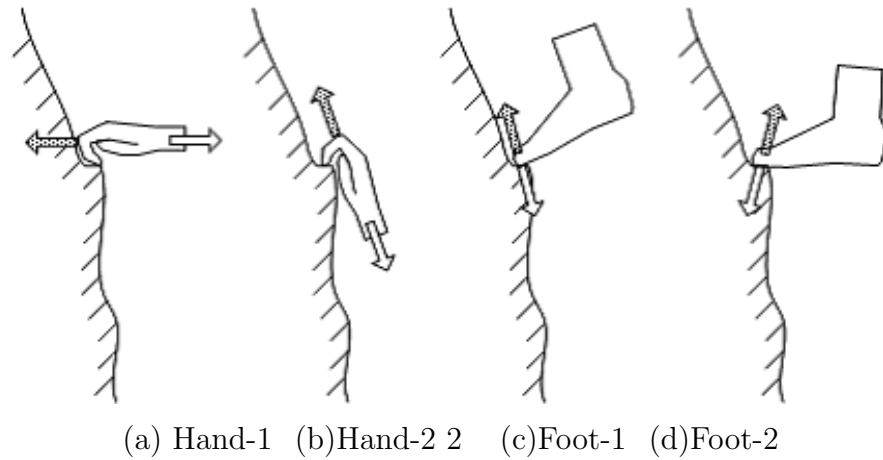


Figure 4.5: Appropriate force with the different shape of holds

weight of body depends upon the shape of holds and climbers technique. The technique means performance of appropriate force and moment generation vectors to keep the balance. Moreover, the ability to keep balance is also swayed the shape of holds that shown in the Figure 4.5. The white arrows denote forces generated by climber. The hatching arrows denote reaction forces against the above forces, which act on the climbers body to keep balance. It is obvious that

the pattern Figure 4.5 (a),(c) are impossible to keep balance, (b),(d) are possible.

4.2.2 Climbing Technical for my Humanoid Climbing Robot

With only bracket hands to make contact with the terrain, the humanoid climbing robot needs at least three simultaneous contacts in order to maintain static equilibrium. Hence, at least four limbs are required, to allow one limb to move to a new hold, while the other three maintain balance.

The robot as more DOFs would have had to be coordinated to avoid self-collision among limbs (hands and feet).

In general, a human climber tries to keep her body as close as possible to the terrain, in order to reduce the magnitude of the forces that must be exerted at the contacts to maintain balance. The same is also true for a climbing robot. Therefore, our motion planning and motion control aim at keeping the center of mass of the robot as close to the climbing terrain as possible

4.3 Humanoid Climbing Robot: Kinematics

The theory to analyze the relationship between the position and attitude of a link and the joint angles of a mechanism is called Kinematics. It is the basic on which robotics is formed, but the exact same theory is used for computer graphics as well. Both require mathematics and algorithm which can clearly represent a moving object in 3D space.

A humanoid robot is a multi-jointed mechanism that mechanically emulates a humans functions, movements and activities. It can be considered as a biped robot with an upper main body, linking two arms, a neck and a head, or as a combination of multiple manipulators, which are themselves linked together through waist and neck joint to emulate a human's functions. Because of its human-like, bipedal movement, the kinematic structure of a humanoid robot has no fixed

route node and has a large number of degree-of-freedom (DOF). Since the robot servo system requires the reference inputs to be in joint coordinates and a task is generally stated in the Cartesian coordinate system, controlling the position and orientation of the end point of a limb (an arm or a leg) of a humanoid robot requires the understanding of the kinematics and inverse kinematic joint solution of a humanoid robot. Kinematics is the formulation of a model as a set of differential equations for robot motion, with joint forces/torques as inputs. Such models are useful in simulations and dynamic evaluations of robots. Inverse-kinematics is concerned to express joints motion in terms of end-effector motion, which is in general more complex. The inverse problem in robot dynamics is directly applicable to computed-torque control (also known as feed forward control), and also somewhat indirectly to the nonlinear feedback control method employed.

4.3.1 Definition of coordinate frames

Generally, kinematics for humanoid robots is often used to describe relationship between the joint angles of the arms and legs and the resulting robot position and orientation. Especially, the kinematics is used to calculate configuration of end-effectors (i.e. hands or feet of robots) from coordinate frames of focus which may be on base or adjacent links of the target robot.

Table 4.1: Degree of freedom of a Kondo KHR-3V robot

Head	Waist	Hand	Leg	Total
1/Neck	1/Waist	2/Shoulder	3/Hip	
		1/Elbow	1/Knee	
		2/Wrist	2/Ankle	
1 DOF	1 DOF	8 DOF	12 DOF	22 DOF

In our study, a Kondo robot (see Figure 4.6 (a) and Table.4.1) is used as a prototype climbing robot. We first define the base coordinate frame ΣO at the

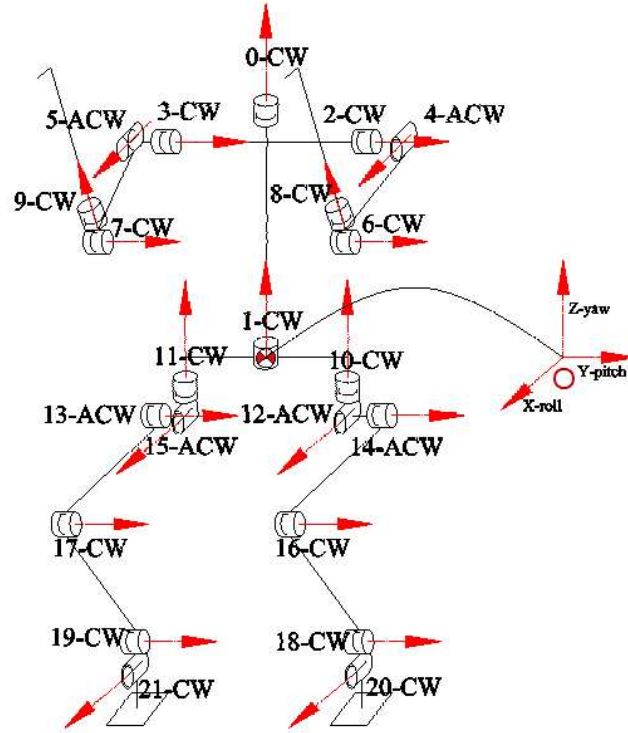


Figure 4.6: Base coordinate frame "O"

center of body of the robot. The ΣO is also used as a reference coordinate frame of hands and legs. Since the general kinematic structure of the left hand/leg is identical to those of the right hand/leg, we assign identical coordinate frames to the left and right limbs. In fact, there is no difference when two-dimensional analysis is performed.

Figure 4.7 shows the left lateral view of the prototype robot and the assigned coordinate frames corresponding arm and leg. The pose of the robot simulates climbing motion. As mentioned above, forward and inverse kinematics of the robot should be analyzed in order to perform desired climbing pose in Figure 4.7. Based on the defined coordinate frames, classically, the forward kinematics map can be derived by composing the rigid motions due to the individual joints.

Then, products of exponential formulas are utilized to calculate position and orientation of the end-effectors equivalent to the limb [79]. Combining the individual joint motions, the forward kinematic map is defined as $g_{ot}:Q \rightarrow SE(3)$ [79].

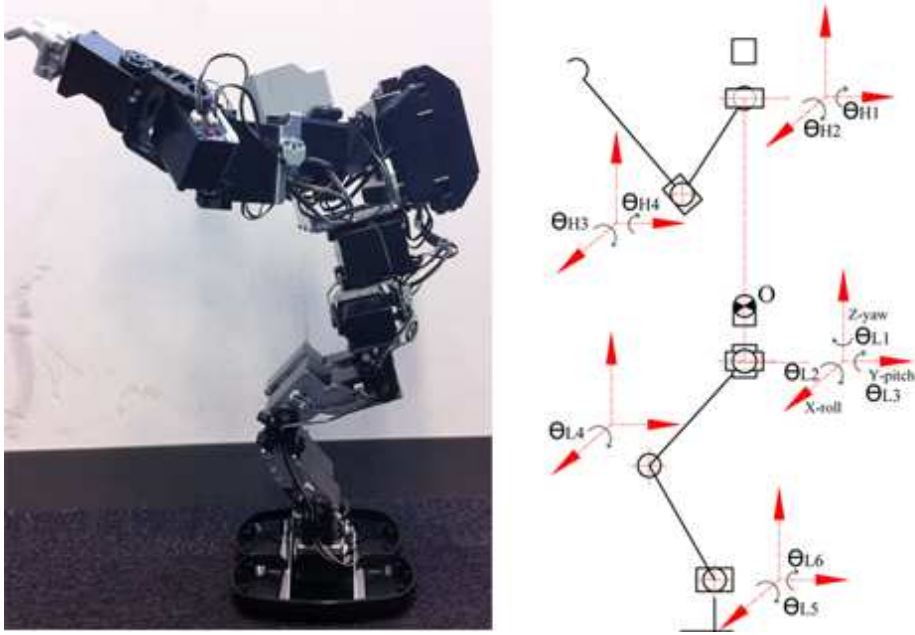


Figure 4.7: Link coordinate frames of the Left Hand/Leg

Where the suffix 'o' denotes the coordinate frame ΣO , and the suffix 't' denotes any terminal coordinate frame Σt .

Now, let us define the configuration, twists, parameters and variables that should be used for solving the robot kinematics. The right hand and leg kinematics are solved; the left ones should be solved in the same way.

Let's consider the coordinate of the hand of robot shown in Figure 4.7, it consists of four revolute joints. The forward kinematics map of the right hand of the robot is given as

$g_{Hst}(0)$: Initial manipulator configuration (right hand)

$g_{Hst}(\theta)$: Goal manipulator configuration (right hand)

$g_{Lst}(0)$: Initial manipulator configuration (right leg)

$g_{Lst}(\theta)$: Goal manipulator configuration (right leg)

θ_{H1} to θ_{H4} . Where $g_{Hst}(\theta), g_{Lst}(\theta) \in SE(3)$

$$g_{Hst}(\theta) = e^{\hat{\xi}_1 \theta_{H1}} \cdot e^{\hat{\xi}_2 \theta_{H2}} \cdot e^{\hat{\xi}_3 \theta_{H3}} \cdot e^{\hat{\xi}_4 \theta_{H4}} \cdot g_{Hst}(0) \quad (4.4)$$

Where $\xi := (v, w) \in \mathbb{R}^6$ represent twist coordinate for the twist $\hat{\xi} \in se(3)$.

And $e^{\widehat{\xi}\theta}$ is the matrix exponential of the 4x4 matrix $\widehat{\xi}\theta$. Thus, $e^{\widehat{\xi}\theta} \in SE(3)$.

As the same manner, the kinematics of the leg can be considered shown in the same figure. It consists of six revolute joints. The forward kinematics map of the right leg of the robot is expressed as

$$g_{Lst}(\theta) = e^{\widehat{\xi}_1\theta_{L1}} \cdot e^{\widehat{\xi}_2\theta_{L2}} \cdot e^{\widehat{\xi}_3\theta_{L3}} \cdot e^{\widehat{\xi}_4\theta_{L4}} \cdot e^{\widehat{\xi}_5\theta_{L5}} \cdot e^{\widehat{\xi}_6\theta_{L6}} g_{Lst}(0) \quad (4.5)$$

They are basically the same as normal robotic kinematics, so these equations can be also used to calculate the corresponding inverse kinematics calculation.

4.3.2 Inverse kinematics of Humanoid climbing robots

When we execute some climbing process, inverse kinematics equations should be derived. Furthermore, the degrees of freedom should be managed in an intelligent way to overcome the problem of kinematic redundancy and to obtain a unique solution. Because some of humanoid robots have redundant degrees of freedom. Negatively, some humanoid robots may not have enough degrees of freedom for climbing walls.

To achieve any desired climbing motion, one-step motion should be done by making use of the corresponding inverse kinematics, which needs to be transferred into a motion sequence, so called motion macro. The motion macro is a kind of simple sequence consisting of "hook into hold", "place foot onto hold" effecting one kinematic chain or more complex motions to keep balance or to move upwards affecting every single joint of the robot.

The hold configuration on real climbing wall is a desired configuration $g_d \in SE(3)$, we need to solve the following equation

$$g_{oh}(\theta) = g_d \quad (4.6)$$

4.3.2.1 Inverse kinematic for the hands

Figure 4.8 illustrates a kind of four degrees of freedom manipulator and we can use a method originally by Paden[76] and built on the unpublished work of

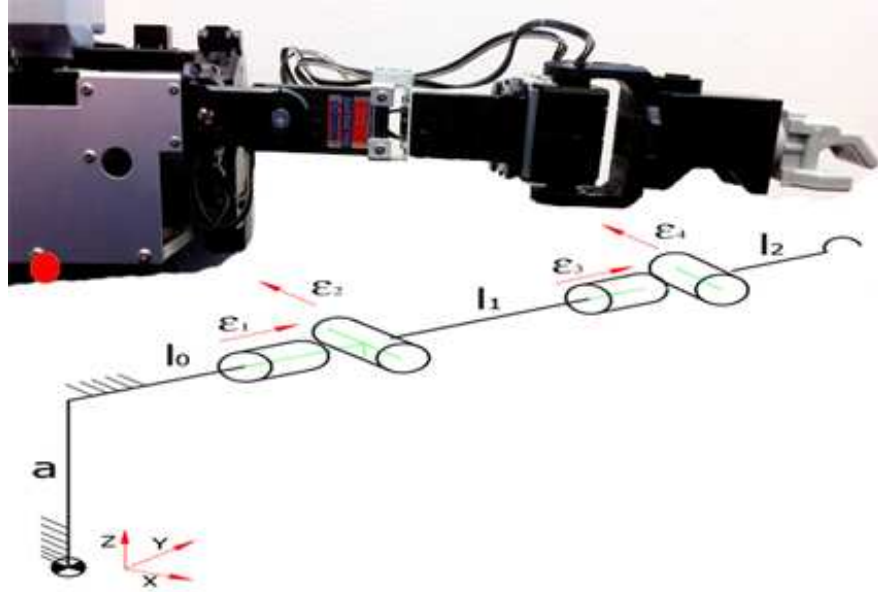


Figure 4.8: Left hand is initial position

Kahan[44] in order to solve

$$g_{oh}(\theta) = e^{\hat{\xi}_1 \theta_{H1}} \cdot e^{\hat{\xi}_2 \theta_{H2}} \cdot e^{\hat{\xi}_3 \theta_{H3}} \cdot e^{\hat{\xi}_4 \theta_{H4}} \cdot g_{oh}(0) = g_{Hd} \quad (4.7)$$

where g_{Hd} is given by the forward kinematic and $g_{oh}(0)$ represents the initial configuration of the left hand robot(see in Figure 4.8). Post multiplying this equation by $g_{oh}^{-1}(0)$

$$e^{\hat{\xi}_1 \theta_{H1}} \cdot e^{\hat{\xi}_2 \theta_{H2}} \cdot e^{\hat{\xi}_3 \theta_{H3}} \cdot e^{\hat{\xi}_4 \theta_{H4}} = g_{Hd} \cdot g_{oh}^{-1}(0) = g_1 \quad (4.8)$$

We determine the requisite joint angles in two steps[79]

Step1 (Solve for θ_1 and θ_2). Apply both sides of equation (4.8) to a point $p \in R^3$ which is the common point of intersection for ξ_4 and ξ_5 . Since $\exp(\hat{\xi}\theta)p = p$ if p is on the axis of ξ , this yields

$$e^{\hat{\xi}_1 \theta_{H1}} \cdot e^{\hat{\xi}_2 \theta_{H2}} \cdot p = g_1 \cdot p \quad (4.9)$$

Applying Subproblem 2 gives the values of θ_{H1} and θ_{H2}

Step2 (Solve for θ_3 and θ_4) The equation (4.8) can be written as

$$e^{\hat{\xi}_3\theta_{H3}} \cdot e^{\hat{\xi}_4\theta_{H4}} = e^{-\hat{\xi}_2\theta_{H2}} \cdot e^{-\hat{\xi}_1\theta_{H1}} g_1 \quad (4.10)$$

Applying Subproblem 2 gives the values of θ_{H3} and θ_{H4}

4.3.2.2 Inverse kinematic for the legs

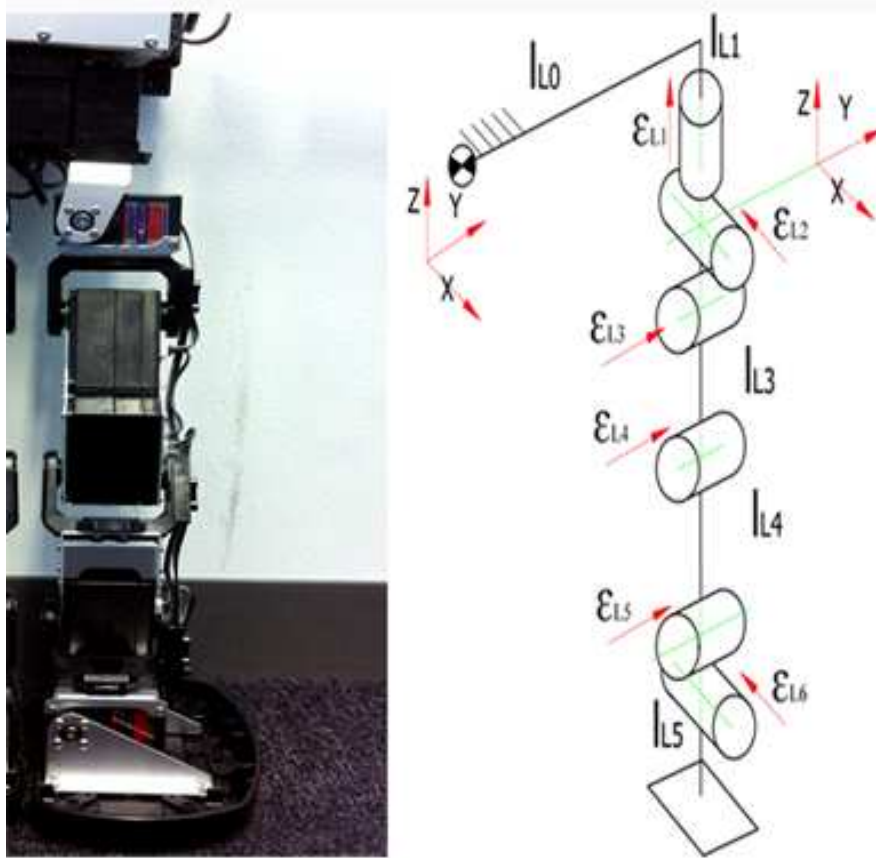


Figure 4.9: Left leg is initial position

Figure 4.9 shows the left leg and the leg consists of four degrees of freedoms joints and the inverse kinematics solution is similar to the inverse kinematics on

the left hand. The corresponding equation is expressed as

$$g_{ol}(\theta) = e^{\widehat{\xi_{L1}\theta_{L1}}} \cdot e^{\widehat{\xi_{L2}\theta_{L2}}} e^{\widehat{\xi_{L3}\theta_{L3}}} e^{\widehat{\xi_{L4}\theta_{L4}}} e^{\widehat{\xi_{L5}\theta_{L5}}} e^{\widehat{\xi_{L6}\theta_{L6}}} \cdot g_{ol}(0) = g_{Ld} \quad (4.11)$$

where g_{Ld} is given by the forward kinematics and $g_{ol}(0)$ represents the initial configuration of the left leg of the robot. Post multiplying this equation by $g_{ol}^{-1}(0)$,

$$e^{\widehat{\xi_{L1}\theta_{L1}}} \cdot e^{\widehat{\xi_{L2}\theta_{L2}}} e^{\widehat{\xi_{L3}\theta_{L3}}} e^{\widehat{\xi_{L4}\theta_{L4}}} e^{\widehat{\xi_{L5}\theta_{L5}}} e^{\widehat{\xi_{L6}\theta_{L6}}} = g_{Ld} \cdot g_{ol}^{-1}(0) = g_2 \quad (4.12)$$

We determine the requisite joint angles in three steps.

Step1 (solve for θ_{L4}) Apply both sides of equation (4.12) to a point $p \in R^3$ which is the common point of intersection of axis ξ_{L4} and ξ_{L5} , this yields

$$e^{\widehat{\xi_{L1}\theta_{L1}}} \cdot e^{\widehat{\xi_{L2}\theta_{L2}}} e^{\widehat{\xi_{L3}\theta_{L3}}} e^{\widehat{\xi_{L4}\theta_{L4}}} \cdot q = g_2 \cdot q \quad (4.13)$$

Subtract from both sides of equation (4.13) to a point $s \in R^3$ which is the common point of intersection of axis ξ_{L1} , axis ξ_{L2} and axis ξ_{L3} , this yields

$$e^{\widehat{\xi_{L1}\theta_{L1}}} \cdot e^{\widehat{\xi_{L2}\theta_{L2}}} e^{\widehat{\xi_{L3}\theta_{L3}}} (e^{\widehat{\xi_{L4}\theta_{L4}}} \cdot q - s) = g_2 \cdot q - s \quad (4.14)$$

Take the magnitude of equation (4.14)

$$\|e^{\widehat{\xi_{L4}\theta_{L4}}} \cdot q - s\| = \|g_2 \cdot q - s\| \quad (4.15)$$

This equation is in the form required for Subproblem 3[79]. Applying Subproblem 3, we solve θ_{L4}

Step2 (Solve for θ_{L1}, θ_{L2} and θ_{L3}) The equation (4.8) can be written as We apply both sides of equation (4.13) to a point $r \in R^3$ which is the common point of axis ξ_{L3} and does not belong axis ξ_{L1} or axis ξ_{L2} , this gives

$$e^{\widehat{\xi_{L1}\theta_{L1}}} \cdot e^{\widehat{\xi_{L2}\theta_{L2}}} \cdot r = e^{-\widehat{\xi_{L4}\theta_{L4}}} \cdot q^{-1} \cdot g_2 \cdot q \cdot r \quad (4.16)$$

Since θ_{L4} is know, we apply Subproblem 2 gives the values of θ_{L1} and θ_{L2} . After that we substitute θ_{L1} and θ_{L2} in the equation (4.13) to find θ_{L3}

Step3 (Solve for θ_{L5} and θ_{L6}) Since are know, we substitute them in the equation (4.12) and Applying Subproblem 2 to find θ_{L5} and θ_{L6}

4.3.3 The stability analysis of humanoid climbing robot

When the humanoid climbing robot climbs a steep slope or a climbing wall, the robot locomotion like quadruped walking. In this case, the Zero-Moment Point (ZMP) to confirm the stability must be considered. However, ZMP is not related to the stability of vertical ladder climbing because the COG is always out from the supporting polygon of soles. Therefore we remark the principles of Newtonian mechanics in order to understand how the vertical and the horizontal forces were distributed on the holds.

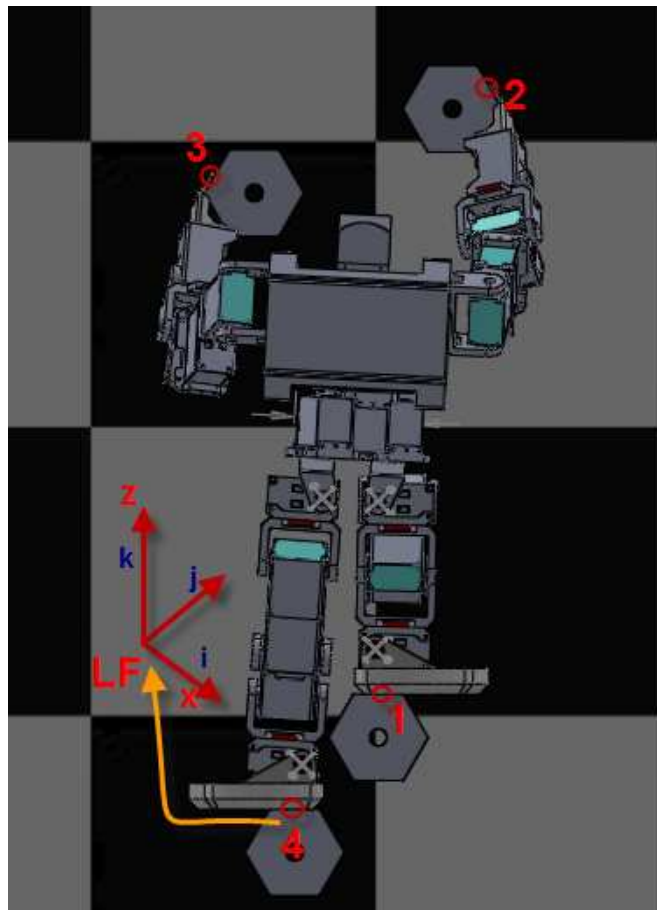


Figure 4.10: The three components of the force applied to each hold are recorded with respect to the reference system (LF, i, j, k)

In a climbing frame as presented in Figure4.10 the climbing holds was num-

bered from 1 to 4 (1=RF hold, 2=RH hold, 3=LH hold and 4=LF hold). The location of LF corresponded to the central area of the left foot hold. These numbers were used when writing general equations governing the movement of the climber. The motion of the humanoid climbing robot was defined by two general equations governing the translation and the rotation in the reference system.

$$\begin{cases} \sum F = ma \\ \sum M = I\alpha \end{cases} \quad (4.17)$$

The sum of all the supporting forces ($\sum F$) acting on the center of mass equals the product of the mass (m) of the climber by its linear acceleration (a). The sum of the moment reactions ($\sum M$) about the left foot hold equals the product of the moment of inertia (I) of the climber by its angular acceleration (α).

It was assumed that the hands and the feet did not exert a torque on the holds. The projection of equation 4.17 along each axis gives:

$$\begin{cases} \sum_1^4 F_i x = ma_x \\ \sum_1^4 F_i y = ma_y \\ \sum_1^4 F_i z - W_k = ma_z \end{cases} \quad (4.18)$$

$$\begin{cases} M(\sum_1^4 F_i z/LF + \sum_1^4 F_i y/LF) \\ + M(W_z/LF) = M_x \\ M(\sum_1^4 F_i z/LF + \sum_1^4 F_i x/LF) \\ + M(W_z/LF) = M_y \\ M(\sum_1^4 F_i x/LF + \sum_1^4 F_i y/LF) = M_z \end{cases} \quad (4.19)$$

\sum_1^4 represented the sum of forces applied to four holds. W_z is the body's weight. During the humanoid climbing robot stable state, the sum of the moment reactions about the left foot hold was equal zero. It means that $M_x = M_y = M_z = 0$. Therefore the expansion of equation (4.17) along pitch, and roll axes leads to the scalar equations to solve initial coordinates of the center of gravity:

$$\begin{cases} y_{CG} = \frac{M(\sum_1^4 F_i z/LF + \sum_1^4 F_i x/LF)}{W} \\ x_{CG} = \frac{M(\sum_1^4 F_i x/LF)}{W} \end{cases} \quad (4.20)$$

4.4 Modeling of Humanoid Climbing Robot by Using Simmechanics

4.4.1 Introduction of Simmechanics

Simmechanics is a toolbox for physical modeling developed by Mathworks from version R2007a of MATLAB suite. Simmechanics extends Simulink with tools for modeling systems spanning mechanical, electrical, hydraulic, and other physical domains as physical networks. Simmechanics has a number of blocks of physical components, such as body, joint, constraint, coordinate System, actuator, and sensor and so on. Simmechanics provides a variety of simulation and analysis modes for mechanical: Forward dynamic analysis, reverse dynamic analysis, kinematic analysis, linear analysis, and equilibrium point analysis determine the steady state equilibrium point for system analysis linear [Zhao]. The most advantage of physical model in Simmechanics is that using physical network approach allows us to describe the physical structure rather than underlying mathematics as in Simulink environment.

4.4.2 Export CAD to Simmechanics diagram

When exporting an assembly file from CAD file we will receive 2 kinds of file which are XML import file and STL file The SimMechanics XML import file mirrors the hierarchical structure of a CAD assembly. The organization of Root

Assembly or Assemblies contains InstanceTree and Constraint which organize the information into reference frame and sets of constraint between Assemblies or parts, respectively. The structure of Part is specified by name, physical unit and especially solid parameters such as mass, center of mass and inertia moments. The STL file specifies 3D geometry of the solid surface for each part.

The mechanical design was developed on Solidworks, and was inspired on various commercial designs. The robot has 22 degrees of freedom, 6 per leg and 4 per arm. The Solidworks design provides pretty much all the necessary information (dimensions, mass and inertia) for a dynamic simulation (see in Figure 4.11)

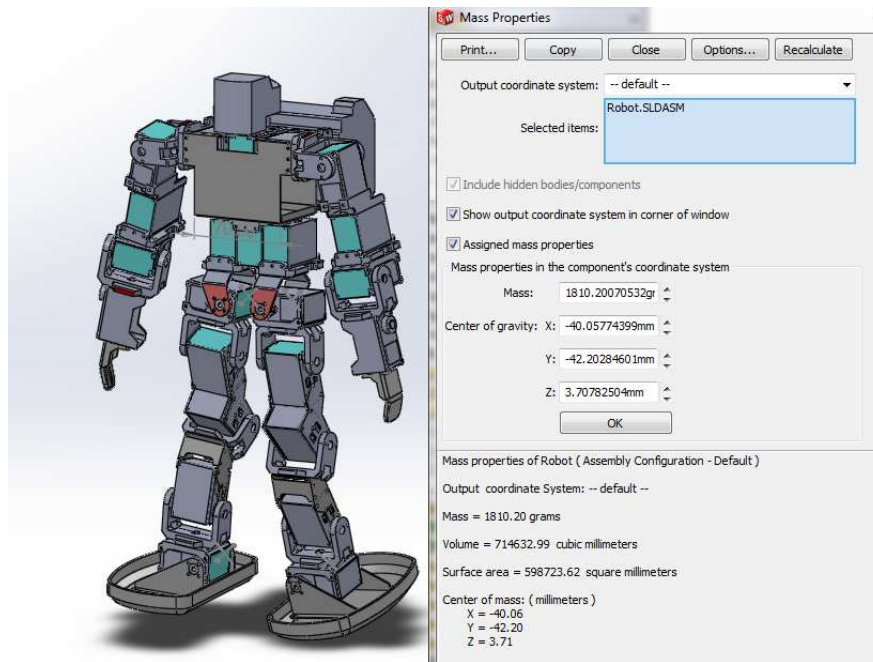


Figure 4.11: Mass properties from Solidwork.

4.4.3 Modeling of humanoid climbing robot

4.4.3.1 Modeling the bodies, legs, hands and joints for the climbing robot

We used the plugin for Solidworks called Simmechanics Link, which allows the conversion from a Solidworks assembly to Simulink model. However, the bodies and joints were laid out manually for greater flexibility and control. The rest of the work consisted in assigning each body its inertial parameters and its 3D model (.stl) and then gluing everything together with the servomotors. The final result is shown below in Figure 4.12 The model of the robot includes main body, head, two arms, two legs, two foot, bushings, machine environment, ground, sine wave generator and constant generator.

Simmechanics provides body and joint 17 blocks to construct various mechanical assemblies. A body holds the inertial information necessary for a dynamic simulation. And two bodies can be connected via a joint, this joint can add

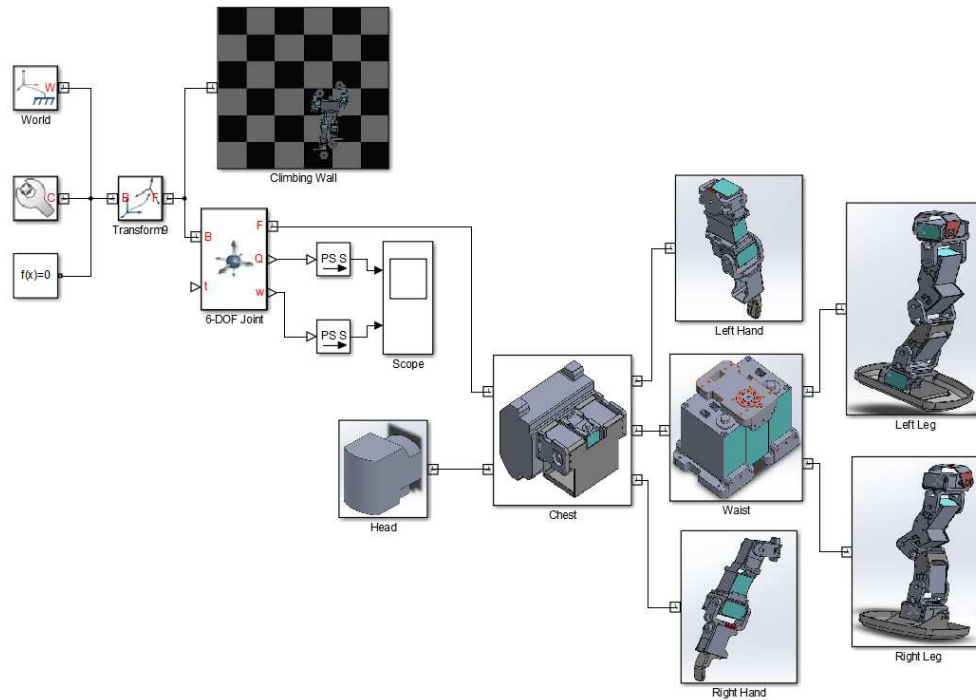


Figure 4.12: Mechanical model of HCR in Simmechanics

zero or more degrees of freedom between the bodies. The bodies and joints are referenced to each other via Coordinates Systems (CS), which can be absolute or relative. Also, sensors and actuators can be attached to the bodies or to the joints for control applications.

4.4.3.2 Modeling the servomotor and actuated joint

For the servomotor model, specifications like the maximum angular speed and the maximum torque were used to produce an accurate DC motor model. For the servomotor controller model, a position + speed controller with gravity compensation and angular speed feed forward was used. Full block diagram is shown in Figure 4.13. Each servomotor was attached to each joint via a joint actuator and joint sensors, as shown in the Figure 4.13

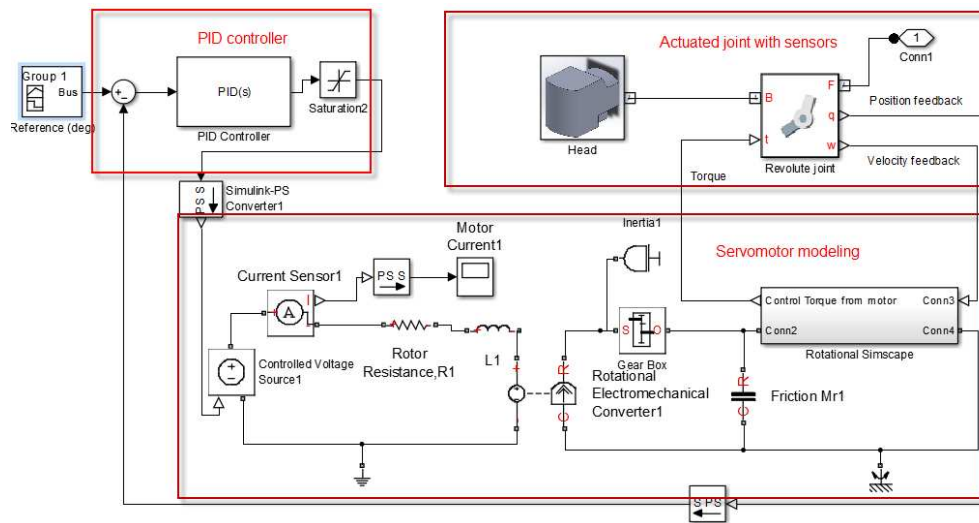


Figure 4.13: Modeling a Servo motor system

4.5 Simulation results

4.5.1 Humanoid climbing robot model in Matlab

In the previous section, by using the tools of SimMechanics we build the model of body, head, feet, arms and legs. By analyzing the robot's mechanical structure correctly, choosing the module rightly, setting parameters reasonably, and colligating the above sections, we eventually get a complete biped robot model in MATLAB. Shown as Figure 4.14

4.5.2 Perform simple task of the climbing activities

When humanoid robot climbs, there are always three limbs touching onto the climbing wall at least. The static gait that will first be considered is the one in which a limb begins return motion after the former limb has touched the wall and completed its climbing.

Climbing consists of repetition of stop and move. The stop means keeping climbing robot's body balance without move against gravity. The move means

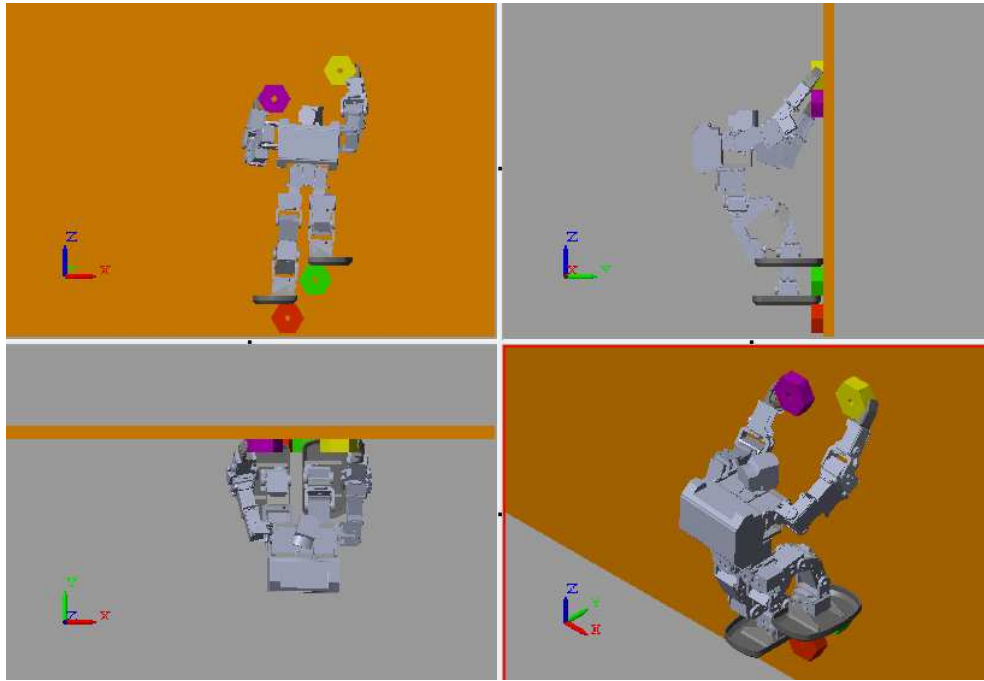


Figure 4.14: 3D model of HCRobot in Matlab

movement of a hand or foot position from current position to next position. Furthermore, the move consists of three kinds of move: Preparing-move, catching-move, and transitional-move [25]. At the first, analysis of stop is the most important because climbing robot should keep its balance and the pose without fall. During the stop, the climbing robot has to find next optimal hand or foot hold to move up its body, and avoid consumption of physical strength concurrently. So we focus on the stop first, and statics should be considered to analyze the stop motion, this action is simulated in 3D model shown in Figure 4.15. By using this model we can get the data of the changed center of gravity's position (see in Figure 4.15).

While balancing, robot has to determine the next hold to climb. This hold must be in robot's work-space. After determine the position of next hold, robot has to determine the orientation of action force in order to ensure the balance of robot in new position. This action is simulated in 3D model shown in Figure 4.16

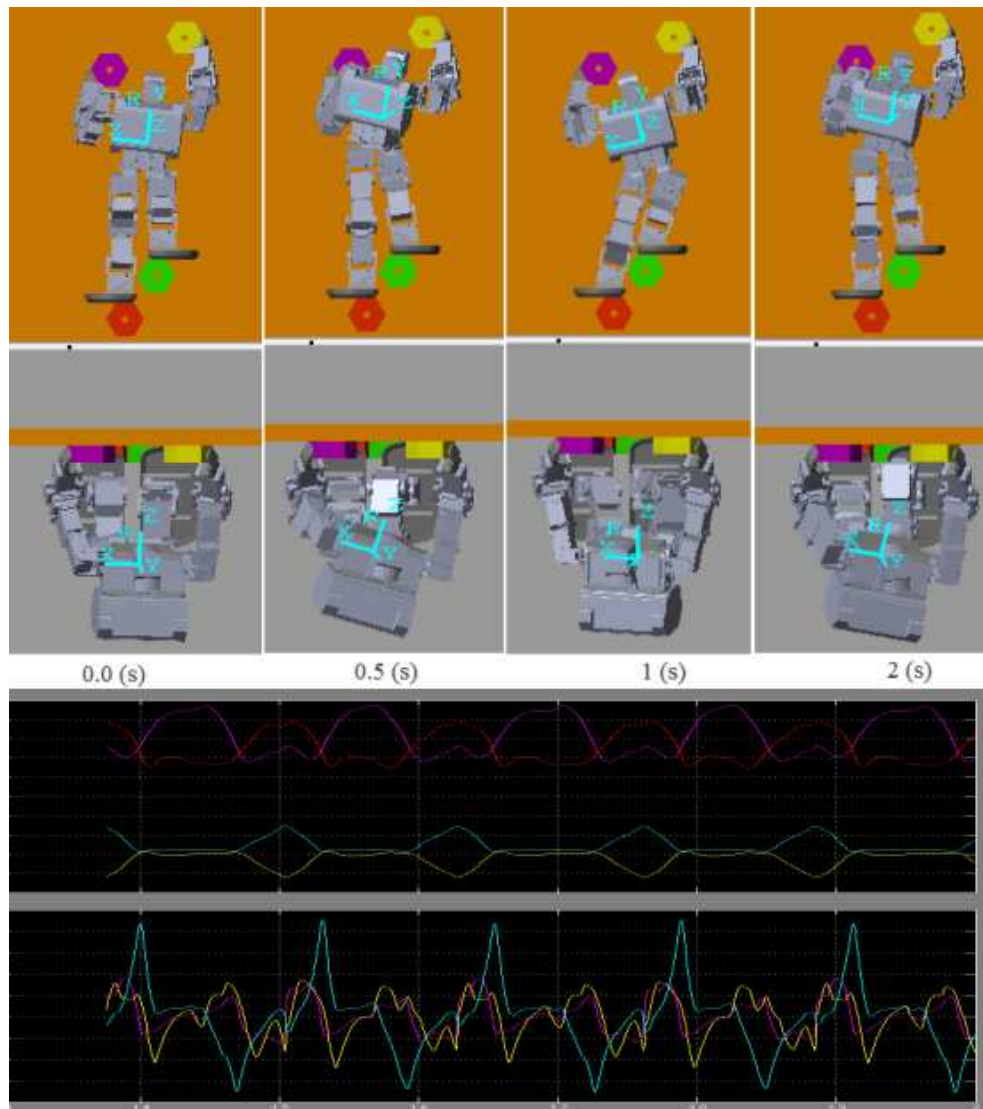


Figure 4.15: Snapshot of stop motion and COG's position

4.6 Discussion

Based on the research of humanoid climbing robot, and using Simmechanics of Matlab, a computer 3D model of humanoid climbing robot was build. With this 3D model we can simulate some basic climbing actions. The center of gravity's positions of robot while balancing during moving time are calculated and recorded

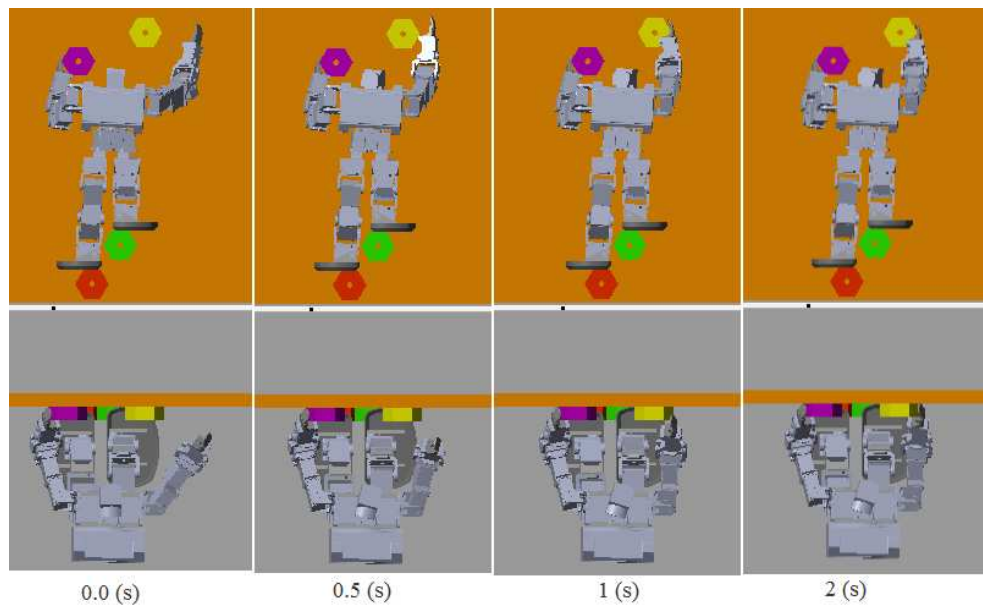


Figure 4.16: Snapshot of dynamic motion

for further research.

In the next step, we use this model to evaluate some motion planning for climbing robot.

Chapter 5

Equilibrium Control on Four-Limbed Climbing Robot

This chapter represents a method to improve the technology that enables the design and simulation of a four-limbed climbing robot. It is equipped with planning capabilities to free climb vertical terrain. It means to extend the robot's ability to a vertical direction under the gravity force. However, we need to analyze climbing and create the theory in parallel with hardware development. In this chapter, the equilibrium allowance area of the four-limbed climbing robot is introduced and the corresponding torque is calculated. Hence, this chapter starts with a rudimentary analysis of mechanical structure and kinematics of four-limb robot. Finally, the corresponding motion planning and control method is performed considering statics and dynamics.

5.1 Four limb model

As an example of a robot to be finally used in this study, it is assumed a humanoid robot having 22 joints as seen in Figure 5.1. However, at the initial stage of humanoid climbing robot research, a four limb model is analyzed. Figure 5.2 is an illustration of thirteen cases when choosing the four limb climbing model. Thereafter, Figure 5.3 show an analysis of four limb climbing model when this

model keep balance on the wall with four limbs.



Figure 5.1: Humanoid Climbing Robot

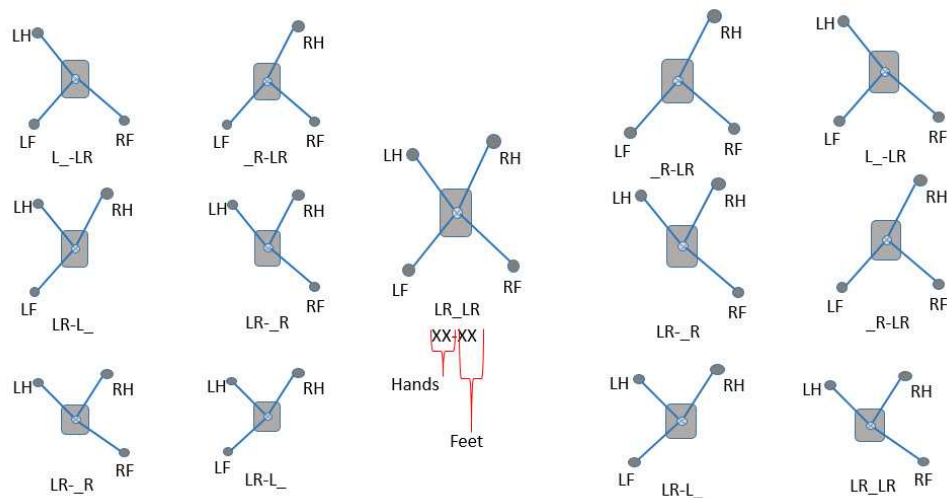
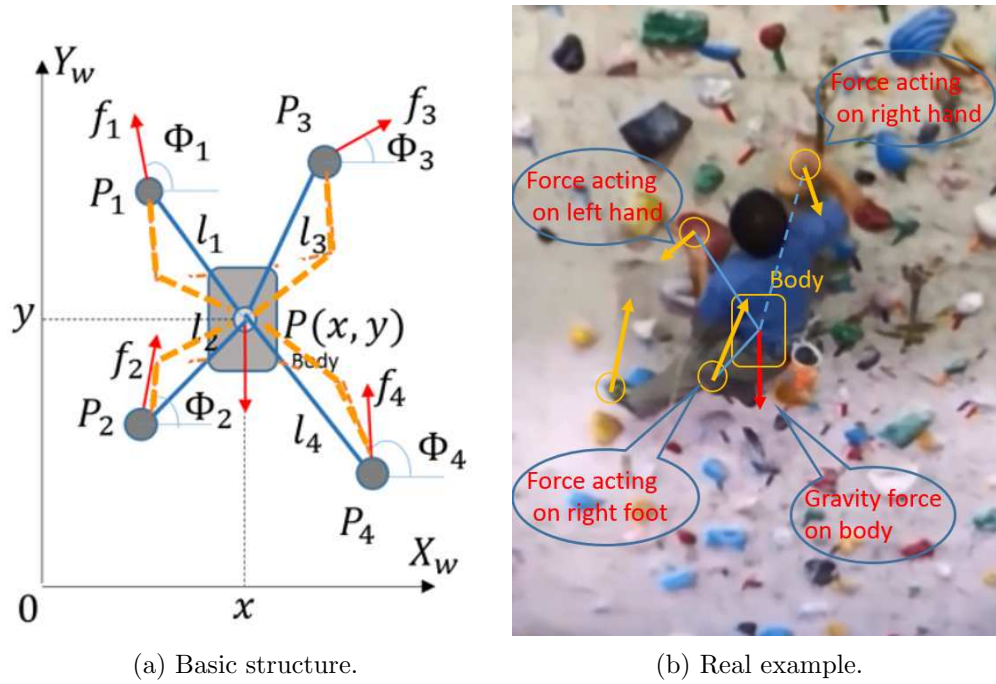


Figure 5.2: The center model keep balance by using 4 limbs. The others maintain equilibrium by just 3 limbs, one free limb is used to reach a new hold.



(a) Basic structure.

(b) Real example.

Figure 5.3: Basic structure and real climbing example

In Figure 5.3(a), the red arrow pointing downwards from the body express the force of gravity. The force f_1 , f_2 , f_3 and f_4 represent the force exerted at P_1 , P_2 , P_3 , and P_4 respectively. Point P_1 is at the left hand, point P_2 is at the left foot, point P_3 is at the right hand, and point P_4 is at the right foot. If the climber grip holds, to resist the attractive force, the climber receives a reaction force of the attractive force from the climbing holds. In Figure 5.3(b), the yellow arrows represent the climbing force of the climber. In addition, the attitude angle of f_1 , f_2 , f_3 , and f_4 at P_1 , P_2 , P_3 , and P_4 are represented by ϕ_1 , ϕ_2 , ϕ_3 , and ϕ_4 respectively. The body position is defined by $P(x, y)$. The length of each limb is represented by l_i (i from 1-4).

On the other hand, Figure 5.3 (b) shows the the actual motion corresponding to the model shown in Figure 5.3 (a). The climber use his limbs to make friction forces with holds, which could help he balance on a climbing wall. In Figure 5.3 (B), the yellow arrows denote the climbing fore.

5.2 Climbing Condition

5.2.1 Static equilibrium constrain

The main propose of this part is to describe how to derive a body's position that can maintain the body balance in the case of the hold position is known. The climbing force $F = [f_1, f_2, f_3, f_4]^T$, and the Jacobian matrix J are applied in the equation $\tau = J^T F'$ to find the robot torque.

Conditions for the body to keep the static stable is the sum of the forces exerted on the body equal 0, and the sum of all moment exerted on the body equal 0 (explain in detail at section 4.3.3). These conditions lead to the following equations (5.1, 5.1, 5.3). Here, we are using the same notation introduce in Section 4.3. We use subscript x and y to distinguish the horizontal and vertical direction.

$$f_{1x} + f_{2x} + f_{3x} + f_{4x} = 0 \quad (5.1)$$

$$(f_1 \cos \phi_1 + f_2 \cos \phi_2 + f_3 \cos \phi_3 + f_4 \cos \phi_4 = 0)$$

$$f_{1y} + f_{2y} + f_{3y} + f_{4y} - mg = 0 \quad (5.2)$$

$$(f_1 \sin \phi_1 + f_2 \sin \phi_2 + f_3 \sin \phi_3 + f_4 \sin \phi_4 - mg = 0)$$

$$\begin{aligned} f_{1x}(y - y_1) - f_{1y}(x - x_1) + f_{2x}(y - y_2) - f_{2y}(x - x_2) \\ + f_{3x}(y - y_3) - f_{3y}(x - x_3) + f_{4x}(y - y_4) - f_{4y}(x - x_4) = 0 \end{aligned} \quad (5.3)$$

Combine(5.1),(5.2) we get the equation(5.4).

$$\begin{bmatrix} \cos \phi_1 & \cos \phi_2 & \cos \phi_3 & \cos \phi_4 \\ \sin \phi_1 & \sin \phi_2 & \sin \phi_3 & \sin \phi_4 \end{bmatrix} \begin{bmatrix} f_1 \\ f_2 \\ f_3 \\ f_4 \end{bmatrix} = \begin{bmatrix} 0 \\ mg \end{bmatrix} \quad (5.4)$$

$$\text{We set: } A = \begin{bmatrix} \cos \phi_1 & \cos \phi_2 & \cos \phi_3 & \cos \phi_4 \\ \sin \phi_1 & \sin \phi_2 & \sin \phi_3 & \sin \phi_4 \end{bmatrix}, F = \begin{bmatrix} f_1 \\ f_2 \\ f_3 \\ f_4 \end{bmatrix}, \text{ and } B = \begin{bmatrix} 0 \\ mg \end{bmatrix}.$$

From the equation 5.4, we get the equation 5.5.

$$F = A^+ B + (I - A^+ A).w \quad (5.5)$$

In the equation 5.5, I is the 4 by 4 identity matrix and w is a one by four arbitrary vector. The equation 5.5 to define the value of forces f_1, f_2, f_3, f_4 .

5.2.2 Equilibrium condition of movement

From the equation 5.3

$$\begin{aligned}
 & f_1 \cos \phi_1 (y - y_1) - f_1 \sin \phi_1 (x - x_1) + f_2 \cos \phi_2 (y - y_2) - f_2 \sin \phi_2 (x - x_2) \\
 & + f_3 \cos \phi_3 (y - y_3) - f_3 \sin \phi_3 (x - x_3) + f_4 \cos \phi_4 (y - y_4) - f_4 \sin \phi_4 (x - x_4) \\
 & = 0
 \end{aligned} \tag{5.6}$$

Here $x_1, x_2, x_3, x_4, y_1, y_2, y_3, y_4$ and $\phi_1, \phi_2, \phi_3, \phi_4$, we already known, we assumed f_1, f_2, f_3, f_4 are calculated from the previous section. The equation (5.6) is written by the equation (5.7).

$$\begin{aligned}
 & (f_1 \cos \phi_1 + f_2 \cos \phi_2 + f_3 \cos \phi_3 + f_4 \cos \phi_4) y \\
 & - (f_1 \sin \phi_1 + f_2 \sin \phi_2 + f_3 \sin \phi_3 + f_4 \sin \phi_4) x \\
 & = (f_1 \cos \phi_1 y_1 + f_2 \cos \phi_2 y_2 + f_3 \cos \phi_3 y_3 + f_4 \cos \phi_4 y_4) \\
 & - (f_1 \sin \phi_1 x_1 + f_2 \sin \phi_2 x_2 + f_3 \sin \phi_3 x_3 + f_4 \sin \phi_4 x_4) = \text{const}
 \end{aligned} \tag{5.7}$$

Set $C = (f_1 \cos \phi_1 + f_2 \cos \phi_2 + f_3 \cos \phi_3 + f_4 \cos \phi_4)$, $D = (f_1 \sin \phi_1 + f_2 \sin \phi_2 + f_3 \sin \phi_3 + f_4 \sin \phi_4)$, and $E = (f_1 \cos \phi_1 y_1 + f_2 \cos \phi_2 y_2 + f_3 \cos \phi_3 y_3 + f_4 \cos \phi_4 y_4) - (f_1 \sin \phi_1 x_1 + f_2 \sin \phi_2 x_2 + f_3 \sin \phi_3 x_3 + f_4 \sin \phi_4 x_4)$

Form the equation (5.1), (5.2), we have $C = 0$, $D = mg$, and E is a constant. Therefore, $x = -E/mg = \text{const}$ and y is not only solution. It means that with four specific holds the robot could has several solution for the body's position to keep balance on the climbing wall.

5.2.3 Relationship between Torque and Length of Limb

l_i is the length of each limb, it dose not appear in the above expression. This part we consider about this problem. The length l_i is not the length of actual link, it is just a distance form the hold to the body's position. You can image that,

each limb consider two parts (such as upper arm and forearm), and L is length of each part of limb. While the distance from the position of holds P_i to the center of mass at the point $P_{x,y}$ are l_i . To maintain a balanced body position, joint torque τ_i is calculated by using the equation: $\tau_i = J_i^T f_i$. We get the equation (5.8). In addition, joint angle of each limb can be determined by using the inverse kinematic operators (for two link manipulator).

$$\begin{bmatrix} \tau_{i1} \\ \tau_{i2} \end{bmatrix} = \begin{bmatrix} -Ls\theta_{i1} - Ls\theta_{i1+i2} & Lc\theta_{i1} - Lc\theta_{i1+i2} \\ -Ls\theta_{i1+i2} & -Lc\theta_{i1+i2} \end{bmatrix} \cdot \begin{bmatrix} c\phi_i \\ s\phi_i \end{bmatrix} f_i, \quad (i = 1, 2, 3, 4) \quad (5.8)$$

5.2.4 Examples

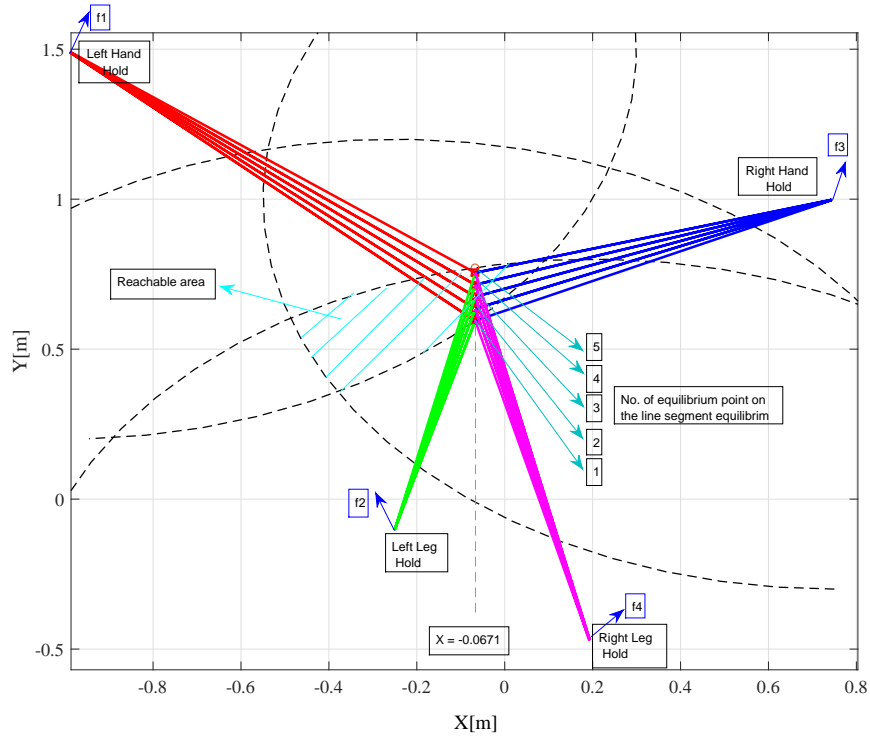


Figure 5.4: Reachable Area and Equilibrium Line Segment

We assumed that the position of 4 holds are known

$P_1 = [x_1, y_1]^T = [-1, 1.5]^T m$, $P_2 = [x_2, y_2]^T = [-0.25, -0.1]^T m$, $P_3 = [x_3, y_3]^T = [0.75, 1.0]^T m$, $P_4 = [x_4, y_4]^T = [0.2, -0.5]^T m$, the maximum length of each limb is $l_i = 1.3m$, $mg = 100N$, $\phi_1 = 2/3\pi$, $\phi_2 = 3/4\pi$, $\phi_3 = \pi/4$, $\phi_4 = \pi/6$.

In this case $[f_1, f_2, f_3, f_4]^T = [37.68, 41.17, 35.40, 26.46]^T N$ be obtained (after selecting $w = [1, 10, 10, 10]$). In the Figure 5.4 the red, blue, pink, and green line represent the connecting line form body to P_1, P_3, P_4 and P_2 respectively. Intersection of four circles with a center of P_1, P_3, P_4 and radius of l_i is called reachable area. The four arcs with maximum value of each limb, in other words they represent reachable area of each limb. Inside the reachable area, the four color lines intersect at a line segment with $x = -0.0671m$ (see in Figure 5.4).

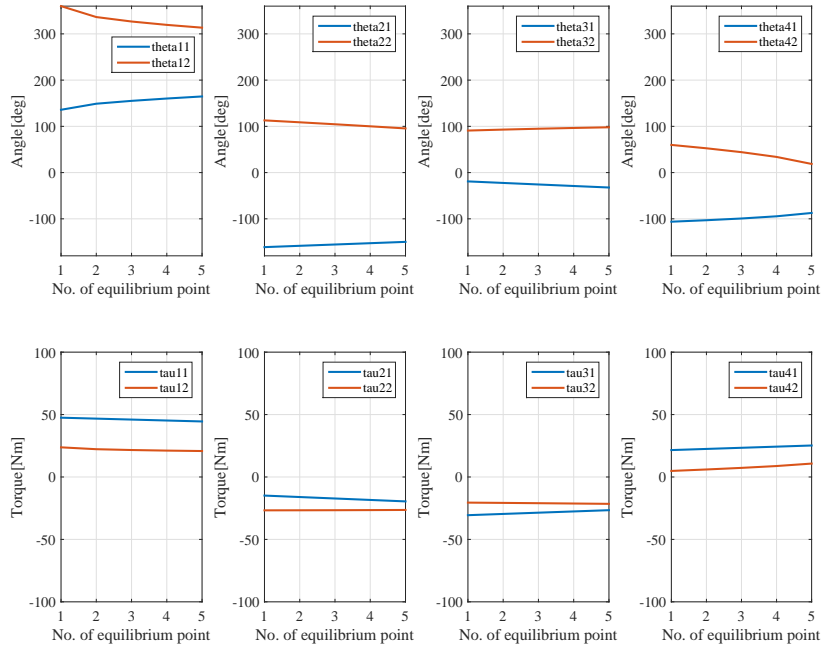


Figure 5.5: Jount angles and Torques at equilibrium points

Figure 5.5 shows the result of joint torque and joint angle for each model limb (for above example). In the variable name, the first digit number of the subscript represents the name of limb, and the second element denotes the joint number (on each limb, counted form body side).

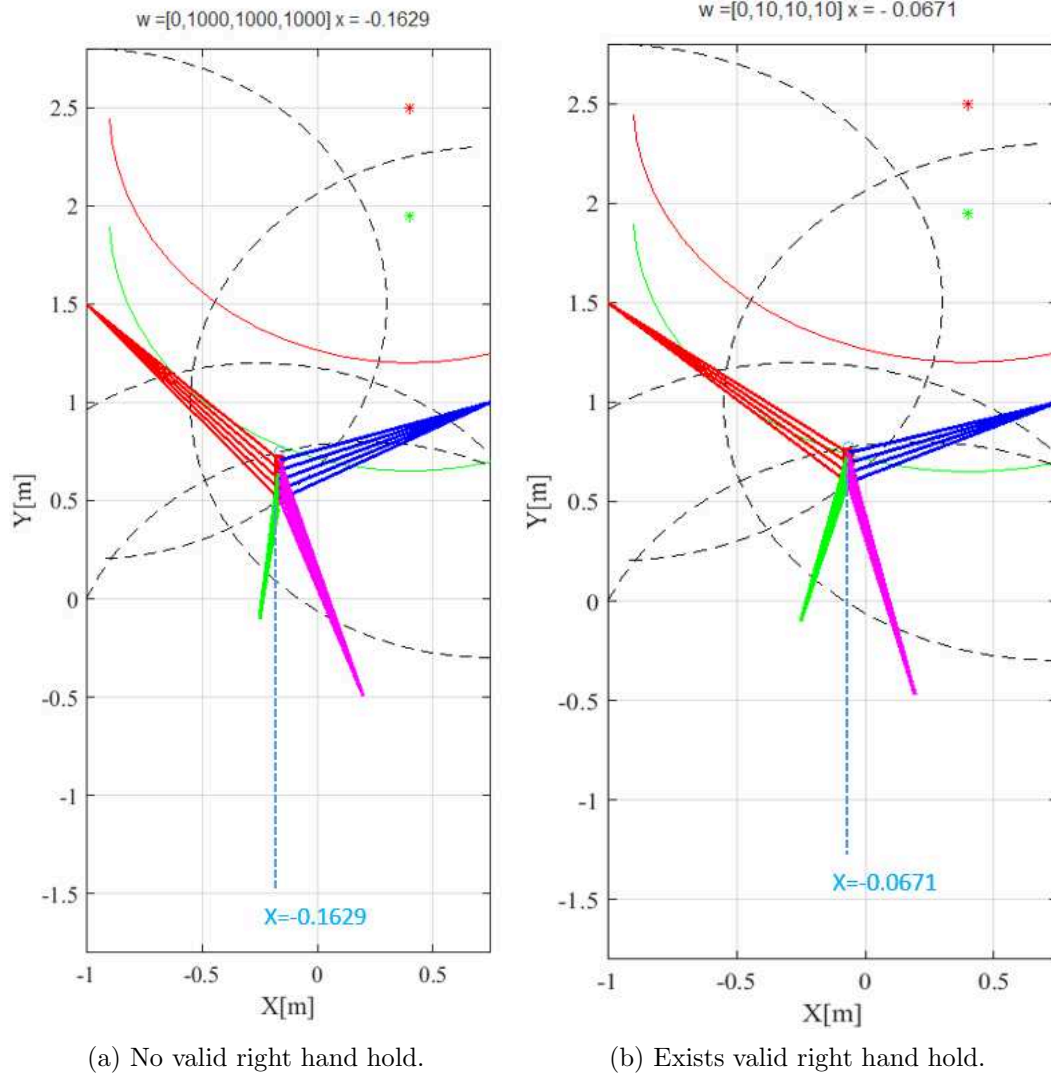


Figure 5.6: Equilibrium line segment position changing

Additional examples are proposed in Figure 5.6. The same initial condition with previous example are applied. In addition, green hold (at the position $P_5 = [x_5, y_5]^T = [0.4, 2.5]^T m$) and red hold (at the position $P_6 = [x_6, y_6]^T = [0.4, 1.95]^T m$) are considered to robot using as a next valid right hand hold or not. The red and green arc (with the center at red and green hold, respectively) represent the reachable area of each holds.

When the value of $w = [0,1000,1000,1000]$ is selecting, the equilibrium line segment position at $x = -0.1629[m]$. In this case the red and the green hold are not next valid right hand hold, since the red and green arc do not intersect with the equilibrium line segment (see Figure 5.6 (a)). When the value of $w = [0,10,10,10]$ is selecting, the equilibrium line segment position at $x = -0.0671[m]$. In this case the green hold is next valid right hand hold while the red hold is not, since the intersection of the equilibrium line segment and the green arc exists (see 5.6 (b)).

5.3 Discussion

The goal of motion control is to make the robot follow the motion path computed by the planner at the progressive stances. Assuming that the position of the hand at the holds are computed in the planner. Then, humanoid climbing robot use the position control to reach his hands and foot to selected holds. Therefore a position control is propose in detail in this part.

5.3.1 Platform for Humanoid Robot

We select KHR-3HV as a prototype to develop humanoid climbing robot. In this part, I have implemented my position control on this robot. Figure 5.7 shows the concept of this humanoid platform. Motion-based humanoid robots are generally controlled by reading motion files which set the key poses in a sequence created by using Motion Editor. **Human Interface**

The motion files to be read by the humanoid robot are invoked by user through the directions using a remote controller. Radio control method is generally used for the motion-based humanoid robot.

Motion Editor and Motion Files

Motion Editor is used to generate motion files by user through operating GUI on a PC.

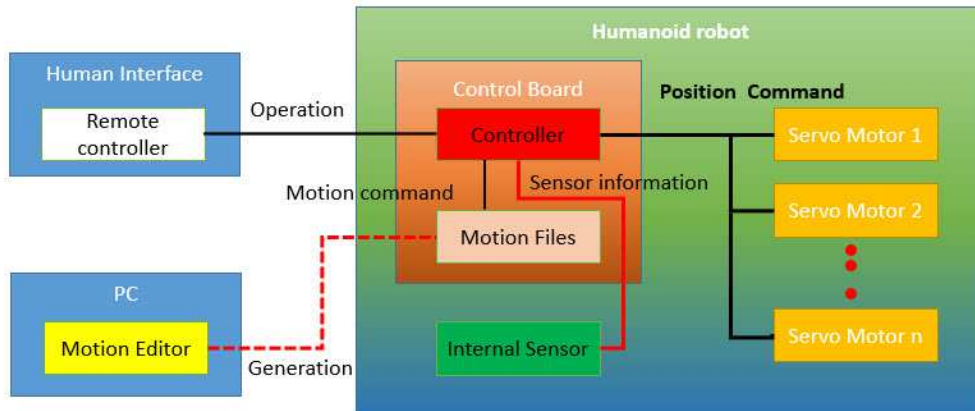


Figure 5.7: Humanoid robots platform

Internal Sensor

Sensor is used to monitor the situation of the humanoid robot using acceleration sensor, gyro sensor, etc., and to feedback the information to the controller.

Internal Sensor

Sensors like kinect sensor will be detect by PC.

Servo Motor

Servo motor is a small actuator module performing positioning. By receiving a position command from controller, servo motor holds at the assigned position by the internal module. In addition, it can measure and send some data to controller, such as current position, internal temperature and current value.

Controller

It controls servo motors by reading motion file from Human Interface to assigned position at assigned speed. Further, it can do feedback control using sensor value from internal sensors and servo motors.

5.3.2 Proposition of Position Control

The controller should try to follow the motion path computed by the planner as closely as possible. We propose the position control for humanoid kondo robot

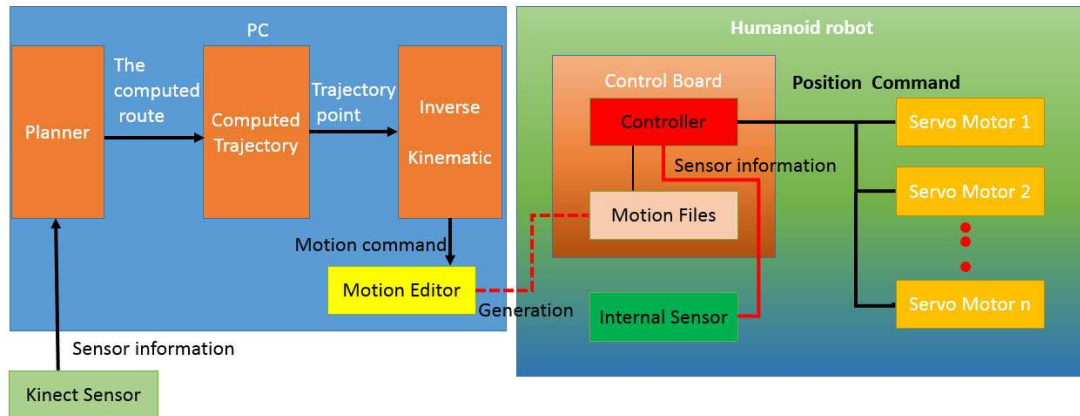


Figure 5.8: Position control diagram

as in Figure 5.8. In this motion control, twenty two joints of humanoid robot are computed at each control cycle, the joint angles to be achieved at the next trajectory point are computed using simple inverse kinematics from the position/orientation of the robot's body and the positions of the new holds that define for new limb's position.

Chapter 6

Global Path and Local Motion Planning for Humanoid Climbing Robot

This chapter focuses on a path planning and local planning algorithm for humanoid robot wall climbing as the initial phase of our development. The first step is to acquire a depth map to extract accurate information about climbing holds on the vertical wall. Secondly, we propose a global planning algorithm for the humanoid robot using data from Kinect. The proposed algorithm ensures that the climbing robot finds the best route to climb up the wall. During climbing, the humanoid robot utilizes the local planning algorithm, based on quasi static equilibrium, to adjust its body posture in order to remain in equilibrium state. Finally, all algorithms are evaluated with a simple practical example for a humanoid climbing robot system, and its effectiveness is demonstrated experimentally in a real environment.

6.1 Introduction

To climb a climbing wall, a humanoid robot typically starts by looking at the entire wall to detect a map of the major terrain features, such as climbing hold

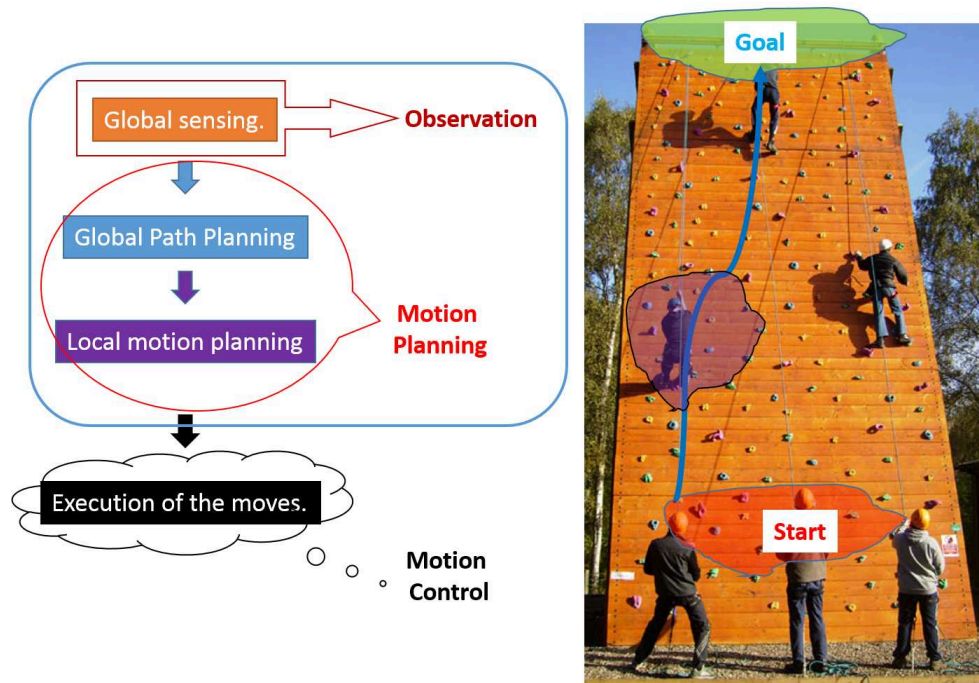


Figure 6.1: General Overview

positions, as well as climbing hold shapes (discussed in section 6.3). Based on this map, the best route is planned (discussed in section 6.4). This route only gives height level direction, since the local motion planning for each fundamental movement is still lacking. To start the algorithm of trajectory planning for free climbing, the humanoid robot also acquires a detail local planning around its current position. With the local motion planning, the robot identifies candidate holds that can be reached in order move up. Therefore, a general scenario of climbing consists of the following steps (see Figure 6.1):

Step 1: Global sensing.

Step 2: Global Path Planning.

Step 3: Local motion planning (detailed planning for series of moves 4-3-4 contact-holds)

Step 4: Execution of the moves. Base on the general scenario, our project is divided into three technical parts: observation, planning, and motion control.

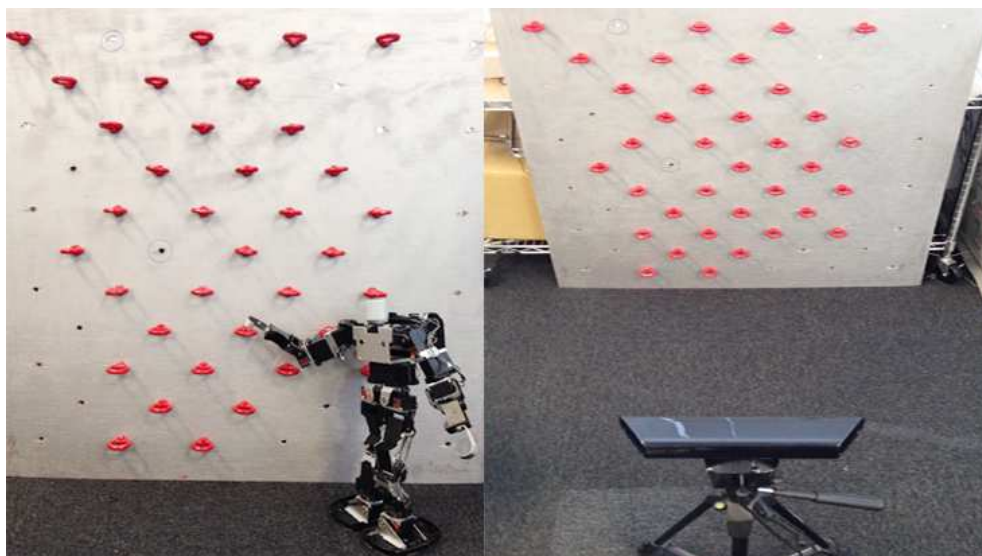


Figure 6.2: Climbing Wall and System Location

Here we focus on the first two parts. In the observation part, we use a Kinect for global sensing (step 1) to get information about the climbing wall, such as all of the climbing holds positions and the climbing wall’s dimensions. After acquiring the current environment, the path planning (step 2) begins the special motion planning algorithm named “Right Hand Search Algorithm” (RHSA) is utilized to identify the best route to climb up the wall. This algorithm can be used to construct a trajectory that connects the start position to the goal position. While following the route, the robot uses the local motion planning (step 3) to identify target holds, and adjusts its center of mass to perform short-term goals.

This chapter is organized as follows. In section 6.3, we use the Kinect [10] to obtain the environment’s information in 3D. Kinect is a motion sensing device produced by Microsoft for the Xbox game system, based on underlying technology from PrimeSense, and provides real time point clouds as well as 2D images. Kinect, which is not only a normal camera sensor but also a special device, can provide a depth map. The depth map is acquired from the OpenNI [11] library, and is then processed to extract accurate information about the environment, such as the climbing hold’s position and the climbing wall dimensions. This information will be used in the planning part to find the best route for the humanoid climbing

robot.

In the path planning (section 6.4), the robot system observes the entire climbing wall to find out the climbing route before the robot actually begins climbing. This algorithm is named the “Right Hand Search Algorithm” and it consists of two phases: a scanning phase and a query phase. In the scanning phase, the algorithm generates a “reachable area” on the climbing wall through the “reference scan point” S . It is a kind of a graph algorithm, and queries to see if it is a useful hold, while also taking into account the specific abilities of the robot. A road map is constructed and stored as a graph whose nodes correspond to “right hand reachable hold” (RHRH) and whose edges correspond to feasible paths between these “RHRHs”. This algorithm defines “adjacent hold” and evaluates the cost between RHRHs. In the query phase, the Dijkstra algorithm is applied to find the best route from the road map in the previous phase. Any given start and goal RHRHs of the road-map are connected and evaluated for total cost, with the best route being the one with the lowest total cost. Section 6.5 describes in detail the local motion planning, which is based on a climbing behavior. Finally, the experiment described in section 6.6 will demonstrate that the humanoid climbing robot climbs up freely along the designed route.

6.2 Precondition and Preliminary Work

6.2.1 Hardware Structure

We selected the KHR-3HV manufactured by Kondo [7] as a prototype to develop humanoid climbing robot. The humanoid robot has 22 degrees of freedom (DOF), with of the 22 degrees being in the open leg in order to enable climbing in the open leg.

The humanoid robot does not have any special mechanism to grasp holds, but angled brackets are used as hands. Hence, the only chances to grab holds are obtained by performing press on pull motions.

6.2.2 Assumptions on the research

This paper addresses the problem of global motion planning and local planning of a humanoid climbing robot in order to “free climbing” on vertical surfaces. To our knowledge, vertical surfaces are categorized into natural walls and artificial walls. However, it is not easy to develop humanoid climbing robot in natural environments. Therefore, this paper focus on an artificial climbing wall.

Climbing wall and climbing wall configuration. The robot’s workspace is a square vertical wall. The wall is made from wood with multi-holes (shown in Fig.6.2). The holds are made by metallic rings which the climbing hands can hook into and the feet can be placed on, shown in Fig.6.3. All information about the climbing hold positions is defined as a climbing wall configuration. In addition, climbing hold positions are arbitrary arranged and can be relocated, hence climbing wall configuration is versatile.

Equilibrium. To remain balanced, the robot must apply contact forces with hands and legs at holds that compensate for gravity. In addition, the robot is assumed that it always maintains contact with either three or four holds. For instance, two hands and left leg are at holds while the right hand is moving. In this case the robot performs 3-contact-holds posture to remain balance. If the robot keeps balance by 4 holds, the posture is called 4-contact-holds.

Motion and transition. In this research, we assumed the robot’s motion to be quasi-static [28]. A motion of humanoid climbing robot consists of a sequence of 3-contact-holds and 4-contact-holds posture. If 3-contact-holds and 4-contact-holds posture share three hold, then they are adjacent and transition exits between them.



Figure 6.3: Climbing holds

6.2.3 Climbing Wall Structure

6.3 Observation part

The overview of our proposed systems is shown in Fig.6.4 Kinect receives all of information of the climbing wall, then it finds the locations of all of the climbing holds. From the size of the robot, the controller creates the working area. Using this working area, and applying the right hand search algorithm, the best route can be found accordingly.

6.3.1 Pre-processing of Kinect Depth Data

Microsoft's Kinect is a sensor creating full 3D images comprised of 640x480 RGB plus depth. Similar to other RGB-D sensors, the basic unit for the Kinect is pixel, which stores the depth values. Basically, each pixel in the color image be assigned with a depth value. However, when the sensor cannot generate a proper depth value due to strong light or other noises, a value of 0 is assigned.

The depth value represents the vertical distance between the target point and the XOY plane of the Kinect coordinates, which is defined as a right handed coordinate with the Kinect's facing direction as the positive Z direction and Kinect's right side direction as the positive X direction (Fig.6.4).

In OpenNI, the Kinect depth map is saved as a one dimension array. Like the

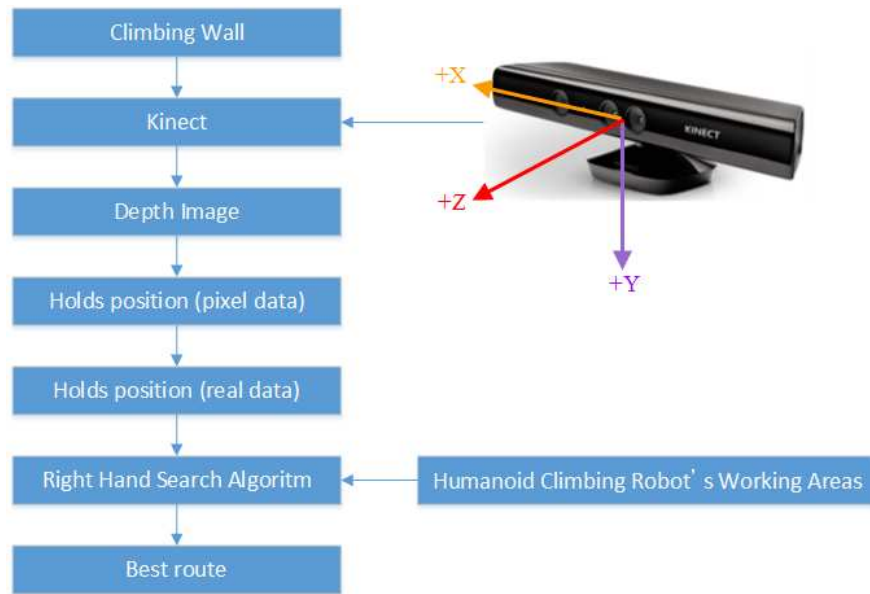


Figure 6.4: Overview proposed Systems

color image, the pixel at the top left corner of the depth value starts the array. When the resolution is 640x480, the positions of the pixel in the array can be illustrated as Table 6.1, where each square stands for a pixel. The first row in the square is the position index of the pixel in the depth-map array, and the second row is the two-dimension position index of the pixel in the depth map.

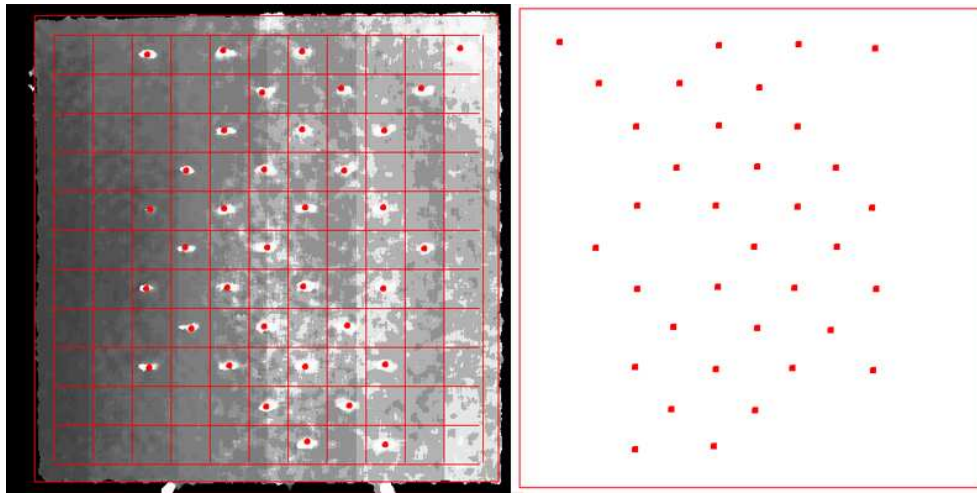
OpenNI saves the depth image in a left-to-right and up-to-down manner as shown in Table.6.1. The depth value for the pixel, located in the column “ i ” and row “ j ” in the depth image can be found in the element “ k ” of the array, where k can be obtained as follows, $k = (j - 1) \times 640 + i$.

6.3.2 Searching Climbing Holds Position (pixel data)

To find out the climbing hold positions, the controller uses the difference values of the holds and climbing wall. Because the climbing holds’s depth value is smaller than the depth value of the wall. Assuming the climbing holds are the same size and the square shape of climbing wall, we divided the wall into 11 rows and 11 columns for total of 121 areas (Fig.6.5a)for example. The controller checks

Table 6.1: The storing rule of Kinect depth values

1 (1,1)	2 (1,2)	...	639 (1,639)	640 (1,640)
641 (2,1)	642 (2,2)	...	1279 (2,639)	640 (2,640)
...
306561 (480,1)	306562 (480,2)	...	307199 (480,639)	307200 (480,640)



(a) Finding climbing holds

(b) Mirror data

Figure 6.5: Pixel Data

all areas to identify which areas have holds and which do not, using the simple algorithm shown below.

Each area is defined as an area with a hold if this area contains pixels whose depth value is smaller than the climbing wall's standard depth value. Any pixels with smallest depth value are defined as the pixels linked to a climbing hold (x , y depth value).

Since the depth values of the Kinect are opposite from the real dimensions. The pixel data is converted to the new pixel.

Each climbing hold position (X, Y - pixel) is converted as equation (6.1).

$$\begin{cases} Y_{new} = Y \\ X_{new} = 640 - X \end{cases} \quad (6.1)$$

The result of every climbing hold position is shown in Fig. 6.5(b)

6.3.3 Climbing holds position (real data-mm)

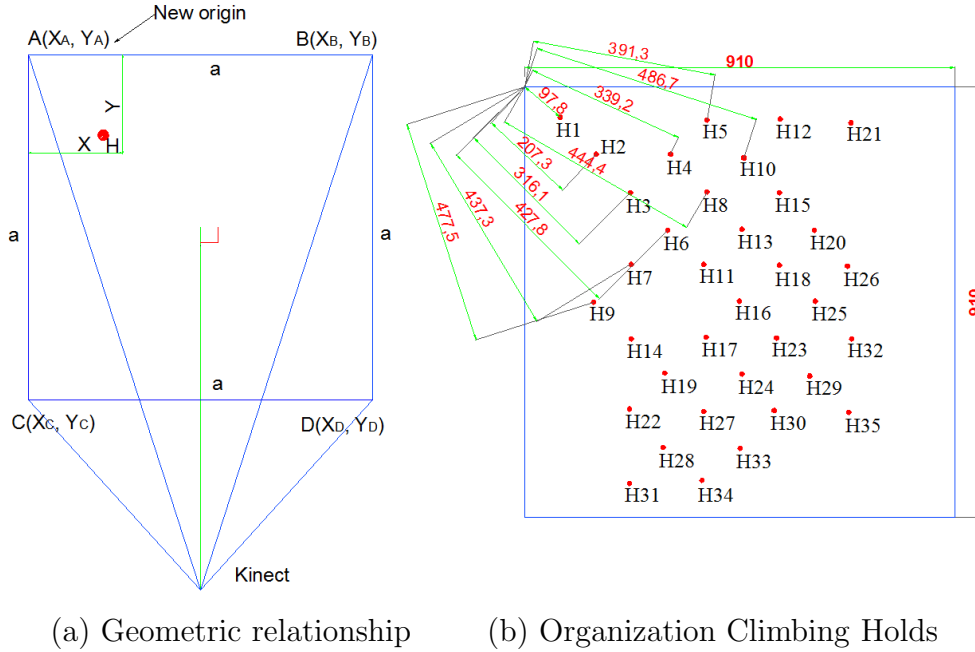


Figure 6.6: Convert and Label Climbing Holds

The controller should rebuild up the climbing wall information with the climbing hold positions (real dimension). From the Kinect data, the controller recognizes the four corners position (A, B, C, and D) of the climbing wall (see Fig.6.6(a)) and also the real dimension of the climbing wall (a-mm). Then, the controller defines point A as a new origin; H denotes the climbing hold (with X_H, Y_H pixel), point H's position can be converted to real dimensions using the following equations (6.2).

$$\begin{cases} x = (x_H - x_A) * a / (x_B - x_A) \\ y = (y_H - y_A) * a / (y_C - y_A) \end{cases} \quad (6.2)$$

In the same manner, the controller converts all of the climbing hold positions from pixel data to real data. To use the set of the climbing holds in the Right Hand Search Algorithm, we define the set of all climbing holds as H . The order of climbing holds in the set H regulatory compliance: A hold that has a smaller distance (compared with the left top point) has a smaller index in the set H (see in Fig.6.6(b)).

6.4 Global Path Planning

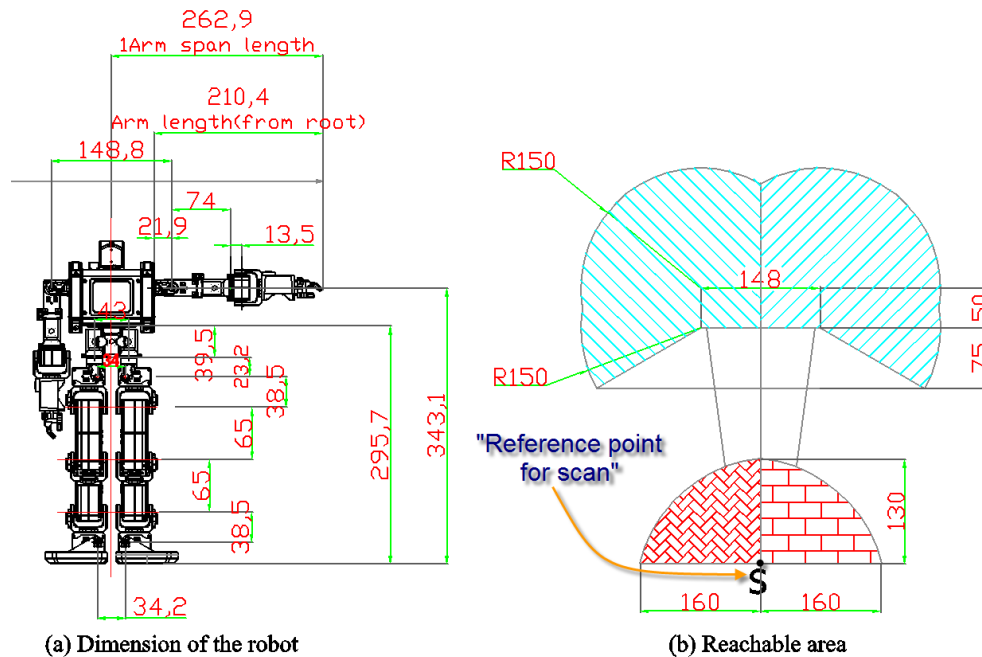


Figure 6.7: Definition of “reachable area” and “reference point for scan”-S

The presented planning algorithm is developed to decide the best route to climb up the wall. The algorithm is similar to graph algorithms on clustering. It analyzes whether hold candidates are useful or not. Moreover, the algorithm takes into account the specific abilities of the robot. The algorithm is labeled “Right Hands Search Algorithm”.

6.4.1 Defining robot “reachable area”

The basic idea of RHSA is to consider only the holds that can be reached by the robot’s right hand while the robot keeps balance. Figure 6.7 describes reachable area, reference point for scan. The reachable area for the hands and feet that is obtained depends on the size of the robot. The reachable area can be moved along with the robot’s motion on the wall. Here it is assumed that the robot can not intersect one leg with another. As the same manner, the robot can not intersect one arm with another. Then the robot finds “right hand reachable holds” under the robot’s configurations. When the robot’s right hand hooks into RHRH, the robot can find at least one hold located within the left hand reachable area, and can also find a hold for each leg within the reachable area.

6.4.2 Scanning Phase

We now describe our planning method in general terms for the prototype humanoid robot without focusing on any specific type of robot. As the first step of the presented right hand search algorithm, RHSA, the robot needs to find a “right hand reachable hold” by scanning the wall through a reference scanning point, S , shown in Fig.6.7(a). First, depending on the size of robot illustrated in Fig6.7(b), the robot controller automatically finds the “reachable area” from S .

The controller uses the set of grid points O to sample the scan point S . The set O is generated as follows: The controller generates vertical and horizontal parallel lines through AB and AC (see in Fig.6.6) with an equal offset distance. Then, we have O as the set of intersection points for those horizontal and vertical lines.

6.4.2.1 Scanning Valid Right Hand Holds

One “right hand reachable holds (RHRH)” can be found for the reference scanning position S . Then the robot can find, at least one hold located in the left hand reachable area, as well as find one hold for each legs reachable area. The point S is sampled from the set O (defined in section6.4.2); (similar with sampling

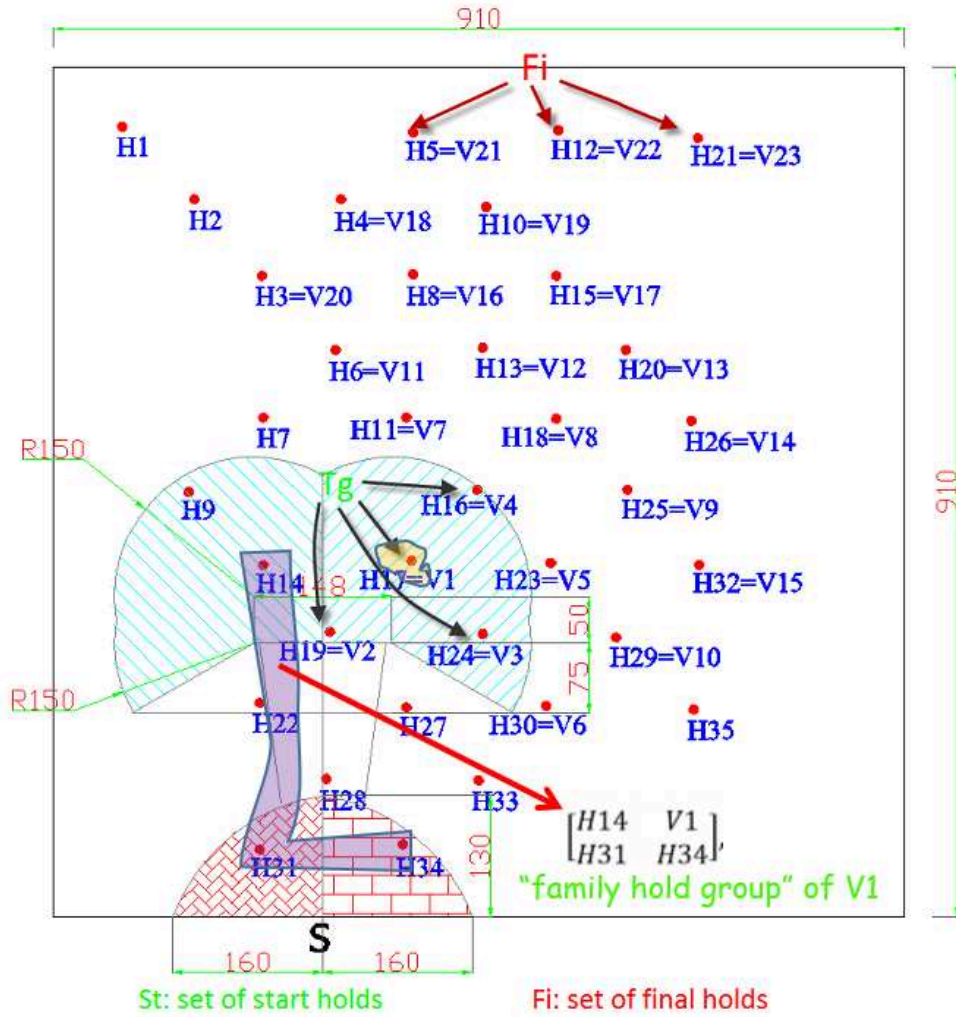


Figure 6.8: Scan example using “Right hand reachable holds”

algorithm in [35]). When the corresponding S is found, the controller can find the robot’s reachable area on the climbing wall. The RHRH is the hold existing in the reachable space of the right hand, and simultaneously at least one group consisting of three holds in the reachable spaces of the left hand, right foot, and left foot. We call this group is the “family hold group”. Note that one RHRH have multiple “family hold groups”.

An example is introduced as the following: Select a scan point “ S ” shown in Fig.6.8. The controller finds out one RHRH $V1$ as a its family hold group, $H14$;

$H31$; $H34$, which are left hand hold, left foot and right foot holds respectively.

V[1] (When V1 is hold H17) (red is new update VRHP)
$\begin{bmatrix} H9 & V1 \\ H31 & H34 \end{bmatrix} \begin{bmatrix} H14 & V1 \\ H31 & H34 \end{bmatrix}, \begin{bmatrix} H19 & V1 \\ H31 & H34 \end{bmatrix}$
V[2] (When V2 is hold H19)
$\begin{bmatrix} H9 & V2 \\ H31 & H34 \end{bmatrix}, \begin{bmatrix} H14 & V2 \\ H31 & H34 \end{bmatrix},$
V[3] (When V3 is hold H24) red is new update VRHP
$\begin{bmatrix} H9 & V3 \\ H31 & H34 \end{bmatrix}, \begin{bmatrix} H14 & V3 \\ H31 & H34 \end{bmatrix}, \begin{bmatrix} H19 & V3 \\ H31 & H34 \end{bmatrix}$
V[4] (When V4 is hold H16 (new VRHP))
$\begin{bmatrix} H9 & V4 \\ H31 & H34 \end{bmatrix} \begin{bmatrix} H14 & V4 \\ H31 & H34 \end{bmatrix}$

Figure 6.9: The updating information of RHRHs when point S at(910,290)

A set, V , is defined as a set of all the right hand reachable holds, and RHRHs are stored as the array of V sets with order of priority: left to right, bottom to top. For instance, RHRH $V1$ is stored in $V[1]$ which contains one element $[H14, V1, H31, H34]$. If one $V[i]$ set has n elements, there are n “family hold group” with respect to the RHRH. Now, by scanning successively the point S from $(910,0)$, $(910,10)$, $(910,910)$,..., $(0,0)$, $(0-910)$ (sampling from the set O), the controller finds every RHRHs. For the point S from $(910,0)$ to $(910,910)$, the controller finds out 4 RHRHs (Table.6.2). The controller adds these 4 RHRHs to the set of all candidates of start holds which is denoted by St

$$St = V1, V2, V3, V4 \text{ (see in Fig.6.8)}$$

Algorithm 1 Scanning “Right Hand Reachable Hold”

```

1: Generate initial V:
2:  $V \leftarrow \emptyset$ 
3:  $O :=$  the set of all area addresses of the wall;
4: while ( $O$  is not empty) do
5:    $S \leftarrow$  a chosen vertex from the set  $O$ ;
6:    $O \leftarrow O \cap \{S\}$ 
7:   if (RHRH in right hand reachable area) and (at least one hold located in
      the left hand, left leg and right leg reachable areas) then Adds new RHRH to
      set  $V$ ;
8:   end if
9:   Update RHRH’s “family hold groups”;
10: end while

```

Table 6.2: 3 First right hand reachable holds for S (910,270-mm)

V1=H17	V2=H19	V3=H24	V4=H26
H14, V1	H14, V2	H14, V3	H14, V4
H31, H34	H31, H34	H31, H34	H31, H34

Temporarily: $V = V1, V2, V3, V4$

The controller continues to choose the point S from the set O . We remember that the “family hold groups” of old RHRHs maybe be updated related to a new point S , and a new RHRH could be found. For example, when the point S is at the address (910,290), the controller update the information on the RHRHs (Fig.6.9). Finally, we have set V .

$V = V1, V2, V3, \dots, V23$ (see in Fig.6.8)

Similar to “start hold” we define the “final hold”. The “final hold” belongs to the RHRH that is located in the highest row, as shown in Fig.6.8. The controller adds these “final hold” to the set of all final holds (denoted by Fi). Completing the scanning process, we have the result:

$St = V1, V2, V3, V4$

$Fi = V21, V22, V23$

$V = V1, V2, V3, \dots, V23$

6.4.2.2 Cost Evaluations and Building the Graph of “Right Hand Reachable Holds”

In this subsection, we define “adjacent hold” and evaluate the cost between RHRHs; in addition, the controller builds the graph of RHRHs based on these costs. A RHRH[i] is called “adjacent hold” of RHRH[j] if RHRH[i] and RHRH[j] have at least one common family hold group. The cost between two RHRHs is the number of similar “family hold groups”. When moving (climbing) between two adjacent holds having the largest cost, robot has many options to utilize the most advantageous “family hold group” for minimizing energy or avoiding obstacles and also singularity or optimizing the moving distance of desired limb and so on. Therefore, it is obviously beneficial when robot can climb between adjacent holds with the largest costs. Now, we set up the algorithm to find out the cost between two RHRHs (see in Algorithm.2).

First, we define each VRHP as a structure containing elements such as

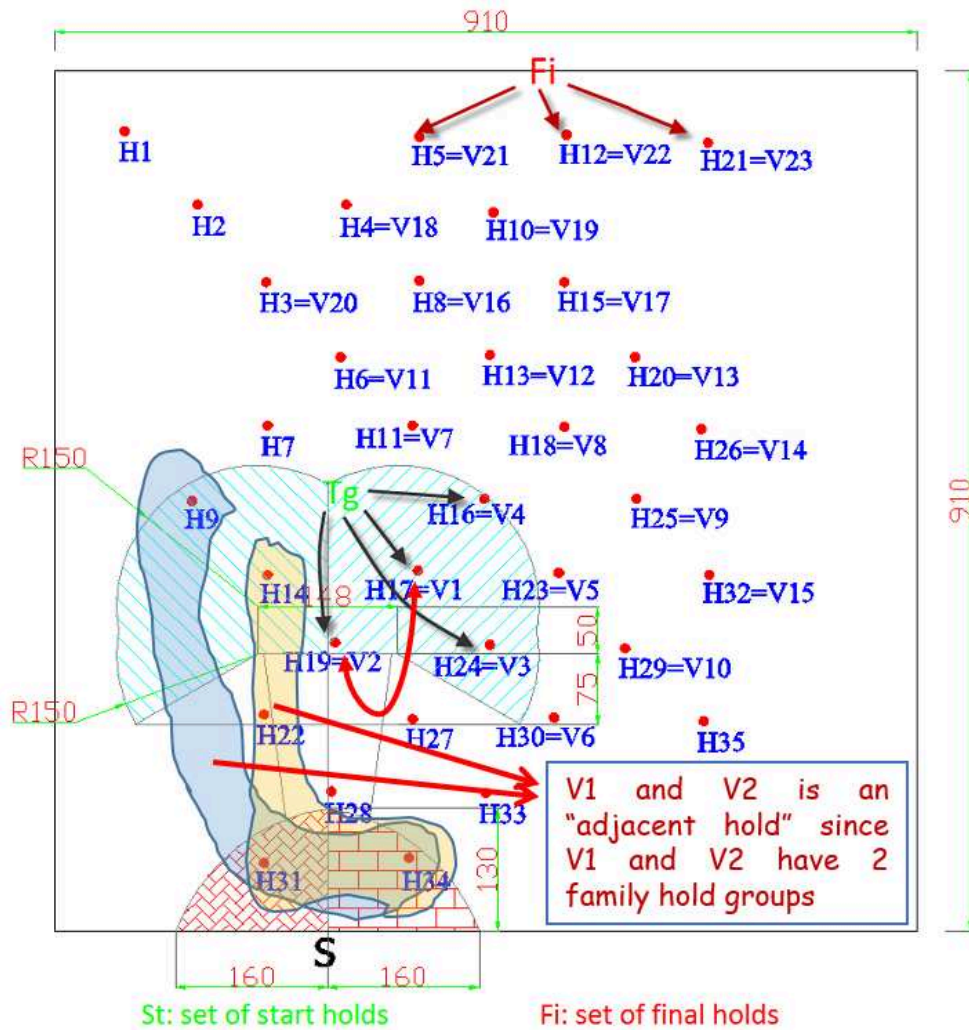


Figure 6.10: Adjacent hold V1 and V2 as an example

$V[3]=$

- $[[H9, V3; H31, H34], [H14, V3; H31, H34], [H19, V3; H31, H34],$
- $[H14, V3; H31, H28], [H7, V3; H31, H34], [H7, V3; H31, H28]]$

$V[3]$ is the third element in the $V[]$ set (in above section), while $V3$ is the valid right hand hold (the hold H24).

Second, we define the “similar operator” between two elements. Elements A and B are similar to each other if $A[1,1]$, $A[2,1]$ and $A[2,2]$ are equal to

Algorithm 2 Cost Evaluations and Building the Graph of “RHRHs”

Input: RHRHs in array

Output: Cost between “adjacent holds”

```

1: Define RHRH;
2: Define the similar operator between two family hold groups: family hold
   groups are similar if the position of both legs and the left hand are similar;
3: Define cost: number of family hold groups between two RHRHs;
4: cost:=0;
5: for (i from 0 to the number of family hold group of  $k^{th}$  RHRH -1 ) do
6:   for (j from 0 to the number of family hold group of  $h^{th}$  RHRH -1) do
7:     if ( $i^{th}$  and  $j^{th}$  family hold group of  $k^{th}$ RHRH and  $h^{th}$ RHRH are similar)
8:       then Set new RHRH to set  $V$ ;
9:     end if
10:  end for

```

$B[1, 1]$, $B[2, 1]$ and $B[2, 2]$ respectively. Using the “for” loop to compare elements between two structures, we increase cost by one if a similar operator occurs. By this way, after comparing all RHRHs with each other, the controller has a matrix containing the cost between every RHRHs.

From this cost result the controller can create the graph (is called Ma-graph) between the “right hand reachable holds”. Obviously climbing robot can move easily between two RHRHs have the large cost (more common “family holds group”), so the goal is to find a path of maximum total cost from “start hold” to “final hold”.

6.4.3 The Query Phase

By using the way where the total cost is maximal, the robot can climb easily. First, the controller builds a new graph in which the complement costs with the maximum value (in the Ma-graph) substitute the old values being the costs

Algorithm 3 Apply Dijkstra Algorithm

Input: The graph from the scanning phase

Output: A path between start and target nodes

```
1: Build the new graph;
2: for (each vertex V in Graph) do
3:   dist [V]:= infinity;
4:   Previous [V]:= undefined;
5: end for
6: dist[source]:=0;
7: Q:= the set of all nodes in Graph;
8: while (Q is not empty) do
9:   u := vertex in Q with smallest distance in dist[];
10:  remove u form Q;
11:  if (dist[u]=infinity:) then
12:    Break;
13:  end if
14:  for (each neighbor v of u) do
15:    alt:=dist[u]+distbetween(u,v);
16:    if (alt<dist[v]) then
17:      dist[v]:=alt;
18:      previous[v]:=u;
19:      decrease - key v in Q;
20:    end if
21:  end for
22: end while
23: return dist;
```

between RHRHs, but the infinity values are kept to identify that robot cannot move between RHRHs which have a zero cost, and we have new graph in Fig.6.11.

With new graph, the easiest route to climb is the path of maximum total cost from “start hold” to “final hold”. The Dijkstra algorithm [23] is used to solve this problem (See Algorithm.3).

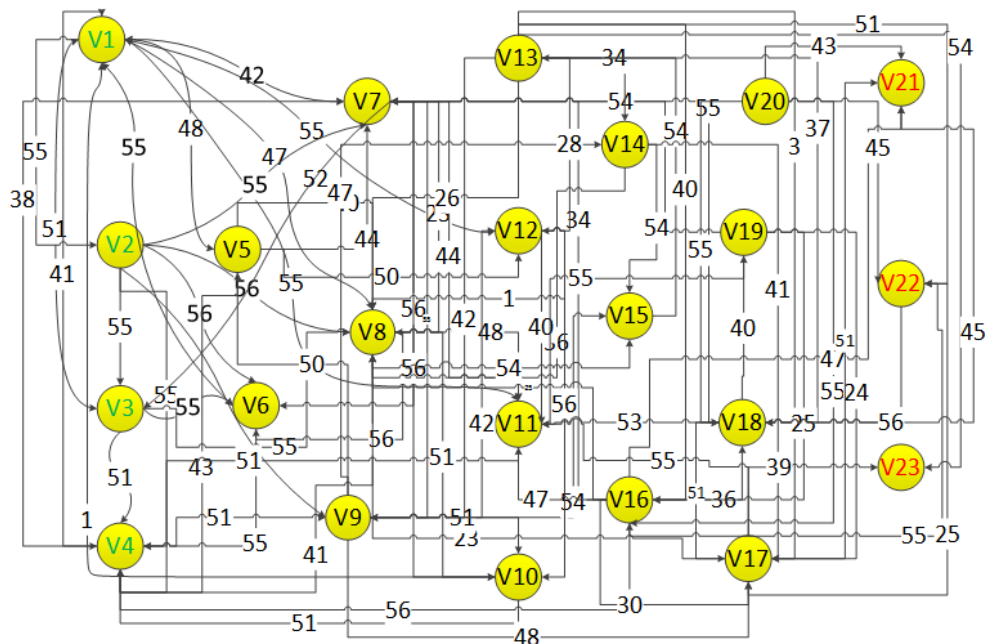


Figure 6.11: The new graph RHRHs

6.5 Local Motion Planning

During the moving, the humanoid robot identifies candidate holds that can be used for contacts in order to move up. Robots usually plan a few moves to reach an intermediate point along the route and then executes. At the beginning and end of each move either a new contact with the terrain is achieved or an existing contact is broken. Therefore, each move is performed at fixed set of contacts, usually three or four contacts. The postures between four and three contacts are adjusted to change the position of the robot’s CoM.

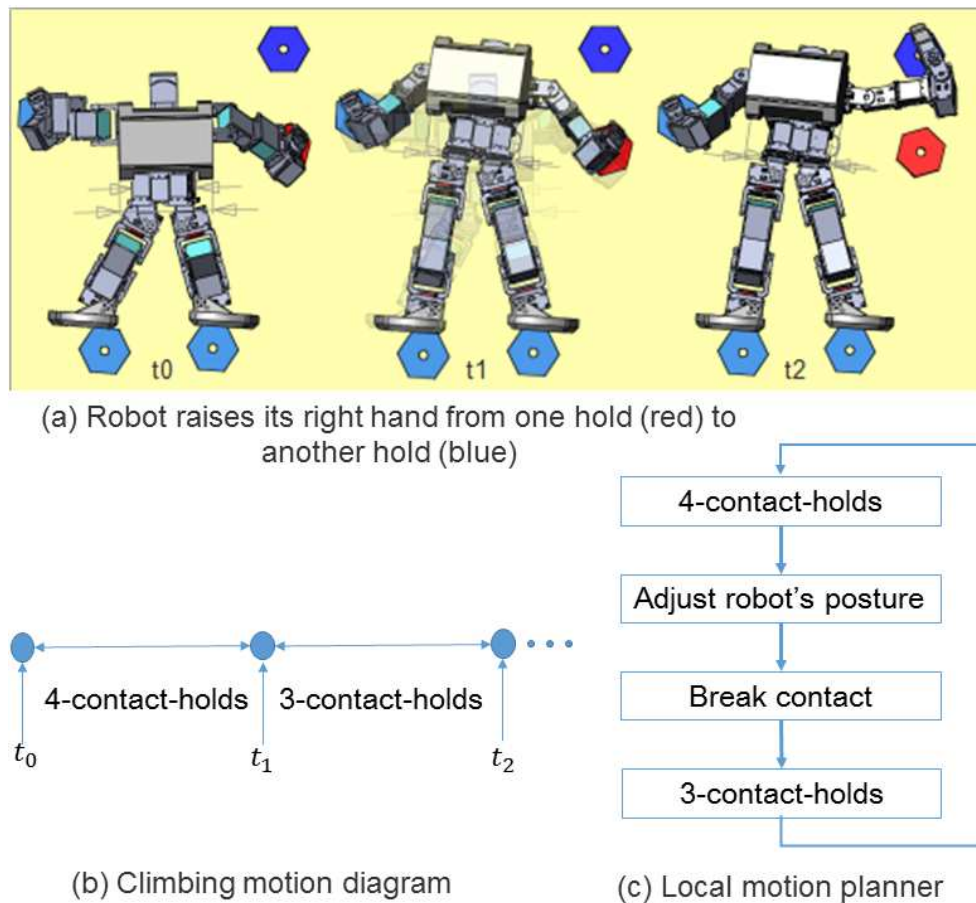


Figure 6.12: Detail local motion planning

In local motion planning, we assume that the short-term goal is to move the robot right hand, currently at a red hold, to a new blue hold (see in Fig6.12(a)). To break the contact, the robot must first adjust its posture to redistribute the contact forces over the other three limbs, so that the contact force applied on the red hold by the right hand becomes 0. See Fig6.12(a). At the time t_0 where each of robot limbs are positioned at the 4 climbing holds. We call this set a 4-contact-holds. The robot breaks the contact at the red hold at time t_1 , and move at a 3-contact-holds (set of 3 contacted holds). The robot's right hand reaches the blue hold (local target hold) at the time t_2 (see in Fig6.12(b)).

To continue climbing, the robot will then have to break contact at one of the other three limbs, and then reach a new hold with the corresponding limb,

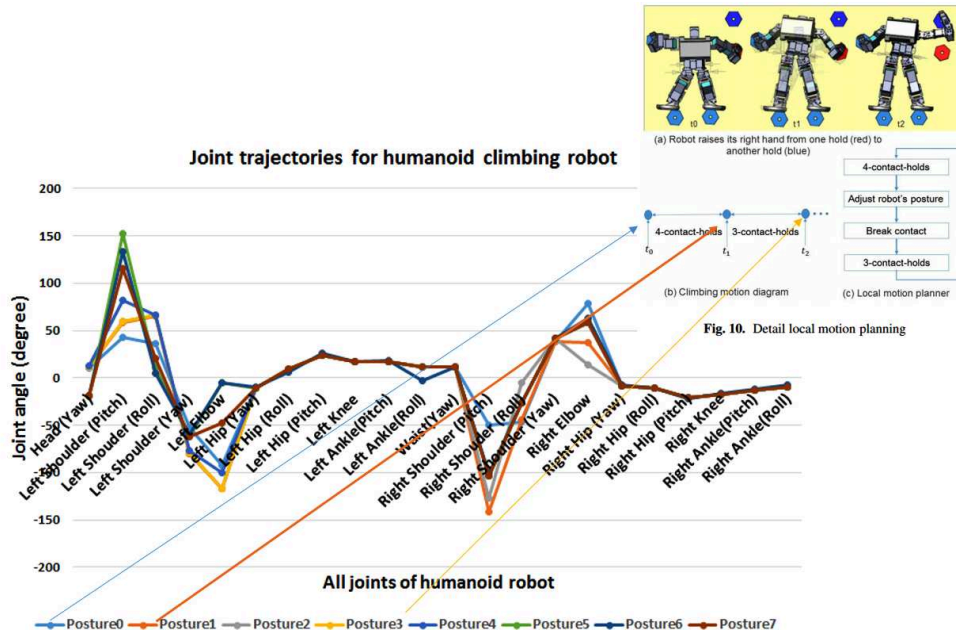


Figure 6.13: Joint trajectories example

etc...(see in Fig6.12(c)). So overall, the entire climbing motion consists of successive moves. By applying this local planning, the humanoid robot can calculate the individual joint angles for each of the robot's joints. In Fig6.13 is an example of applying local motion planning to determine all joint angles. At the posture 0 (at the time t_0), the robot keeps balance on the wall by 4-contact-holds. From the posture 0 to posture 1, robot adjusts the its body (at the time t_1). Therefore at the posture 3, the robot raises its right hand to reach a new climbing hold (at the time t_2). In the same manner, from the posture 4 to posture 7, robot raises its left hand to reach a new climbing hod.

6.6 Experiment with an Example

We implemented our global path and local motion planning on KHR-3HV robot. Using the planner, the robot can climbs up freely along the designed route. Of course, free-climbing also requires various sensor feedback (vision, force sensor...) to make the climbing more precise and robust. However, for our example, an

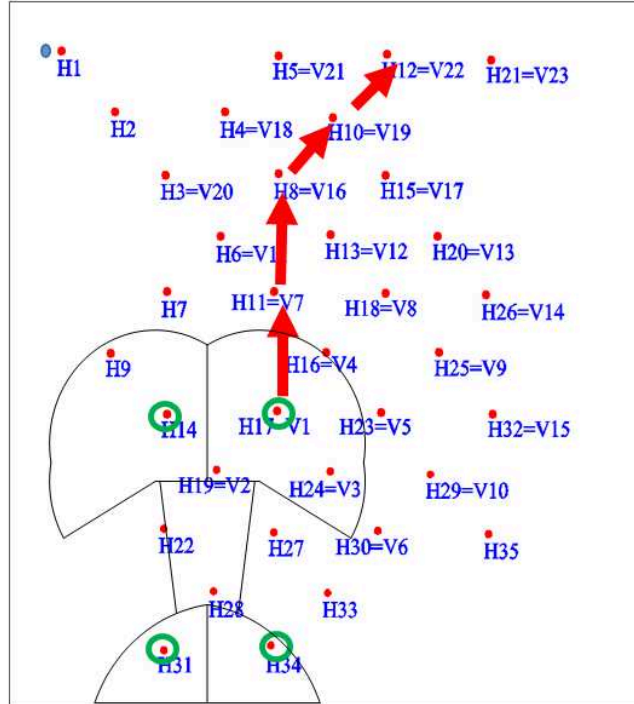


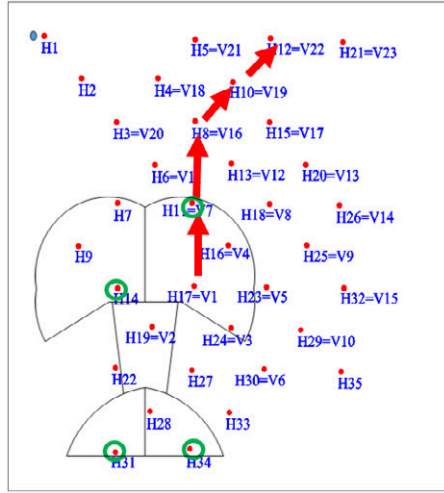
Figure 6.14: Robot start to climb at V1

open-loop position controller is implemented without sensor feedback on the robot to execute the trajectory at very slow velocity to reduce positioning errors and slipping risks.

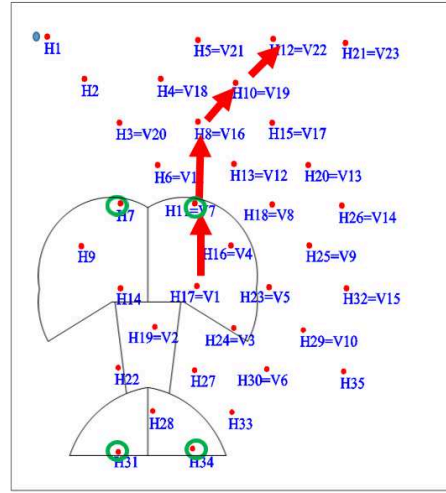
As input, the motion planning through the Kinect sensor receives all information of the climbing wall configuration (a list of all hold's positions) and the robot's initial position. The motion planning is executed. As output, the planner either generates a route (list of all joint-angle waypoints- see in Fig.6.13) to be passed to the control system, or indicates that could not found a route.

In this example, the climbing wall configuration is shown in Fig. 6.2. The path of right hand[V1]-[V7]-[V16]-[V19]-[V22] was found on the current climbing wall configuration.

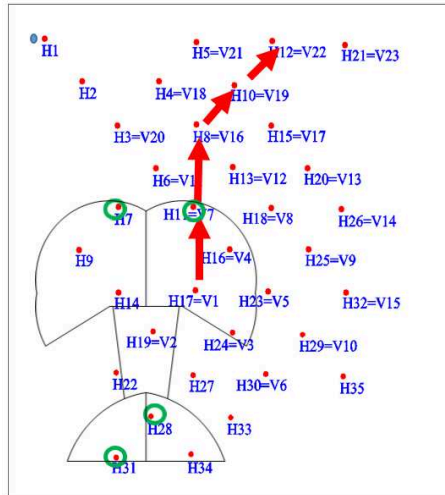
The humanoid robot starts climbing the wall with “the start hold” V[1]. The “family holds group” of V[1] which the robot uses to keep balance in this step is



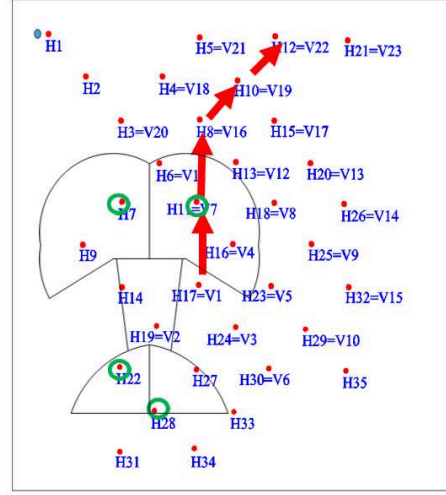
(a) Robot's position at $\begin{bmatrix} H14 & V7 \\ H31 & H34 \end{bmatrix}$



(b) Robot's position at $\begin{bmatrix} H7 & V7 \\ H31 & H34 \end{bmatrix}$



(c) Robot's position at $\begin{bmatrix} H7 & V7 \\ H31 & H28 \end{bmatrix}$

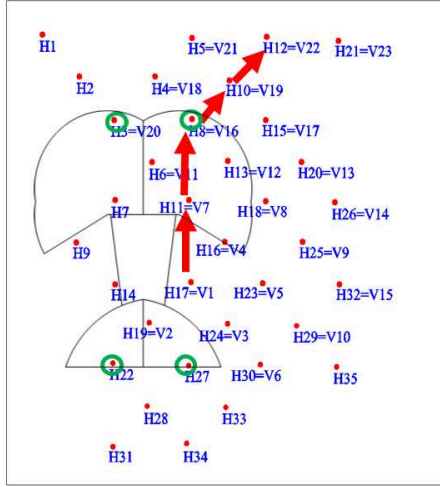


(d) Robot's position at $\begin{bmatrix} H7 & V7 \\ H22 & H28 \end{bmatrix}$

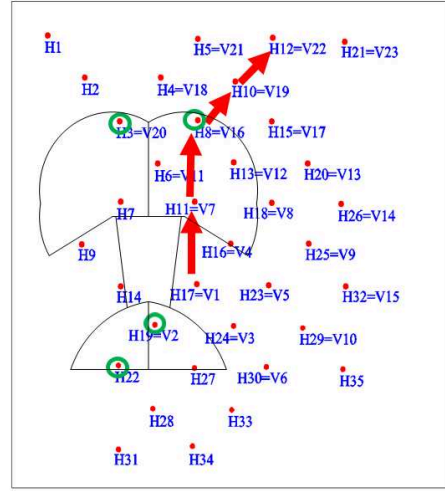
Figure 6.15: Sequence of family hold group from V[2] to V[7]

$\begin{bmatrix} H14 & V1 \\ H31 & H34 \end{bmatrix}$ (show in Figure 6.19(24[s]) and Figure 6.14).

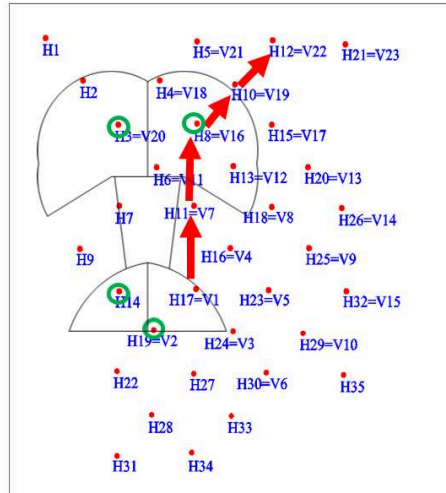
When the robot move the right hand form the V[2] to V[7] (see in Fig.6.19(24[s])-36[s] and Figure 6.15). The sequence of “family holds group” is:



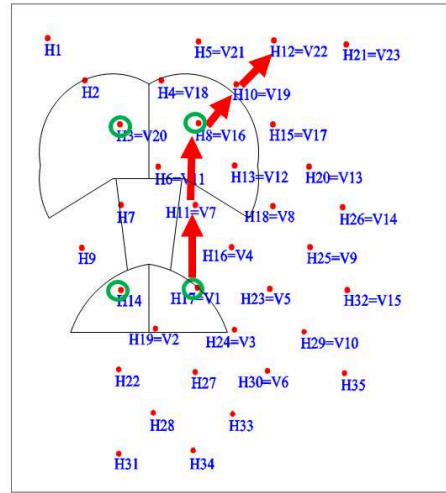
(a) Robot's position at $\begin{bmatrix} H3 & V16 \\ H22 & H27 \end{bmatrix}$



(b) Robot's position at $\begin{bmatrix} H3 & V16 \\ H22 & H19 \end{bmatrix}$



(c) Robot's position at $\begin{bmatrix} H3 & V16 \\ H14 & H19 \end{bmatrix}$

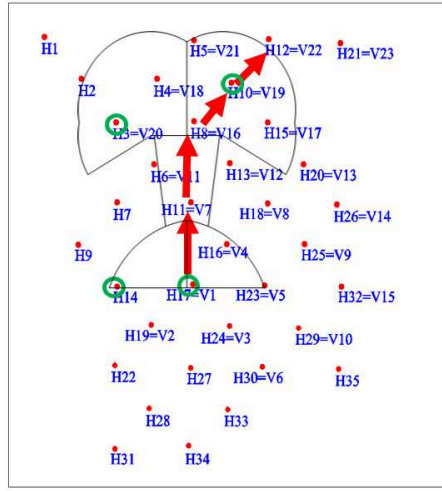


(d) Robot's position at $\begin{bmatrix} H3 & V16 \\ H14 & H17 \end{bmatrix}$

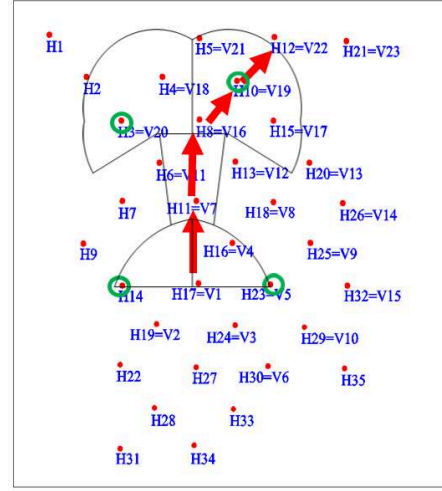
Figure 6.16: Sequence of family hold group from V[7] to V[16]

$$\begin{bmatrix} H14 & V7 \\ H31 & H34 \end{bmatrix} - \begin{bmatrix} H7 & V7 \\ H31 & H34 \end{bmatrix} - \begin{bmatrix} H7 & V7 \\ H31 & H28 \end{bmatrix} - \begin{bmatrix} H7 & V7 \\ H22 & H28 \end{bmatrix}$$

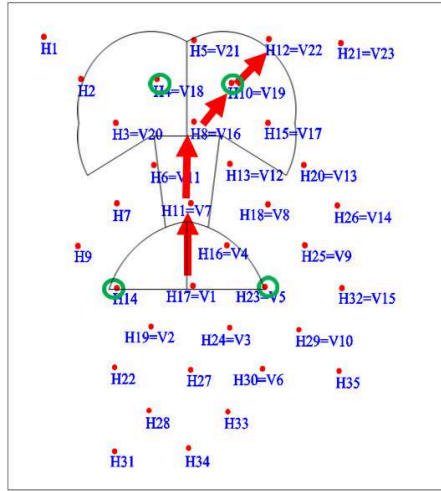
When the robot move the right hand form the V[7] to V[16] (see in Fig.6.19(36[s]-64[s])and Figure 6.16). The sequence of “family holds group” is:



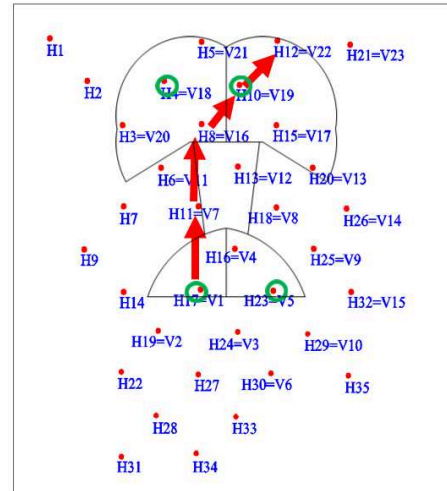
(a) Robot's position at $\begin{bmatrix} H3 & V19 \\ H14 & H17 \end{bmatrix}$



(b) Robot's position at $\begin{bmatrix} H3 & V19 \\ H14 & H23 \end{bmatrix}$



(c) Robot's position at $\begin{bmatrix} H4 & V19 \\ H14 & H23 \end{bmatrix}$

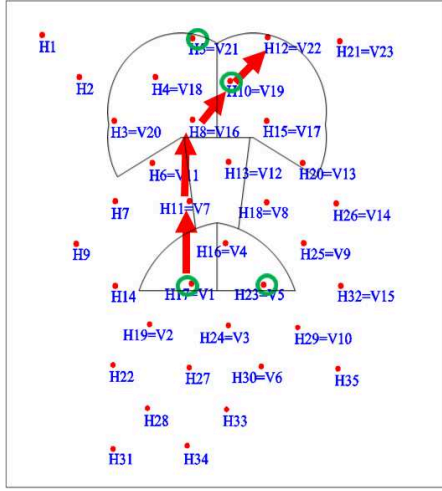


(d) Robot's position at $\begin{bmatrix} H4 & V19 \\ H17 & H23 \end{bmatrix}$

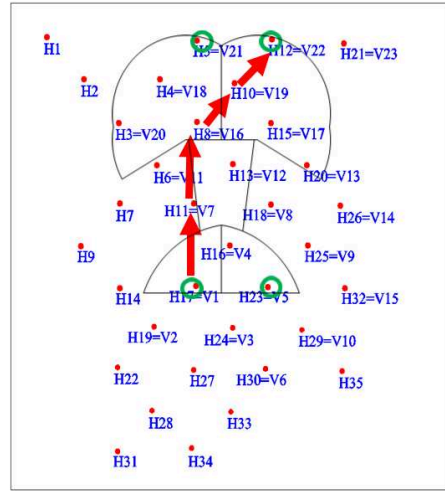
Figure 6.17: Sequence of family hold group from V[16] to V[19]

$$\begin{bmatrix} H3 & V16 \\ H22 & H27 \end{bmatrix} - \begin{bmatrix} H3 & V16 \\ H22 & H19 \end{bmatrix} - \begin{bmatrix} H3 & V16 \\ H14 & H19 \end{bmatrix} - \begin{bmatrix} H3 & V16 \\ H14 & H17 \end{bmatrix}$$

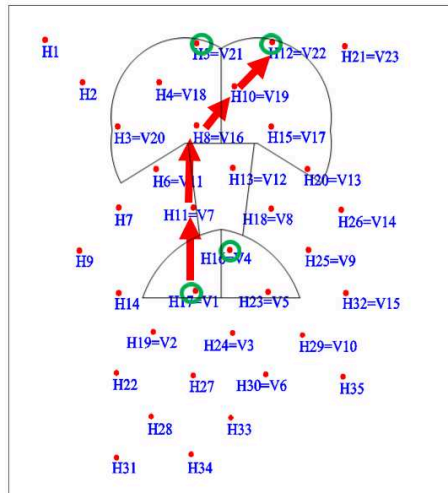
When the robot move the right hand form the V[16] to V[19] (see in Fig.6.19(64[s]-94[s]) and Figure 6.17). The sequence of “family holds group” is:



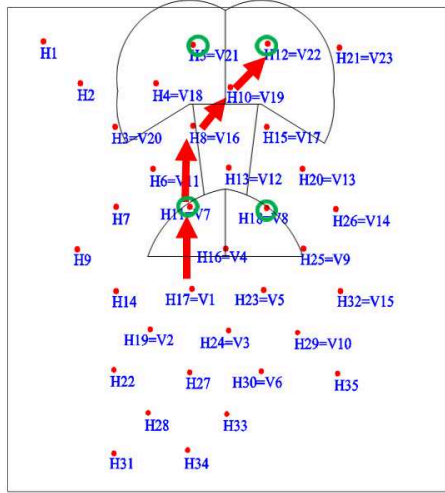
(a) Robot's position at $\begin{bmatrix} H5 & V19 \\ H17 & H23 \end{bmatrix}$



(b) Robot's position at $\begin{bmatrix} H5 & V22 \\ H17 & H23 \end{bmatrix}$



(c) Robot's position at $\begin{bmatrix} H5 & V22 \\ H17 & H16 \end{bmatrix}$



(d) Robot's position at $\begin{bmatrix} H5 & V22 \\ H11 & H18 \end{bmatrix}$

Figure 6.18: Sequence of family hold group from V[19] to V[22]

$$\begin{bmatrix} H3 & V19 \\ H14 & H17 \end{bmatrix} - \begin{bmatrix} H3 & V19 \\ H14 & H23 \end{bmatrix} - \begin{bmatrix} H4 & V19 \\ H14 & H23 \end{bmatrix} - \begin{bmatrix} H4 & V19 \\ H17 & H23 \end{bmatrix}$$

When the robot move the right hand form the V[19] to V[22] (see in Fig.6.19(104[s]-154[s])and Figure 6.18). The sequence of “family holds group” is:

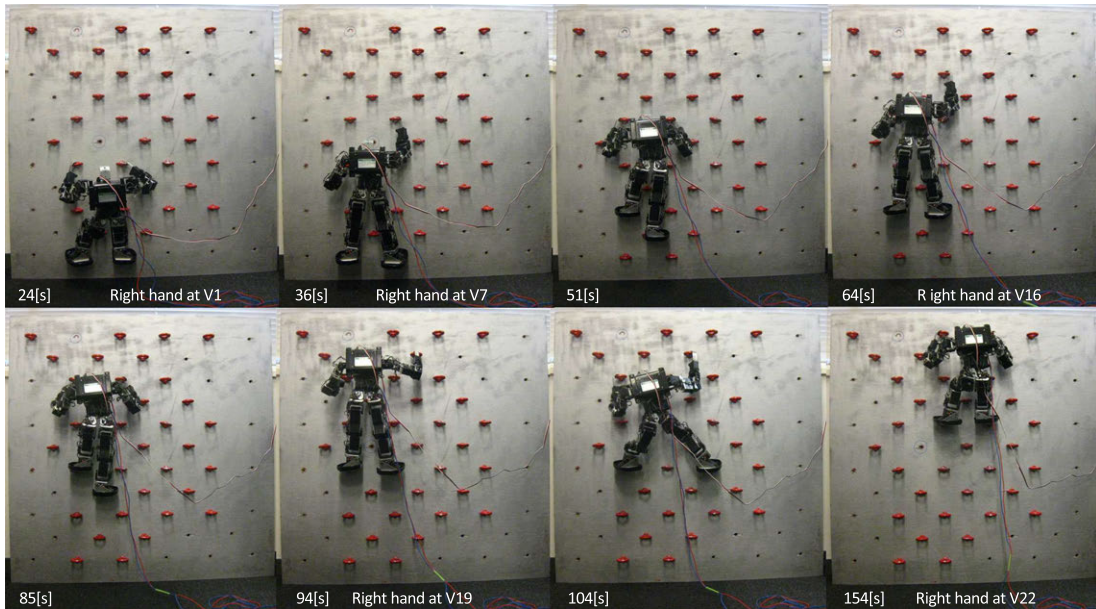


Figure 6.19: Snapshots of humanoid climbing robot along the best route.

$$\begin{bmatrix} H5 & V19 \\ H17 & H23 \end{bmatrix} - \begin{bmatrix} H5 & V22 \\ H17 & H23 \end{bmatrix} - \begin{bmatrix} H5 & V22 \\ H17 & H16 \end{bmatrix} - \begin{bmatrix} H5 & V22 \\ H11 & H18 \end{bmatrix}$$

Lessons from experiments.

KHR-3HV is well designed and robust, capable of precise joint angle control. However, in this experiment several limitations remain. For example, the robot is controlled by joint-angle control, achieving desired posture but not always desired force. In addition, the robot is unable to measure its position by lacking sensing. There is main reason leading to the falling of the robot during the experiment.

Given these limitations, it is remarkable that the humanoid robot can climb at all. With any climbing wall configuration as input, the planner computed to give the easiest route for the right hand. Combining with a “family hold group” of each right-hand holds on this route, the planner generates a joint-angle trajectory for the robot.

6.7 Conclusion and Future work

In this paper, the trajectory for an autonomously operating humanoid robot to climb up a wall has been described. The Kinect sensor is used to detect the climbing hold positions, and we addressed the problem of motion planning for humanoid climbing robots. Then the “Right Hand Search Algorithm” is developed to determine the route to climb up the wall. This algorithm compared these paths to find out the best route based on the ease of the climbing (which is described in subsection 4.2.2). Then, local motion planning is proposed to support the robot in each rudimentary movement while the humanoid robot is following the global path. Finally, experiments demonstrate that our humanoid robot can reliably climb the rudimentary climbing wall.

6.7.1 Future work

In this paper, we only consider the global sensing to discern a global path, and the local motion planning for a humanoid climbing robot. In the next step, a local camera is used to allow the robot to acquire information about the details of local terrain while climbing. The robot controller is applied the vision feedback; consequently a robot’s limbs can accurately reach climbing holds at a computed location. Thank for this, the robot’s trajectory can be modified in real-time when other small errors occur. In addition, each limb will be equipped with a force sensor, which is used by the robot controller to not only keep robot balanced on the wall, but also to adjust the robot’s center of mass. We propose that additional new sensors will increase the ability of humanoid climbing robot.

Chapter 7

Conclusion and Future Work

7.1 Conclusion

This dissertation describes a research with respect to humanoid free climbing robot. The main object is develop humanoid robot, which which can climb up autonomously a vertical climbing wall while using the climbing technical similar to those develop by climber. At the beginning, robot typically starts by looking at the entire wall to propose an effective strategy. During the moving, humanoid climbing robot without any special tool, just only use climbing technical that developed by human. This robot is expected to be useful to support rescue teams in disaster area searching trapped climbers on the mountain, or even exploring rock faces on the solar system.

In this dissertation, my first contribution was the development of hard ware for humanoid climbing robot. Then, a rudimentary analysis of mechanical structure, and kinematic aspects of humanoid climbing robot are analyzed in detail. Moreover, there are many useful climbing technical that developed by human is presented and applied to humanoid climbing robot. At last, a 3D humanoid climbing robot is simulated in Matlab-Simmechanics environment. With this 3D model we can simulate some basic climbing actions. The center of gravity's positions of robot while maintaining balance are calculated and recorded for further research.

My second dissertation was motion control for four limb climbing robot, and a set of algorithm to support humanoid climbing robot: I propose a global planning algorithm for the humanoid robot using data from Kinect. The proposed algorithm ensures that the climbing robot finds the best route to climb up the wall. During climbing, the humanoid robot utilizes the local planning algorithm, base on quasi static equilibrium, to adjusts its body posture in order to remain in equilibrium state.

My third contribution was integrated implementation for a real humanoid robot (Kondo KHR-3HV robot). Using the planning algorithm presented in this dissertation, my controller could find the best route for robot, and free climbed the ring climbing wall (Chapter 5).

7.2 Future works

This section briefly outlines the directions of future work.

Hardware development

Humanoid robot's foot will be modified to increase the working area. Moreover, the robot's hands should be wrapped with rubber. Conceptually, this modification is quite similar to which climbers use shoes to increase the friction contact between their limbs and climbing holds.

Incremental sensing

The robot should be quipped with local camera (attracted robot's head), and force sensor that will be used by motion controller.

Developing motion planning Many useful climbing technique should be apply to humanoid robot to develop motion planning. Such that, "best pose" for the robot when robot keeps balance, or "changing pose" before release climbing holds

References

- [1] Humanoid robots from Honda. [Online]. Available: <http://www.asimo.honda.com/>.
- [2] [Online]. Available: <http://www.humanoid.waseda.ac.jp/>.
- [3] Boston Dynamics [Online]. Available: <http://www.bostondynamics.com/>.
- [4] Aldebaran robotics [Online]. Available: <https://www.aldebaran.com/en>.
- [5] ROBOTIS. Open platform humanoid project [Online]. Available: <http://www.robotis.com/xen/darwin-en>.
- [6] Fujisoft, Inc. PALRO (in japanese) [Online]. Available: <http://palro.jp/>.
- [7] Products of Kondo Kagaku Co. Ltd. (in Japanese) [Online]. Available: <http://kondo-robot.com/product/>.
- [8] Schaft team. [Online]. Available: <http://spectrum.ieee.org/automation/robotics/humanoids/schaft-robot-company-bought-by-google-darpa-robotics-challenge-winner>.
- [9] DARPA Robotics Challenge. [Online]. Available: <http://www.theroboticschallenge.org/>.
- [10] Kinect Sensor [Online]. Available: <http://www.microsoft.com/en-us/kinectforwindows/>.
- [11] OpenNI [Online]. Available: <http://www.openni.org/>.

-
- [12] ALAN T ASBECK, SANGBAE KIM, MARK R CUTKOSKY, WILLIAM R PROVANCHER, AND MICHELE LANZETTA. Scaling hard vertical surfaces with compliant microspine arrays. *The International Journal of Robotics Research*, **25**(12):1165–1179, 2006.
- [13] CARLOS BALAGUER, ANTONIO GIMENEZ, AND ALBERTO JARDÓN. Climbing robots mobility for inspection and maintenance of 3d complex environments. *Autonomous Robots*, **18**(2):157–169, 2005.
- [14] PETER BEAL. *Bouldering: Movement, Tactics, and Problem Solving*. Mountaineers Books, October 2011.
- [15] TIM BRETTL, STEPHEN ROCK, JEAN-CLAUDE LATOMBE, BRETT KENNEDY, AND HRAND AGHAZARIAN. Free-climbing with a multi-use robot. In *Experimental Robotics IX*, pages 449–458. Springer, 2006.
- [16] TIMOTHY BRETTL, TERESA MILLER, STEPHEN ROCK, AND JEAN-CLAUDE LATOMBE. Climbing robots in natural terrain. *terrain (eg, ducts and pipes)*, **1**:12, 2003.
- [17] TIMOTHY BRETTL, STEPHEN ROCK, AND J-C LATOMBE. Motion planning for a three-limbed climbing robot in vertical natural terrain. In *Robotics and Automation, 2003. Proceedings. ICRA '03. IEEE International Conference on*, **3**, pages 2946–2953. IEEE, 2003.
- [18] TIMOTHY WOLFE BRETTL. *Multi-step motion planning: Application to free-climbing robots*. PhD thesis, Citeseer, 2005.
- [19] W. BROCKMANN. in *Climbing and Walking Robots*, M. O. Tokhi, G. S. Virk, and M. A. Hossain, Eds. Springer, pp.107-114., 2006.
- [20] G. CARBONE, HUN OK LIM, A. TAKANISHI, AND M. CECCARELLI. Numerical and experimental estimation of stiffness performances for the humanoid robot wabian-rv. In *Advanced Intelligent Mechatronics, 2003. AIM 2003. Proceedings. 2003 IEEE/ASME International Conference on*, **2**, pages 962–967 vol.2, July 2003.

-
- [21] BAEK-KYU CHO, SANG-SIN PARK, AND JUN-HO OH. Controllers for running in the humanoid robot, hubo. In *Humanoid Robots, 2009. Humanoids 2009. 9th IEEE-RAS International Conference on*, pages 385–390, Dec 2009.
- [22] JEANNE DIETSCH, BRETT KENNEDY, AVI OKON, HRAND AGHAZARIAN, MIRCEA BADESCU, XIAOQI BAO, YOSEPH BAR-COHEN, ZENSHEU CHANG, BORNA E DABIRI, MIKE GARRETT, ET AL. Lemur iib: a robotic system for steep terrain access. *Industrial Robot: An International Journal*, **33**(4):265–269, 2006.
- [23] E. W DIJKSTRA. A note on two problems in connexion with graphs. *Numerische Mathematik 1: 269-271*. DOI:10.1007/BF01386390., 1959.
- [24] LE TIEN DUNG, HEE-JUN KANG, AND YOUNG-SHICK RO. Robot manipulator modeling in matlab-simmechanics with pd control and online gravity compensation. In *Strategic Technology (IFOST), 2010 International Forum on*, pages 446–449, Oct 2010.
- [25] AKIRA SHIMADA DUNG ANH NGUYEN. A consideration of mechanical structure for climbing robots. In *IEEJ Technical meeting, IIC-12-80*, 2012.
- [26] G. ZURLO F. CEPOLINA, M. ZOPPI AND R. MOLFINO. A robotic cleaning agency. in *Proc. of IAS2004 8th Conf. on Intelligent Autonomous Systems, The Netherlands*, pp. 1153-1161., 2004.
- [27] XUESHAN GAO AND KOKI KIKUCHI. Study on a kind of wall cleaning robot. In *Robotics and Biomimetics, 2004. ROBIO 2004. IEEE International Conference on*, pages 391–394. IEEE, 2004.
- [28] BILL GOODWINE AND JOEL W BURDICK. Motion planning for kinematic stratified systems with application to quasi-static legged locomotion and finger gaiting. *Robotics and Automation, IEEE Transactions on*, **18**(2):209–222, 2002.
- [29] N. XI H. CHEN, W. SHENG AND J. TAN. Motion control of a micro biped robot for nondestructive structure inspection. in *Proc. of the IEEE ICRA, Barcelona, Spain*, pp. 480-485, 2005.

-
- [30] T. H. KANG J. H. LEE H. R. CHOI, S. M. RYEW AND H. M. A wall climbing robot with closed link mechanism. In *in Proc. of the IEEE/RSJ IROS, pp. 2006-2011*, 2000.
- [31] R. LIU H. ZHANG, J. ZHANG AND G. ZONG. A novel approach to pneumatic position servo control of a glass wall cleaning robot. *in Proc. of the IEEE/RSJ IROS , Sendai, Japan, pp 467-472*, 2004.
- [32] KRIS HAUSER. *MOTION PLANNING FOR LEGGED AND HUMANOID ROBOTS*. PhD thesis, STANFORD UNIVERSITY, 2008.
- [33] KRIS HAUSER, TIMOTHY BRETLE, AND J-C LATOMBE. Learning-assisted multi-step planning. In *Robotics and Automation, 2005. ICRA 2005. Proceedings of the 2005 IEEE International Conference on*, pages 4575–4580. IEEE, 2005.
- [34] KRIS HAUSER AND JEAN-CLAUDE LATOMBE. Multi-modal motion planning in non-expansive spaces. *The International Journal of Robotics Research*, 2009.
- [35] SETH HUTCHINSON GEORGE A. KANTOR WOLFRAM BURGARD LYDIA E. KAVRAKI SEBASTIAN THRUN HOWIE CHOSET, KEVIN M. LYNCH. *Principles of Robot Motion: Theory, Algorithms, and Implementations*,. A Bradford Book,, May, 2005.
- [36] H. KOBAYASHI K. SHIRAI I. KATO, S. OHTERU AND A. UCHIYAMA. Information-power machine with senses and limbs (wabot -1). In *1st CISM-IFTOMM Symposium on theory and practice of Robots and Manipulators*, 1973.
- [37] TACHI S. ET AL. INOUE, H. Hrp: Humanoid robotics project of meti. In *Proc. IEEE-RAS Int. Conf. Humanoid Robots*, 2000.
- [38] TACHI S. ET AL. INOUE, H. Overview of humanoid robotics project of meti. In *Proc. Int. Symp. Robotics 1478 - 482*, 2001.

-
- [39] A. GIMENEZ J. C. RESINO, A. JARDN AND C. BALAGUER. Analysis of the direct and inverse kinematics of roma ii robot. *in Climbing and Walking Robots*, M. O. Tokhi, G. S. Virk, and M. A. Hossain, Eds. Springer, pp.869-874, 2006.
- [40] J. XIAO J. XIAO, N. XI AND J. TAN. Multi-sensor referenced gait control of a miniature climbing robot. *in Proc. of the IEEE/RSJ IROS, Las Vegas, Nevada, USA*, pp. 3656-3661, 2003.
- [41] N. XI J. XIAO, J. XIAO AND W. SHENG. Fuzzy system approach for task planning and control of micro wall climbing robots. *in Proc. of the IEEE ICRA*, pp. 5033-5038, 2004.
- [42] D. SUN J. ZHU AND S.-K. TSO. Application of a service climbing robot with motion planning and visual sensing. *Journal of Robotic Systems*, vol. 20, no. 4, pp. 189-199, 2003.
- [43] C. HILLENBRAND K. BERNS, T. BRAUN AND T. LUKSCH. Developing climb-ing robots for education. *in Climbing and Walking Robots*, M. Armada and P. de Santos, Eds. Springer, pp. 981-988., 2005.
- [44] W. KAHAN. Lectures on computational aspects of geometry. *Department of Electrical Engineering and Computer Sciences*, 1983.
- [45] K. KANEKO, K. HARADA, F. KANEHIRO, G. MIYAMORI, AND K. AKACHI. Humanoid robot hrp-3. In *Intelligent Robots and Systems, 2008. IROS 2008. IEEE/RSJ International Conference on*, pages 2471–2478, Sept 2008.
- [46] K. KANEKO, F. KANEHIRO, S. KAJITA, H. HIRUKAWA, T. KAWASAKI, M. HIRATA, K. AKACHI, AND T. ISOZUMI. Humanoid robot hrp-2. In *Robotics and Automation, 2004. Proceedings. ICRA '04. 2004 IEEE International Conference on*, **2**, pages 1083–1090 Vol.2, April 2004.
- [47] K. KANEKO, F. KANEHIRO, M. MORISAWA, K. AKACHI, G. MIYAMORI, A. HAYASHI, AND N. KANEHIRA. Humanoid robot hrp-4 - humanoid robotics platform with lightweight and slim body. In *Intelligent Robots and*

-
- Systems (IROS), 2011 IEEE/RSJ International Conference on*, pages 4400–4407, Sept 2011.
- [48] TAEHUN KANG, HYUNGSEOK KIM, TAEYOUNG SON, AND HYOUKRYEOL CHOI. Design of quadruped walking and climbing robot. In *Intelligent Robots and Systems, 2003. (IROS 2003). Proceedings. 2003 IEEE/RSJ International Conference on*, **1**, pages 619–624. IEEE, 2003.
- [49] SANGBAE KIM, MATTHEW SPENKO, SALOMON TRUJILLO, BARRETT HEYNEMAN, VIRGILIO MATTOLI, AND MARK R. CUTKOSKY. Whole body adhesion: hierarchical, directional and distributed control of adhesive forces for a climbing robot. In *In IEEE International Conference on Robotics and Automation*, pages 1268–1273, April 2007.
- [50] S. P. KROSURI AND M. A. MINOR. A multifunctional hybrid hip joint for improved adaptability in miniature climbing robots. in *Proc. of the IEEE ICRA , Taipei, Taiwan, 2003*.
- [51] HONG D. LAHR, D. The development of charli: A linear actuated powered full size humanoid robot. In *In: Proceedings of the International Conference on Ubiquitous Robots and Ambient Intelligence (URAI 2008)*, November.
- [52] BOKMAN LIM, JUSUK LEE, JOOHYUNG KIM, MINHYUNG LEE, HOSEONG KWAK, SUNGGU KWON, HEKUK LEE, WOONG KWON, AND KYUNGSHIK ROH. Optimal gait primitives for dynamic bipedal locomotion. In *Intelligent Robots and Systems (IROS), 2012 IEEE/RSJ International Conference on*, pages 4013–4018, Oct 2012.
- [53] STEPHEN PAUL LINDER, EDWARD WEI, AND ALEXANDER CLAY. Robotic rock climbing using computer vision and force feedback. In *Robotics and Automation, 2005. ICRA 2005. Proceedings of the 2005 IEEE International Conference on*, pages 4685–4690. IEEE, 2005.
- [54] JIANHUA LIU, GUOJIN CHEN, YOUPING GONG, AND HUIPENG CHEN. Modeling and simulation of loader working device based on simmechanics. In *Transportation, Mechanical, and Electrical Engineering (TMEE), 2011 International Conference on*, pages 2054–2057, Dec 2011.

-
- [55] S. LOHMEIER, T. BUSCHMANN, AND H. ULBRICH. Humanoid robot lola. In *Robotics and Automation, 2009. ICRA '09. IEEE International Conference on*, pages 775–780, May 2009.
- [56] D. LONGO AND G. MUSCATO. Design of a single sliding suction cup robot for inspection of non porous vertical wall. In *in Proc. of the 35th Int.Symp. on Rob. , Paris, France, pp. 1153 -1161*, 2004.
- [57] ZHIGUO LU, T. AOYAMA, K. SEKIYAMA, Y. HASEGAWA, AND T. FUKUDA. Vertical ladder climbing down motion with internal stress adjustment for a multi-locomotion robot. In *Micro-NanoMechatronics and Human Science (MHS), 2011 International Symposium on*, pages 403–408, Nov 2011.
- [58] JINGRU LUO, YAJIA ZHANG, K. HAUSER, H.A. PARK, M. PALDHE, C.S.G. LEE, M. GREY, M. STILMAN, JUN HO OH, JUNGHO LEE, IN-HYEOK KIM, AND P. OH. Robust ladder-climbing with a humanoid robot with application to the darpa robotics challenge. In *Robotics and Automation (ICRA), 2014 IEEE International Conference on*, pages 2792–2798, May 2014.
- [59] E. GARCA M. PRIETO M. A. ARMADA, P. G. DE SANTOS AND S. NABULSI. Design of mobile robots. *in Proc. of the CLAWAR: Introductory Mobile Robotics Workshop , London, UK, pp. 2890-2895.*, 2005.
- [60] G. DANGHI R. MUKHERJEE R. L. TUMMALA M. MINOR, H. DULIMARTA AND D. ASLAM. Design, implementation, and evaluation of an under-actuated miniature biped climbing robot. *in Proc. of the IEEE/RSJ IROS, pp. 1999-2005*, 2000.
- [61] G. NELSON M. RAIBERT, K. BLANKESPOOR AND R. PLAYTER. Bigdog, the rough-terrain quadruped robot. In *Proc. 17th IFAC World Congress*, pages 10822–10825, June 2008.

-
- [62] GIRISH DANGHI RANJAN MUKHERJEE R.LAL TUMMALA DEAN ASLAM MARK MINOR, HANS DULIMARTA. Design, implementation, and evaluation of an under-actuated miniature biped climbing robot. *in Proc. of the IEEE/RSJ IROS, Takamasu*, 2000.
- [63] GIORGIO METTA, LORENZO NATALE, FRANCESCO NORI, GIULIO SANDINI, DAVID VERNON, LUCIANO FADIGA, CLAES VON HOFSTEN, KERSTIN ROSANDER, MANUEL LOPES, JOSÉ SANTOS-VICTOR, ET AL. The icub humanoid robot: An open-systems platform for research in cognitive development. *Neural Networks*, **23**(8):1125–1134, 2010.
- [64] TERESA G. MILLER. *Control of a Climbing Robot Using Real-time Convex Optimization*. PhD thesis, Stanford, CA, USA, 2008. AAI3292395.
- [65] TERESA G MILLER, TIMOTHY W BRETL, AND STEPHEN ROCK. Control of a climbing robot using real-time convex optimization. In *Mechatronic Systems*, **4**, pages 409–414, 2006.
- [66] BEHNAM MIRIPOUR. *Climbing and Walking Robots*. In-Tech, March 2010.
- [67] M. SACK J. SAENZ N. ELKMANN, T. FELSCH AND J. HORTIG. Innovative service robot systems for facade cleaning of difficult-to-access areas. *in Proc. of the IEEE/RSJ IROS* , pp. 756-762., 2002.
- [68] GABE NELSON, AARON SAUNDERS, NEIL NEVILLE, BEN SWILLING, JOE BONDARYK, DEVIN BILLINGS, CHRIS LEE, ROBERT PLAYTER, AND MARC RAIBERT. Petman: A humanoid robot for testing chemical protective clothing. *Journal of the Robotics Society of Japan*, **30**(4):372–377, 2012.
- [69] S. NODA, M. MUROOKA, S. NOZAWA, Y. KAKIUCHI, K. OKADA, AND M. INABA. Generating whole-body motion keep away from joint torque, contact force, contact moment limitations enabling steep climbing with a real humanoid robot. In *Robotics and Automation (ICRA), 2014 IEEE International Conference on*, pages 1775–1781, May 2014.

-
- [70] S. NOZAWA, R. UEDA, Y. KAKIUCHI, K. OKADA, AND M. INABA. A full-body motion control method for a humanoid robot based on on-line estimation of the operational force of an object with an unknown weight. In *Intelligent Robots and Systems (IROS), 2010 IEEE/RSJ International Conference on*, pages 2684–2691, Oct 2010.
- [71] YU. OGURA, K. SHIMOMURA, H. KONDO, A. MORISHIMA, T. OKUBO, S. MOMOKI, HUN OK LIM, AND A. TAKANISHI. Human-like walking with knee stretched, heel-contact and toe-off motion by a humanoid robot. In *Intelligent Robots and Systems, 2006 IEEE/RSJ International Conference on*, pages 3976–3981, Oct 2006.
- [72] HUN OK LIM AND A. TAKANISHI. Waseda biped humanoid robots realizing human-like motion. In *Advanced Motion Control, 2000. Proceedings. 6th International Workshop on*, pages 525–530, April 2000.
- [73] C. OTT, C. BAUMGARTNER, J. MAYR, M. FUCHS, R. BURGER, DONGHEUI LEE, O. EIBERGER, A. ALBU-SCHAFFER, M. GREBENSTEIN, AND G. HIRZINGER. Development of a biped robot with torque controlled joints. In *Humanoid Robots (Humanoids), 2010 10th IEEE-RAS International Conference on*, pages 167–173, Dec 2010.
- [74] Y. BAR-COHEN P. G. BACKES AND B. JOFFE. The multifunctional automated crawling system (macs). In *in Proc. of the IEEE ICRA, Albuquerque, New Mexico, USA, pp. 335-340*, 1997.
- [75] ROBERT T PACK, JOEL L CHRISTOPHER JR, AND KAZUHIKO KAWAMURA. A rubbertuator-based structure-climbing inspection robot. In *Robotics and Automation, 1997. Proceedings., 1997 IEEE International Conference on*, **3**, pages 1869–1874. IEEE, 1997.
- [76] B. PADEN. Kinematics and control robot manipulators. *PhD thesis, Department of Electrical Engineering and Computer Sciences*, 1986.
- [77] SANGDEOK PARK, HEE DON JEONG, AND ZHONG SOO LIM. Design of a mobile robot system for automatic integrity evaluation of large size reservoirs

- and pipelines in industrial fields. In *Intelligent Robots and Systems, 2003. (IROS 2003). Proceedings. 2003 IEEE/RSJ International Conference on*, **3**, pages 2618–2623 vol.3, Oct 2003.
- [78] N. XI D. ASLAM H. DULIMARTA J. XIAO M. MINOR R. L. TUMMALA, R. MUKHERJEE AND G. DANGHI. Climbing the walls. *IEEE Robotics and Automation Magazine*, vol. 9, no. 4, pp. 10-19, 2002.
- [79] S.SHANKAR SASTRY RICHARD M. MURRAY, ZEXIANG LI. A mathematical introduction to robotic manipulation. 20 1994. US Patent 6,567,813.
- [80] J. SAVALL, A. AVELLO, AND L. BRIONES. Two compact robots for remote inspection of hazardous areas in nuclear power plants. In *Robotics and Automation, 1999. Proceedings. 1999 IEEE International Conference on*, **3**, pages 1993–1998 vol.3, 1999.
- [81] JOHN SHERMAN. *Better Bouldering (How To Climb Series)*. Falcon Guides; Second Edition edition, November 2011.
- [82] B. E. SHORES AND M. A. MINOR. Design, kinematic analysis, and quasi-steady control of a morpnic rolling disk biped climbing robot. in *Proc. of the IEEE ICRA, Barcelona, Spain, pp. 2732 - 2737*, 2005.
- [83] MANUEL F SILVA AND JA MACHADO. *A survey of technologies and applications for climbing robots locomotion and adhesion*. InTech, 2010.
- [84] MANUEL F SILVA, JA TENREIRO MACHADO, AND JÓZSEF K TAR. A survey of technologies for climbing robots adhesion to surfaces. In *Computational Cybernetics, 2008. ICC 2008. IEEE International Conference on*, pages 127–132. IEEE, March 2008.
- [85] S. SUGANO AND I. KATO. Wabot-2: Autonomous robot with dexterous finger-arm-finger-arm coordination control in keyboard performance. In *Robotics and Automation. Proceedings. 1987 IEEE International Conference on*, **4**, pages 90–97, Mar 1987.

-
- [86] K. TANIE AND FNR. Toward a platform based humanoid project, robotics research. *Eds. Y. Shirai and S. Hirose, Springer, pages 439–450, 1998.*
- [87] J. URATA, K. NSHIWAKI, Y. NAKANISHI, K. OKADA, S. KAGAMI, AND M. INABA. Online walking pattern generation for push recovery and minimum delay to commanded change of direction and speed. In *Intelligent Robots and Systems (IROS), 2012 IEEE/RSJ International Conference on*, pages 3411–3416, Oct 2012.
- [88] J. VAILLANT, A. KHEDDAR, H. AUDREN, F. KEITH, S. BROSSETTE, K. KANEKO, M. MORISAWA, E. YOSHIDA, AND F. KANEHIRO. Vertical ladder climbing by the hrp-2 humanoid robot. In *Humanoid Robots (Humanoids), 2014 14th IEEE-RAS International Conference on*, pages 671–676, Nov 2014.
- [89] BRIAN H. WILCOX, TODD LITWIN, JEFF BIESIADECKI, JARET MATTHEWS, MATT HEVERLY, JACK MORRISON, JULIE TOWNSEND, NORMAN AHMAD, ALLEN SIROTA, AND BRIAN COOPER. Athlete: a cargo handling and manipulation robot for the moon. *Journal of Field Robotics.*, **20**(5):421–434, Apr 2007.
- [90] TAO XIAO, MIN LI, QIANG HUANG, WEIMIN ZHANG, AND LE HE. Analysis of pushing manipulation by humanoid robot bhr-2 during dynamic walking. In *Automation and Logistics, 2007 IEEE International Conference on*, pages 3000–3005, Aug 2007.
- [91] M. TIAN LI Y. LI AND L. NING SUN. Design and passable ability of transitions analysis of a six legged wall-climbing robot. *in Proc.ofthe IEEE Int. Conf. on Mechatronics and Aut., Harbin, China, pp. 800-804, 2007.*
- [92] KAZUHITO YOKOI, FUMIO KANEHIRO, KENJI KANEKO, SHUJI KAJITA, KIYOSHI FUJIWARA, AND HIROHISA HIRUKAWA. Experimental study of humanoid robot hrp-1s. *The International Journal of Robotics Research*, **23**(4-5):351–362, 2004.

- [93] CHEN YUN, CHEN RONG, AND SU JIAN. Simulation design on the 6-dof parallel vibration platform based on simmechanics and virtualreality. In *World Automation Congress (WAC), 2012*, pages 1–4, June 2012.
- [94] RUIXIANG ZHANG. Design of a climbing robot: Capuchin. In *Proc. 5th Intl. Conf. on Computational Intelligence, Robotics, and Autonomous Systems*, 2008.
- [95] RUIXIANG ZHANG AND JEAN-CLAUDE LATOMBE. Capuchin: A free-climbing robot. *Int. J. Adv. Robot. Syst*, **10**, 2013.
- [96] RUIXIANG ZHANG, PRAHLAD VADAKKEPAT, AND CM CHEW. Motion planning of biped robot climbing stairs. In *Proceeding of FIRA Robot World Congress*, pages 1–3, 2003.
- [97] YAJIA ZHANG, JINGRU LUO, K. HAUSER, R. ELLENBERG, P. OH, H.A. PARK, AND M. PALDHE. Motion planning of ladder climbing for humanoid robots. In *Technologies for Practical Robot Applications (TePRA), 2013 IEEE International Conference on*, pages 1–6, April 2013.

List of Publications

International Journal

- [1] Nguyen Anh Dung, Akira Shimada, "Equilibrium Control on Four-Limbed Climbing Robot," *Applied Mechanics and Materials Journal*, Vols. 799-800, pp 1021-1027, Trans Tech Publications, August 2015.

International Conference

- [1] Nguyen Anh Dung, Akira Shimada, "A Path-Planning Algorithm for Humanoid Climbing Robot using Kinect Sensor," *SICE Annual Conference 2014*, pp. 1549 - 1554, Japan, September 2014.
- [2] Nguyen Anh Dung, Akira Shimada, "Humanoid climbing robot modeling in matlab-simechanics", *Industrial Electronics Society, IECON 2013 - 39th Annual Conference of the IEEE*, pp 4162-4167, Austria, November 2013.
- [3] Nguyen Anh Dung, Akira Shimada, "A Path Motion Planning For Humanoid Climbing Robot" *Modelling and Simulation (EUROSIM), 2013 8th EUROSIM Congress on*, Cardiff, Wale, pp 179-184, July 2013.
- [4] Dung Anh Nguyen, Akira Shimada, "Planning with Right Hand Search Algorithm for Humanoid Climbing Robot," *7th South East Asian Technical University Consortium (SEATUC) Symposium*, OS05, Bandung, Indonesia, March 2013.

Domestic Conference

- [1] A. Shimada, D. Anh Nguyen, “A Basic Study of Dynamics for Humanoid Climbing-Robot,” *Automatic Control Joint Conference*, 1B08-1, pp 656-658, Japan, November 2014 [Japanese].